Universidade de São Paulo
Instituto de Astronomia, Geofísica e Ciências Atmosféricas
Departamento de Ciências Atmosféricas

Natália Machado Crespo

A potential vorticity perspective on cyclones over South America (Ciclones na América do Sul sob a perspectiva da vorticidade potencial)

São Paulo
2019

Natália Machado Crespo

A potential vorticity perspective on cyclones over South America (Ciclones na América do Sul sob a perspectiva da vorticidade potencial)

Versão corrigida. O original encontra-se disponível na Unidade.

Tese de Doutorado apresentada ao Departamento de Ciências Atmosféricas do Instituto de Astronomia, Geofísica e Ciências Atmosféricas da Universidade de São Paulo como requisito parcial para a obtenção do título de Doutor em Ciências.

Área de Concentração: Meteorologia
Orientadora: Prof[a] Dr[a] Rosmeri Porfírio da Rocha

São Paulo
2019

À Ciência e a todos os bons cientistas.

Agradecimentos (Acknowledgments)

Primeiramente, agradeço a mim, por ter chegado até aqui. =)

Agradeço à minha família por todo apoio e compreensão, principalmente por eu ter estado/ainda estar longe de casa há mais de 8 anos; à minha orientadora, Rosmeri Porfírio da Rocha, por ter aceitado me orientar por todos estes anos e não desistir de mim, por fazer ciência de qualidade e não desistir dela nunca; aos colegas e amigos, novos e de longa data (Daiane, Maurício, Stefanía, Felipe, Fernando, Ana Maria, Mario, Angel, Carol, Lívia, Eduardo, pessoal do GrEC e da pós-graduação da meteorologia), pela amizade, companheirismo e apoios técnico e emocional; aos funcionários do IAG-USP, docentes e discentes, mas principalmente ao pessoal da informática (Djalma, Sebastião e Samuel) por estarem sempre dispostos a ajudar e sanar problemas inimagináveis; às CAPES e CNPq pelo apoio financeiro durante estes quatro anos de doutorado.

Agradeço à pesquisadora e professora Raquel Nieto por ter me recebido em seu grupo, obrigada pela paciência; não posso deixar de agradecer ao grupo EphysLab e principalmente às amigas Milica e Anita, que tornaram minha estadia em Ourense ainda mais agradável.

A special thanks to Heini Wernli and Michael Sprenger for accepting me in their group of atmospheric dynamics at IAC-ETHZ for six months, even not knowing me previously – I am still a big “fan” of yours! It was an amazing experience of knowledge and traditions exchange. Thank you all in the group! Also Eva for the administrative work during the process of exchange (Um obrigada em especial aos pesquisadores e professores Heini Wernli e Michael Sprenger por terem me aceitado para fazer parte do grupo de dinâmica da atmosfera do IAC-ETHZ por 6 meses, mesmo sem me conhecerem previamente – continuo uma grande “fã” de vocês; foi uma experiência incrível de troca de conhecimento e vivência; obrigada a todos do grupo). Agradeço à Alessandra e ao Gabriel por também sem nem me conhecerem, me receberem em sua casa em Zurique. And, finally, to Christina Marchand’s family, to receive me in their home at the end of my stay in Zurich.

Por fim, agradeço ao Arthur Amador por n motivos, mas principalmente por ser uma pessoa incrível, companheira, e claro, por me aguentar; à sua família por ter me acolhido e apoiado nestes últimos anos.

RESUMO

Crespo, N. M. **A potential vorticity perspective on cyclones over South America**. 2019. 105p. Tese (Doutorado) – Instituto de Astronomia, Geofísica e Ciências Atmosféricas, Universidade de São Paulo, São Paulo, 2019.

Este estudo apresenta uma visão geral da atmosfera do ponto de vista de anomalias e estruturas de vorticidade potencial (VP) em altos níveis, com o objetivo de entender tais estruturas e suas influências em ciclones em superfície na América do Sul. A partir da reanálise ERA-Interim foram rastreados tanto os ciclones em superfície como as estruturas de VP (streamers e cutoffs de VP, referidos como streamers-VP e cutoff-VP) em superfícies isentrópicas no período 1979-2017. Após identificar ciclones em superfície em quatro regiões (*Argentina, Uruguay, SEBrazil* e *Andes*) são analisados seus deslocamentos, intensidade, tempo de vida, associação com estruturas de VP, e relações entre as regiões ciclogenéticas em diferentes estações do ano. O rastreamento de ciclones mostrou que: i) antes da ciclogênese no *Uruguay* existe uma alta frequência ciclogênese em *Andes*; ii) uma distribuição bimodal de ciclones em termos de deslocamento, intensidade e tempo de vida, indicando dois diferentes tipos de ciclones se formando nas *Argentina, Uruguay* e *SEBrazil*. De forma geral, ciclones que se desenvolvem em *Argentina* e *Uruguay* percorrem distâncias maiores e são mais intensos. Nas quatro regiões, streamers-VP ocorrem frequentemente durante a ciclogênese, localizados tipicamente à sudoeste. No entanto, existem diferenças sazonais durante a gênese: em *Argentina* e *Andes*, streamers-VP ocorrem principalmente no verão, em *Uruguay* no verão e inverno, e principalmente no inverno em *SEBrazil*. A frequência de streamers-VP varia para cada região, sendo encontrados mais frequentemente para *Argentina* e *Uruguay* em 320 K, enquanto que no *SEBrazil* e *Andes* em 340 K, no verão. Cutoffs-VP ocorrem com menor frequência que streamers-VP durante a ciclogênese, no entanto tendem a se intensificar ao longo do ciclo de vida do ciclone, o que é mais comum de ocorrer no verão do que no inverno. Composições de campos dinâmicos (Eady growth rate-EGR, ômega quase-geostrófico, VP, ventos em altos e baixos níveis, pressão ao nível médio do mar, altura geopotencial e umidade específica) antes, durante e depois da ciclogênese mostram importantes diferenças entre inverno e verão em cada região. Em *Argentina*, o ambiente é levemente mais baroclínico (medido pela maior intensidade de EGR, ômega e jato em altos níveis) no verão e o ciclone se forma sob a entrada equatorial do jato de altos níveis. Nesta estação, a anomalia de VP associada com os streamers-VP atua intensificando o movimento

ascendente e contribuindo para a ciclogênese em superfície. No inverno, ciclogênese em *Argentina* ocorre sob a saída polar da corrente de jato, com fraco streamer-VP corrente acima. Padrões similares são observados no verão e inverno em *Uruguay*, porém sob baroclinia mais intensa no inverno. Em *SEBrazil* e *Andes* a corrente de jato em altos níveis situa-se distante da região ciclogenética no verão. Nesta estação, em *SEBrazil*, os ciclones apresentam uma estrutura vertical mais próxima barotrópica. No inverno, a maior frequência de streamer-VP e anomalias de VP têm atuação importante nas ciclogêneses em *SEBrazil*. Comparativamente, *Andes* se apresenta como a região com menor contribuição de streamers-VP e de anomalia de VP para as ciclogêneses em superfície.

Palavras-chave: Vorticidade potencial. Ciclones. Ciclogênese. América do Sul. PV streamers. PV cutoffs.

ABSTRACT

Crespo, N. M. **A potential vorticity perspective on cyclones over South America**. 2019. 105p. Tese (Doutorado) – Instituto de Astronomia, Geofísica e Ciências Atmosféricas, Universidade de São Paulo, São Paulo, 2019.

This study presents a general overview of the atmosphere from a potential vorticity (PV) perspective at upper levels, focusing on the influence of upper-level PV anomalies and structures and their influences on surface cyclones over South America. Surface cyclones and PV structures on isentropic surfaces (PV streamers and PV cutoffs) are identified using ERA-Interim reanalysis for the period 1979-2017. After identifying cyclones in four regions (*Argentina, Uruguay, SEBrazil* and *Andes)*, their traveled distance, intensity, lifetime, association with PV structures, and time lags are analyzed in different seasons. The cyclone tracking showed that i) before cyclogenesis in *Uruguay* there is a high frequency of cyclogenesis in *Andes*; ii) a bi-modal distribution of cyclones in terms of displacement, intensity and lifetime, indicating two different types of cyclones occurring in *Argentina, Uruguay* and *SEBrazil*. In general, cyclones from *Argentina* and *Uruguay* travel longer distances and are more intense. In the four regions, PV streamers occur frequently during cyclogenesis, typically located to the southwest. However, there are seasonal differences during genesis: in *Argentina* and *Andes*, PV streamers occur mainly in summer, in *Uruguay* in summer and winter, and in *SEBrazil* mainly in winter. PV streamers frequency for each region varies, e.g., in *Argentina* and *Uruguay* they are more frequent at 320 K, while in *SEBrazil* and *Andes* at 340 K in summer. PV cutoffs occur in lower frequency than PV streamers during cyclogenesis, however, they tend to intensify during the cyclone lifetime, which is more frequent in summer than in winter. Composites of dynamic fields (Eady growth rate-EGR, quasi-geostrophic omega, PV, upper and lower-level winds, sea level pressure, geopotential height and specific humidity) before, during and after cyclogenesis show important differences between winter and summer for each region. In *Argentina*, the environment is slightly more baroclinic (in respect with stronger EGR, omega and upper-level jet) in summer and cyclones develop beneath the equatorial upper-level jet entrance. In this season, the PV anomaly associated with PV streamers acts intensifying ascent and contributing to the surface cyclogenesis. In winter, cyclogenesis in *Argentina* occur beneath the polar exit sector of the jet stream, with weak PV streamer upstream. Similar patterns are observed in summer and

winter in *Uruguay*, but with a stronger baroclinicity in winter. In *SEBrazil* and *Andes* the upper-level jet is far from the cyclogenetic region in summer. In this season, cyclones in *SEBrazil* have a more barotropic vertical structure, whereas in winter, the higher frequency of PV streamers and PV anomalies are more important for cyclogenesis in this region. Comparatively, *Andes* is the region with the lowest contribution of PV streamers and PV anomalies for surface cyclogenesis.

Key-words: Potential vorticity. Cyclones. Cyclogenesis. South America. PV streamers. PV cutoffs.

List of Figures

Contents

Chapter 1

1 Introduction

Cyclones are meteorological phenomena of great importance to the energetic equilibrium of the global atmosphere. Being classified from synoptic to the meso-alfa scales, they redistribute heat, moisture and momentum in the atmosphere since the heating on the Earth's surface is heterogeneous due to the differential radiation energy received from the Sun, from the equator to the poles. There are three main different types of cyclones: extratropical, subtropical and tropical, and they have different characteristics as regarding their formation, location, intensity, and other weather systems associated. Frequently, they are associated with the presence of strong winds, cloud formation and precipitation, cold and warm fronts; in some cases, they are able to create a proper environment for severe weather systems, as tornadoes, or being a precursor of cold surges and storm surges. There are large interests to understand the development of cyclones worldwide. Therefore, this study aims in to better understand the relationship between upper-level forcing, i.e., the upper part of the troposphere, and the formation of surface cyclones over South America (SA).

1.1 Motivation and goals

An important aspect during cyclogenesis, i.e., the cyclone formation, is its interaction with the upper level of the troposphere. This interaction can be studied using potential vorticity (PV), which is a conservative quantity that may modify the environment providing more favorable conditions to the formation or intensification of surface cyclones (Hoskins et al., 1985). Despite all previous studies found in the literature on cyclones and cyclogenesis over SA and the South Atlantic Ocean, a systematic climatology of upper-level PV forcing leading to cyclogenesis over these regions is still not fully explored in the literature. Therefore, the main aim of this thesis is to evaluate the contribution of upper-level PV anomalies on surface cyclogenesis over the main cyclogenetic regions of SA. For this purpose, this work presents:

i) a climatology of PV features in different isentropic levels;

ii) a climatology of the main atmospheric variables associated with the surface cyclone development;

iii) the tracking of surface cyclones over a larger area using relative vorticity (RV) to identify the main cyclogenetic regions over SA;

iv) a detailed analysis to assess where (i.e., in which cyclogenetic region) and when (i.e., in which season; austral summer or winter) the association with PV streamers and PV cutoffs is particularly important for the surface cyclogenesis.

This study is particularly relevant to provide forecasters and scientists with a climatological background of the upper level PV forcing during cyclogenesis over SA; the idea is that this study can enable the use of upper level PV fields together with other relevant atmospheric indicators as a guide for cyclones prediction, since it is discussed the precursors for cyclones in each cyclogenetic region of SA.

This thesis is divided as: chapter 2, a theoretical background on cyclones and the state-of-art knowledge regarding cyclogenesis over SA and the South Atlantic, a discussion on PV and its importance to the development of synoptic weather systems; chapter 3, dataset and methods used to assess cyclones and PV features; chapters 4 and 5, results and discussions; and chapter 6, a summary of main results and future possible studies.

Chapter 2

2 Theoretical background

In this chapter a PV perspective on cyclones development is introduced followed by a summary of cyclone studies over South America.

2.1 Isentropes and PV anomalies on cyclogenesis

"Isentropic" means conservation of entropy, i.e., in a given isentropic surface, the entropy is conserved following the motion. From the thermodynamic equation it is possible to show that, for an "isentropic" flow, the potential temperature (θ) is also a conservative quantity. However, this is only valid when a flow without external heat exchange (adiabatic flow) and frictionless is assumed, hence the quantities transported in this region are conserved (Ertel, 1942). PV, on the other hand, is a combination of vorticity dynamics and thermodynamics (Hoskins and James, 2014), where in an adiabatic and frictionless flow (hence, without dissipating energy), the potential vorticity is conserved.

The barotropic PV was introduced by Rossby (1940) and considers the atmosphere as an incompressible and homogeneous fluid. However, we will discuss the baroclinic version of PV, represented by the Ertel's (1942) equation. Hence, PV is a product between the absolute vorticity and the static stability of the atmosphere. In isentropic vertical coordinates, PV is expressed as:

$$PV = -g\,(\zeta_\theta + f)\left(\frac{\partial\theta}{\partial p}\right) \qquad (1),$$

where g is gravity, $(\zeta_\theta + f)$ is the absolute vorticity (ζ_θ is the relative vorticity in isentropic surface; f is the Coriolis parameter), and $\frac{\partial\theta}{\partial p}$ is the static stability. By conservation, where one term changes, the other must compensate the difference. The unity of measure of PV is normally expressed as 1 PVU = 1 x 10^{-6} m^2 K s^{-1} kg^{-1}. PV is frequently used to separate stratospheric air from tropospheric air and to identify the dynamical tropopause, which is the

region of transition between the troposphere and stratosphere. Values of PV above 1.5 PVU (in module, since PV is negative for the Southern Hemisphere) are typically from stratospheric origin (Hoskins et al., 1985). However, the value of PV used to identify the dynamical tropopause is not fixed; some studies use PV values between 1 and 3 PVU (Reed, 1955; Danielsen, 1959; Shapiro, 1980; Hoskins et al., 1985; WMO, 1986; Wernli and Sprenger, 2007), 3.5 PVU (Hoerling et al., 1991; Hoinka, 1998), and a more recent study shows that the tropopause level can range from 1.5 to 5 PVU (Kunz et al., 2011).

When air masses from the stratosphere (high absolute values of PV due to the strong static stability) move to the troposphere they are referred to as PV anomalies. The material conservation property makes PV anomalies a useful dynamical variable in identifying and tracing the evolution of meteorological disturbances (Holton, 2004).

In that sense, the diagram in Figure 2.1 presents a scheme where the upper level PV anomaly advected downwards to the middle troposphere leads to deformations in the vertical distribution of potential temperature and vorticity as, respectively, i) deforming the isentropes, which imposes ascending motion ahead of the anomaly and subsidence behind it, and ii) generating cyclonic vorticity slightly downward (Hirschberg and Fritsch, 1991).

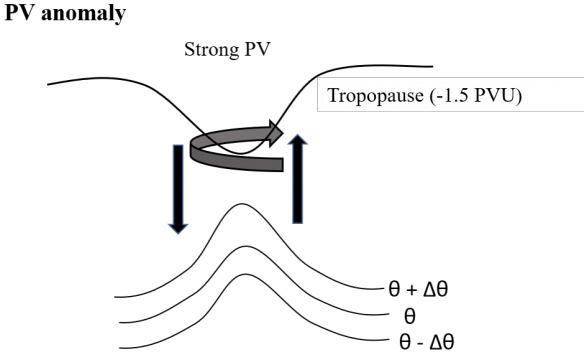

Figure 2.1 Scheme of PV anomaly and dynamical tropopause for the Southern Hemisphere. The black arrows indicate downward and upward motions and the grey arrow indicates the cyclonic circulation.

Figure 2.1 indicates the associations between potential vorticity and surface cyclogenesis; regions to the west and to the east of the upper level PV anomaly will become warm (black arrows), whereas beneath the upper level PV anomaly, however, the air becomes colder (Figure 2.1). The region of warmer air at east of the PV anomaly is where the low levels low-pressure systems will probably form (Hirschberg and Fritsch, 1991).

The diagrams in Figure 2.2 exemplify the process of cyclogenesis through upper level PV forcing and lower level coupling. The upper level PV anomaly induces cyclonic vorticity potentially down to surface where the amplitude of this induced circulation becomes weaker towards the surface (Figure 2.2a). A perturbation in the potential temperature field at surface induces cyclonic vorticity (Figure 2.2b); there is an intensification, as these two anomalies (in upper and lower levels) are not vertically aligned (Figure 2.2c).

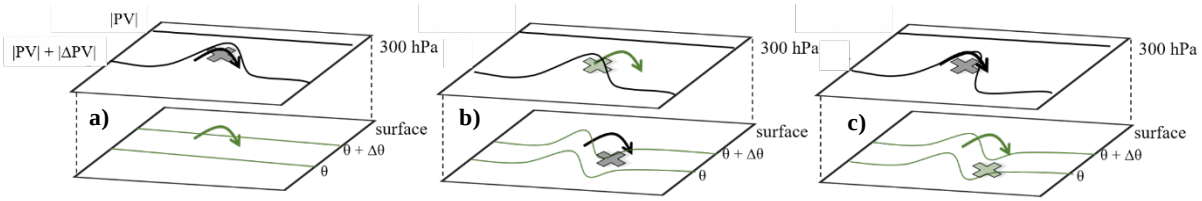

Figure 2.2 Upper tropospheric PV anomaly moving over a low-level baroclinic zone in the Southern Hemisphere. a) Circulation associated with upper PV anomaly ('X' sign) is indicated by the black arrow. The surface reflection of that circulation is given by the green arrow at the surface; b) low-level thermal advections produce a surface warm anomaly (grey 'X' sign) whose circulation, indicated by the black arrow, has an upper tropospheric reflection (green arrow); c) upper tropospheric PV advections intensify the upper PV anomaly (grey 'X' sign) and its circulation, indicated by the black arrow, intensifies. The surface reflection of that circulation (green arrow) results in thermal advections that serve to intensify the surface warm anomaly. Adapted from Martin (2006).

Another important aspect during a cyclone development is the diabatic heating, which occurs due to the latent heat release during condensation. Following Martin (2006), the diabatic heating affecting PV may be better understood considering the conservation of PV (equation 1) in its equivalent isobaric form:

$$PV = -g\left(f\,\boldsymbol{k} + \nabla_p \times \boldsymbol{V}_h\right).\nabla_p\theta \qquad (2),$$

and by deriving (2) into all of its components and keeping only the vertical component, the resulting expression is:

$$\frac{d}{dt}(PV) \approx -g(\zeta + f)\left(\partial\dot{\theta}/\partial p\right) \qquad (3),$$

where $\dot{\theta} = \frac{d\theta}{dt}$ is, according the thermodynamic equation, the diabatic heating and ζ is the relative vorticity in isobaric vertical coordinate.

In summary, PV is increased (decreased) where the vertical gradient of diabatic heating is positive (negative). In a typical mid-latitude cyclone, the maximum diabatic heating is located in the middle troposphere (Martin, 2006). In this case, PV production occurs in the lower troposphere and PV destruction occurs near the tropopause, as presented in Figure 2.3 (Wernli and Davies, 1997). The resultant low-level PV anomaly (negative in the Southern Hemisphere) has an associated cyclonic circulation and can contribute to the intensification of the low-level surface cyclone (Figure 2.3). The maximum heating occurs slightly downstream of an upper-level negative PV (in the Southern Hemisphere) anomaly since it is where the upward motion is more intense (as depicted in Figure 2.2). Consequently, the effects of diabatic heating are to **create** the low-level negative PV anomaly and to **erode** upper tropospheric PV. This erosion is important because it serves to steepen the slope of the PV isopleth downstream of the upper-level negative PV anomaly, contributing to intensify the PV anomaly (Martin, 2006). The penetration of both PV anomalies (one from the stratosphere and the other produced by diabatic heating) is intensified by latent heating, which generally acts to reduce the static stability in such regions. All these mechanisms lead to the intensification of the surface cyclone (Whitaker and Davies, 1994).

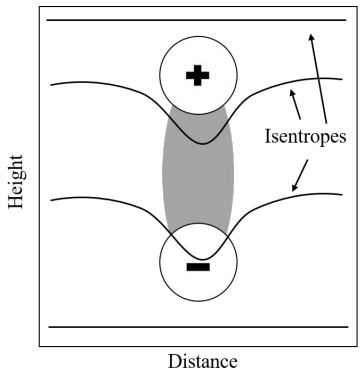

Figure 2.3 Schematic vertical cross-section showing diabatically produced PV anomalies (circles with plus and minus) for an idealized case. Shading indicates the region of diabatic heating and the lower (upper) circle indicates PV production (destruction) for the Southern Hemisphere. Adapted from Wernli and Davies (1997).

2.2 PV streamers and PV cutoffs structures

The term “streamer” was firstly introduced by Appenzeller and Davies (1992), in a study related to structures of stratospheric intrusions into the troposphere, which is usually associated with the development of a surface low-pressure system and cold front (Appenzeller

and Davies, 1992; Hoskins et al., 1985). PV streamers are characterized by “PV tongues”, i.e., narrow stratospheric filaments containing high absolute values of PV from the stratospheric reservoir (Platzman, 1949), as exemplified in Figure 2.4. These structures act as wave guides; for instance, in the planetary scale, the air from the polar vortex expelled in the mid-stratosphere favors a mix of chemical constituents in its surroundings (McIntyre and Palmer, 1983) and from the lower stratosphere to the troposphere (Waugh et al., 1994; Appenzeller et al., 1996), also leading to stratosphere-troposphere exchanges (Sprenger et al., 2007). Nevertheless, PV streamers can be considered as a breaking in the synoptic scale Rossby waves (Thorncroft et al., 1993)

If these PV filaments break up, they form mesoscale vortices called PV cutoffs (Wernli and Sprenger, 2007). PV cutoffs (Figure 2.4) - and similarly PV streamers that feature the same characteristics as PV cutoffs but remain attached to the poleward stratospheric high-PV reservoir - favor the formation or intensification of cyclonic circulations at mid-to-low-tropospheric levels (Hoskins et al., 1985). With that, there is also the concept of cutoff lows (COLs), which are upper-level systems that could generate surface cyclones, and they are usually identified as low-pressure systems at upper levels, i.e., as regions inside closed geopotential isolines or isobars. Nieto et al. (2008) found that a high percentage of COLs is also associated with PV anomalies (or PV cutoffs), which allows the COLs impact to be studied in the PV framework as proposed by Hoskins et al. (1985).

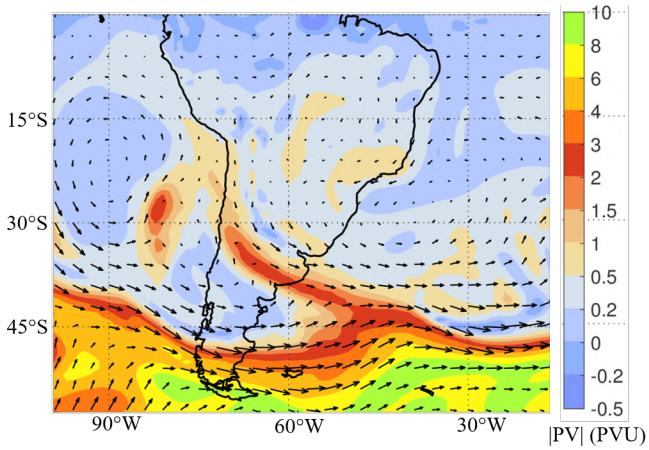

Figure 2.4 Example of PV streamer and PV cutoff over South America and adjacent oceans at 1200 UTC 29 January 2014. The streamer is represented by the red (2-3 PVU) filamentary structure over southern South America and the cutoff is the red center (2-3 PVU) detached from the PV reservoir over the South Pacific. In shaded is PV at 320 K and the vectors are winds at 300 hPa.

2.3 Cyclones over South America

From a general point of view, cyclones over SA and South Atlantic Ocean have different phases during their lifecycle such as extratropical, subtropical or tropical. The only documented tropical cyclone over the South Atlantic was the so-called “Furacão Catarina” (Pezza and Simmonds, 2005). Extratropical cyclones are the most common over the region (Reboita et al., 2017) and, recently, a climatology of subtropical cyclones was performed by Gozzo (2014), showing that around six subtropical cyclones per year occur over the South Atlantic.

Nevertheless, the cyclonic activity near the eastern coast of SA and southwestern South Atlantic significantly influences weather and climate conditions over the South American continent. Previous climatologies have identified three most cyclogenetic regions in eastern SA: south/southeast of Brazil, east of Uruguay, and southern Argentina (Sinclair, 1995; Hoskins and Hodges, 2005; Reboita et al., 2010, 2018; Krüger et al., 2012; Gramcianinov et al., 2019). The main dynamical mechanism for the formation of these cyclones is mainly baroclinic instability of the westerly flow. Thereby, the formation of lee-side troughs east of the Andes can trigger baroclinic instability and induce the development of surface cyclones (Gan and Rao, 1991; Miky Funatsu et al., 2004; Reboita et al., 2012). In addition, there is also the downstream development, where cyclones develop from the available energy exported from the main mid-latitude baroclinic wave (e.g. Orlanski and Katzfey, 1991) and some cyclones are able to develop following the barotropic chain of energy conversion process (Dias Pinto et al., 2013).

The presence of two stationary low-pressure systems over the central part of the continent, Chaco Low and the Northwestern Argentinian Low (Salio et al., 2002; Saulo et al., 2004; Seluchi et al., 2003; Seluchi and Saulo, 2012), acts differently over the region and may contribute to cyclogenesis. The former is located equatorward of the subtropical jet and it is basically absent during winter but still associated with great amount of annual rainfall. The second is located further to the south (around 30°S), associated with less precipitation, and characterized by a distinct diurnal cycle. Whereas the Chaco Low, which at upper levels presents an anticyclonic circulation, only weakly interacts with transient upper-level disturbances crossing over it, the Northwestern Argentinian Low more strongly interacts with these disturbances from mid-latitudes when they pass over the Andes. As shown by Sinclair

(1994), about 50% of cyclones forming close to the Andes remain stationary while the rest move away from the genesis region and potentially influence cyclogenesis downstream (Gan and Rao, 1994). Additional factors have also been found to contribute to cyclone formation: the moisture transport from the Amazonia region to the subtropics subsequent latent heat release, and the propagation of upper-level troughs over the southern part of the Andes (Mendes et al., 2007; Reboita et al., 2012).

2.4 Cutoff Lows and PV perspective on surface cyclones over South America

Some surface cyclones have been found to develop in the presence of upper-level cutoff lows (COLs; Miky Funatsu et al., 2004; Campetella and Possia, 2007; Nieto et al., 2008). They are usually identified as regions inside closed geopotential isolines in the middle or upper troposphere. The accurate prediction of cutoff lows is very important since their interaction with low levels may result in events of intense precipitation, snow, and strong winds. Satyamurty and Seluchi (2007) simulated the lifecycle of a COL (also known in the region as "*Vórtice Ciclônico de Altos Níveis* - VCAN"), developed over the subtropical region of South America in austral winter of 1999. Besides the cold core, stronger values of relative vorticity right beneath the tropopause were found associated with PV anomalies. Recently, Pinheiro et al. (2017) tracked COLs objectively using relative vorticity minimum at 300 hPa for the Southern Hemisphere. Also, they used PV minima to identify COLs. In one hand the method differs from the one using geopotential in the systems' lifetime, since the latter identifies systems with smaller lifetime, but on the other hand the results match seasonally with climatologies obtained by traditional methods using only geopotential height (Fuenzalida et al., 2005; Campetella and Possia, 2007; Reboita et al., 2010).

For the Northern Hemisphere, Nieto et al. (2008) found that a high percentage of COLs is associated with PV anomalies (or PV cutoffs), which allows studying COLs in the PV framework (Hoskins et al., 1985). More specifically, a PV cutoff is a center of high absolute values of PV typically identified on an isentropic surface that detached from the stratospheric reservoir at higher latitudes (Wernli and Sprenger, 2007; Portmann et al., 2018). These upper-level PV anomalies induce a closed circulation at lower levels, as mathematically expressed in the PV invertibility principle (Hoskins et al., 1985). Furthermore, the typically low tropopause in a PV cutoff goes along with a warm anomaly in the lower stratosphere and

a cold anomaly in the middle troposphere (as discussed in section 2.1). This can destabilize the troposphere and favor convection. Hence, PV cutoffs - and similarly filamentary PV streamers that feature similar characteristics as PV cutoffs but remain attached to the poleward stratospheric high-PV reservoir - favor the formation or intensification of cyclonic circulations at mid-to-low-tropospheric levels (Hoskins et al., 1985).

The PV perspective has already been successfully applied to SA cyclogenesis. For instance, Iwabe and da Rocha (2009) analyzed in a case study how a stratospheric PV anomaly was responsible for a secondary cyclogenesis over the western South Atlantic. The enhanced turbulent heat fluxes and moisture content in the marine boundary layer, and a COL at mid-tropospheric levels contributed to reduce the propagation speed of an upper-level Rossby wave resulting in an extended lifecycle of the cyclone. Furthermore, two types of secondary cyclogenesis were identified by Iwabe (2012) in a climatology, whereby one of them forms mainly due to upper-level PV perturbations.

A case of orographic cyclogenesis was studied by Miky Funatsu et al. (2004), where the Andes played an important role in triggering an extratropical cyclone development over Uruguay. In the same study, it was observed by using PV inversion that the surface temperature anomaly was important in the initial development stages, while the upper-level PV anomalies contributed to the maximum intensification of the system at later stages.

A PV perspective was also adopted by Sprenger et al. (2013) to study cold-surge events in the south and southeastern of Brazil. They found that upstream of SA the dynamical tropopause (-2 PVU isoline) on the 320 K isentropic surface gets strongly distorted before and during the cold-surge event, finally leading to an equatorward development of a PV streamer to the east of the Andes, reaching Uruguay and southeastern Brazil.

For cyclones in general, Crespo (2015) developed a methodology to associate surface cyclones over SA with upper-level PV anomalies at 300 hPa for the period 1998-2003. Cyclones associated with PV anomalies during their lifecycle turned out to be more intense, travel longer distances, and have their genesis especially over the extratropical South Atlantic. Also, they occur more frequently during winter. Finally, a recent study on explosive cyclogenesis cases over the South Atlantic found that explosive cyclogenesis develops under an anomalous dynamical tropopause, followed by stratospheric ozone intrusion and high values of PV (Avila, 2018).

Chapter 3

3 Data and methodology

This chapter explains the methods and dataset used for the cyclone tracking as well as PV streamers and PV cutoffs, and, finally, the atmospheric variables and parameters for the composite analysis.

3.1 Data and cyclone tracking

3.1.1 Data

The ERA-Interim (Dee et al., 2011) dataset from the *European Centre for Medium-Range Weather Forecasts* (ECMWF) in both pressure and isentropic levels is the main data source for this study. For the cyclone tracking we used the 925 hPa horizontal wind field with horizontal grip spacing of 1.5° x 1.5° of latitude by longitude. The potential vorticity from ERA-Interim at different isentropic levels from 310 to 360 K, with interval of 5 K (Sprenger et al., 2017) is used to identify PV streamers and PV cutoffs. Other atmospheric variables at pressure levels (horizontal wind field, sea level pressure, geopotential height, specific humidity, etc.) from the same data base are used to create the composites analysis. In these two latter cases, the horizontal grid spacing is of 1° x 1°.

3.1.2 Cyclone tracking

The cyclone tracking algorithm is based on relative vorticity (RV) and first developed by Sugahara (2000) and after adapted by Reboita et al. (2010). The methodology follows that of Sinclair's (1994, 1995, 1997). However, differently from Sinclair's, which calculates the vorticity from the geostrophic wind, our tracking algorithm is applied directly to the reanalysis (or simulated) wind field. As a first step, the vorticity field is smoothed twice with

the Cressman method (Cressman, 1959) to eliminate spurious vorticity centers and signals related to elongated shear regions. As described by Reboita et al. (2010), the cyclone tracking involves three stages: 1) identifying vorticity minima, 2) locating them after the first displacement, and 3) searching for the next positions considering the estimated velocity of the cyclone.

According to the tracking algorithm, cyclones are required to have RV equal or less than -1.5×10^{-5} s^{-1} and a minimum lifetime equal or greater than 24 hours. The tracking is applied to the domain illustrated in Figure 3.1, which extends from 73.5°S – 1.5°S and 138°W – 108°E, and to the period of 1979 to 2017. Since this study uses a large area to apply the tracking algorithm, the surface cyclones climatology provides a higher number of events in comparison to previous studies where this tracking was applied to a smaller domain (e.g., Krüger et al., 2012; Gozzo, 2014; Reboita et al., 2018). This occurs because with the absent of domain boundaries close to the continent, most cyclones reach at least 24 hours of lifecycle inside of the domain. In addition, a large domain allows the inclusion of important areas in the cyclones climatology, such as upstream Andes and all of South Atlantic Ocean.

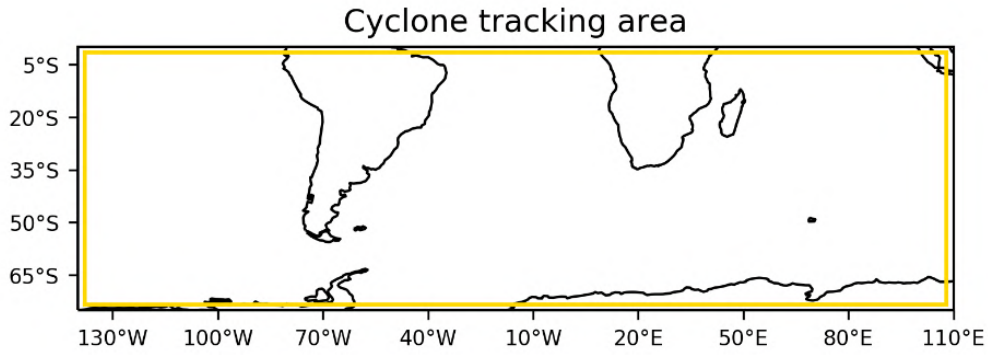

Figure 3.1 Cyclone tracking region (yellow line) delimited by 73.5°S - 1.5°S; 138°W - 108°E.

3.2 PV streamers and cutoffs identification

The method developed by Wernli and Sprenger (2007) is used to identify stratospheric PV streamers and cutoffs. In this methodology, the absolute PV values equal or above 2 PVU is used to separate stratospheric from tropospheric air.

PV cutoffs are identified as regions of stratospheric air embedded in a tropospheric environment on different isentropic levels (Wernli and Sprenger, 2007). High absolute values

of PV could also be related to PV generation by topography (e.g., Aebischer and Schär, 1998) or latent heat release in cyclones (Čampa and Wernli, 2012).

For PV streamers, the identification is based on the geometry of the 2 PVU contour (Wernli and Sprenger, 2007; Sprenger et al., 2017). As illustrated in Figure 3.2, the method depends on two distance thresholds: the direct spherical distance between two points needs to be smaller than 800 km (*d*) and the connection between these two points along the contour has to be larger than 1500 km (*l*). With these specific values, the algorithm is able to identify meso- and synoptic-scale filamentary PV features.

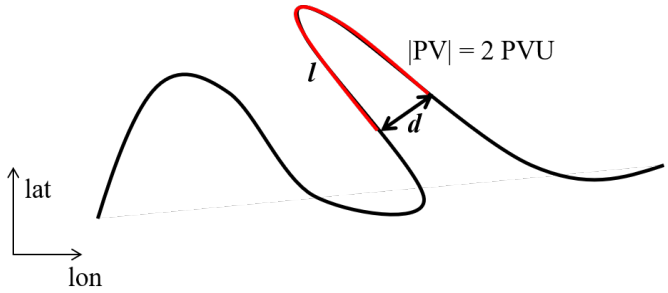

Figure 3.2 Scheme of PV streamer identification. The black line corresponds to the 2 PVU contour on an isentropic surface, where the delimited red line is a stratospheric streamer since **d** (the spherical distance) between two points of the contour is smaller than the threshold D and the distance ***l*** along the contour connecting these points is larger than the threshold value L. Adapted from Wernli and Sprenger (2007).

3.3 Dynamic characterization of cyclones

Several dynamical variables are used to characterize the cyclone development over SA. In particular, PV is considered at specific isentropic levels (as will be discussed in section 5) to identify the different PV structures (streamers and cutoffs) and to analyze the perturbation of the dynamical tropopause at and upstream of the cyclogenesis event. Furthermore, the horizontal wind speed at 300 hPa is used to analyze the upper level jet stream. Other atmospheric variables as geopotential height at 500 hPa and sea level pressure (SLP) are used to discuss the vertical structure of the cyclone. Winds and specific humidity (q) allow discussing the influence of different air masses and the moisture transport influencing cyclogenesis. In addition to the basic atmospheric fields, two other parameters directly linked to cyclone formation complement this list: Eady growth rate (EGR) and quasi-geostrophic Omega forcing (QG-omega).

The Eady model is the simplest model to understand baroclinic instability (Eady, 1949). The EGR, which is the growth rate of the most unstable baroclinic mode, depends on the vertical wind shear, static stability N^2 and the Coriolis parameter f:

$$EGR = 0.31\ \frac{f}{N}\frac{\partial \boldsymbol{v}}{\partial z} \text{ with } N = \left(\frac{g}{\theta}\frac{\partial \theta}{\partial z}\right)^{1/2} \quad (4),$$

where $\boldsymbol{v}$ is the horizontal wind speed, z is height, and θ the potential temperature. According to equation (4), the Eady model of baroclinic instability the growth rate of the most unstable mode is directly proportional to f. Therefore, cyclone intensification most likely occurs faster at higher latitudes, i.e., near the polar jet. The ageostrophic circulation associated with the jet streak dynamics favors baroclinic instability at the jet streak's exit, which is also climatologically the region of frequent cyclone tracks (James, 1995). At mid-latitudes the typical wavelength for the most unstable baroclinic mode is 4000 km with EGR corresponding to ~ 0.5 day^{-1}, which is similar to the high frequency eddy scale. In this study, EGR (equation 4) is calculated in the 850-500 hPa layer (for details, see Sprenger et al., 2017).

The forced vertical motion (in the text referred to as QG-omega) is obtained from the quasi-geostrophic omega equation, according to the **Q**-vector formulation (Davies, 2015):

$$\left(\sigma\boldsymbol{\nabla}^2 + f^2\frac{\partial^2}{\partial p^2}\right)\omega = -2\,\boldsymbol{\nabla}\,.\,\mathbf{Q}\text{ , with } \sigma = -\frac{RT_v}{p\theta}\frac{d\theta}{dp} \quad (5),$$

where σ is the static stability, T_v the virtual temperature, R the gas constant for dry air, f the Coriolis parameter and p the pressure. Hence, the forcing for vertical motion ω is determined by numerically inverting equation (5) with the divergence of **Q** as a forcing term, which in turn is calculated from the geostrophic wind and temperature gradient. More specifically:

$$\mathbf{Q} = \left(\mathrm{Q}_x, \mathrm{Q}_y\right) = f\gamma\left[\left(\frac{\partial \boldsymbol{v}_g}{\partial x}\,.\,\boldsymbol{\nabla}\theta\right),\ \left(\frac{\partial \boldsymbol{v}_g}{\partial y}\,.\,\boldsymbol{\nabla}\theta\right)\right] \text{ where } \gamma = \frac{R}{f\ p_0}\left(\frac{p}{p_0}\right)^{R/C_p} \quad (6).$$

Setting the forcing term $\nabla . \mathbf{Q}$ to zero at lower and upper levels, it is possible to separate between QG-omega forcing attributable to, respectively, upper-level and low-level flow. QG-omega is calculated at the 500 hPa mid-tropospheric level and we specifically considered the forcing from levels above 600 hPa. For further details, see Graf et al. (2017).

3.4 Period and composite analysis

The period of analysis is from 1979 to 2017. Except for the upper and lower level winds, the aforementioned variables are analyzed through anomalies composites, i.e., for all fields, the anomaly is calculated considering the seasonal climatology: “mean of events” minus “seasonal climatology” for timesteps previous, during and after cyclogenesis. The seasons are referred to as austral summer, autumn, winter and spring, which correspond respectively to the months DJF (December-January-February), MAM (March-April-May), JJA (June-July-August) and SON (September-October-November).

Chapter 4

4 Results 1 – Cyclones characteristics

This chapter presents the main results regarding to the cyclogenetic regions and cyclones characteristics over SA. The sections are divided as: 1) a discussion of the cyclogenesis density and a comparison between relative vorticity (RV) and sea level pressure (SLP) tracking; 2) the cyclones characteristics such as tracking, seasonality, lifetime and intensity as well as 3) a comparison between time lag genesis.

4.1 Cyclone tracking and cyclogenetic regions over SA

As a first step, we will show a small comparison of the 925 hPa RV tracking with the i) default two smoothing option and ii) three smoothing on RV field. An additional comparison is presented for the tracking using sea level pressure (SLP) developed by Wernli and Schwierz (2006). This analysis is presented to illustrate that the cyclone detection depends on which method is used and thus the resulting density fields differs partially from each other. The period of analysis is from 1979 to 2017 using the ERA-Interim dataset as input for both comparisons.

Figure 4.1 shows the annual cyclogenetic density for both RV and SLP, where the shaded and blue lines represent, respectively, the two and the three smoothing on the fields of RV (Figure 4.1a) and the two smoothing and SLP (Figure 4.1b) tracking. A clear aspect is that the three smoothing on the RV (Figure 4.1a) presents a smaller number of cyclones, especially near the continental coasts (SA and Africa). However, focusing on SA, the density is similar for both (two and three) smoothing over the continent. An interesting aspect is that there is a small shift equatorward of densities with two smoothing on the RV field compared to three. This indicates that besides the two smoothing being able to capture cyclones at lower latitudes, it can also detect smaller vorticity perturbations that will not necessarily become a classic extratropical cyclone as described in theory (Bjerkenes and Solberg, 1922).

Differently from the three smoothing on the RV field, when comparing the two smoothing with the SLP tracking it is noticeable that the density of cyclogenesis is similar in

the subtropics, over the continent and near the coasts (Figure 4.1b). However, at mid-higher latitudes the RV tracking presents a larger number of cyclogenesis, as already found in Neu et al. (2013) by comparing several algorithms using RV and SLP to identify cyclones. In addition, this also demonstrates that the method using RV has the advantage over the method relying on SLP since it can detect not only closed centers of SLP, intense or slowly moving systems, but it also adds a large number of mobile vortices, especially in the latitude belt of 45°-55°S where many cyclones are not associated with closed isobars in the pressure field due to the strong westerly winds (Sinclair, 1994). Even though the tracks differ in number of cyclones detected (more than double for RV compared to SLP), they show similar regions as hot spots for cyclogenesis over SA, with the SLP track having a center slightly displaced to southwest compared to the center in RV track (~ 50°S).

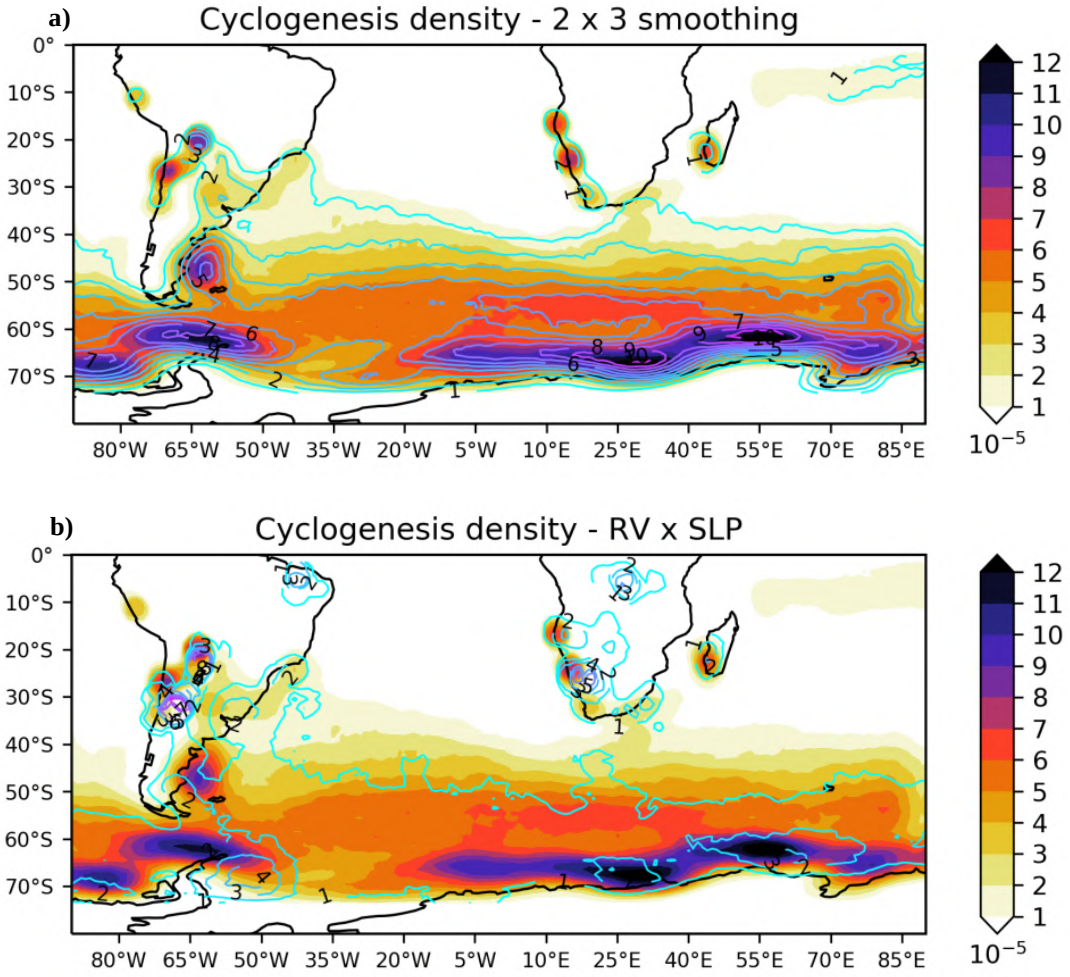

Figure 4.1 Comparison of the annual mean cyclogenesis density (1979-2017) from South America to the mid Indian Ocean for a) RV tracking with two (shaded) and three (blue lines) smoothing at 925 hPa and b) RV with two (shaded) smoothing at 925 hPa and SLP (blue lines) tracking. The unit is cyclogenesis per area (km^2) per year with the values multiplied by 10^5.

For SA, several studies investigate cyclones and cyclogenesis with most of them focusing over the South Atlantic Ocean, since different processes involving continental features occurs especially close to the Andean region. However, the systems occurring over the continent are of great importance for weather and climate conditions due to their contribution to the moisture transport at low-levels from tropics to subtropics with subsequent formation of rainfall and latent heat release (Mendes et al., 2007; Reboita et al., 2012). As Sinclair (1994) also showed, around 50% of cyclones forming very close to the Andes are stationary, while the rest can be accounted as mobile systems.

From Figure 4.1b the RV and SLP tracks present four main concurrent hot spots for cyclogenesis, where three of them are already known and studied (the coastal regions) and the fourth is over the continent, at lower latitudes and in the lee side of the Andes (20°S). This region, for instance, is not seen in Reboita et al. (2010, 2018), Mendes et al. (2007), or in Gramcianinov et al. (2019), even though the latter considered the continent for the tracking. There is another center close to the western coast of SA, but both tracks (RV and SLP) differ regarding its center position. Because of this difference in addition to orographic aspects (this region strongly overlaps with the Andes), this fifth region is discarded from the analysis. Therefore, the study will focus on the four main cyclogenetic regions using the information (date, latitude and longitude) from the RV tracking.

The four boxes in Figure 4.2, which have different sizes, highlight the main geographical hot spots of cyclogenesis. Throughout this work, these areas are named *Argentina* (size 15°x15°, centered at 45.5°S;62.5°W), *Uruguay* (19°x10°, 32°S;56.5°W), *SEBrazil* (10°x10°, 25°S;43°W), and *Andes* (10°x10°, 21°S;61°W). Some hot spots (e.g., *Argentina*, *Uruguay* and *SEBrazil*) agree qualitatively with earlier studies using different methods and datasets to identify cyclones (Taljard, 1967; Gan and Rao, 1991; Hoskins and Hodges, 2005; Reboita et al., 2010, 2018; Neu et al., 2013; Gramcianinov et al., 2019).

Figure 4.3 shows the total (inner pie) and seasonal frequency (outer pie) of cyclogenesis in each cyclogenetic box. *Argentina* contains the largest number of cyclones and is very active during all seasons with a slightly higher frequency in austral summer (Figures 4.2a, 4.3), which is consistent with previous studies (Hoskins and Hodges, 2005; Reboita et al., 2010, 2018; Gramcianinov et al., 2019). *Uruguay*, on the other hand, is more active during winter and spring (Figures 4.2c,d, 4.3), as already documented in the literature (Hoskins and Hodges, 2005; Reboita et al., 2010, 2018). The smallest number of cyclones is found in

SEBrazil, where greater frequencies occur in summer followed by spring (Figures 4.2a,d, 4.3). Finally, *Andes* records greater cyclogenesis activity during winter and spring (Figures 4.2c,d, 4.3), with seasonality comparable to *Uruguay*.

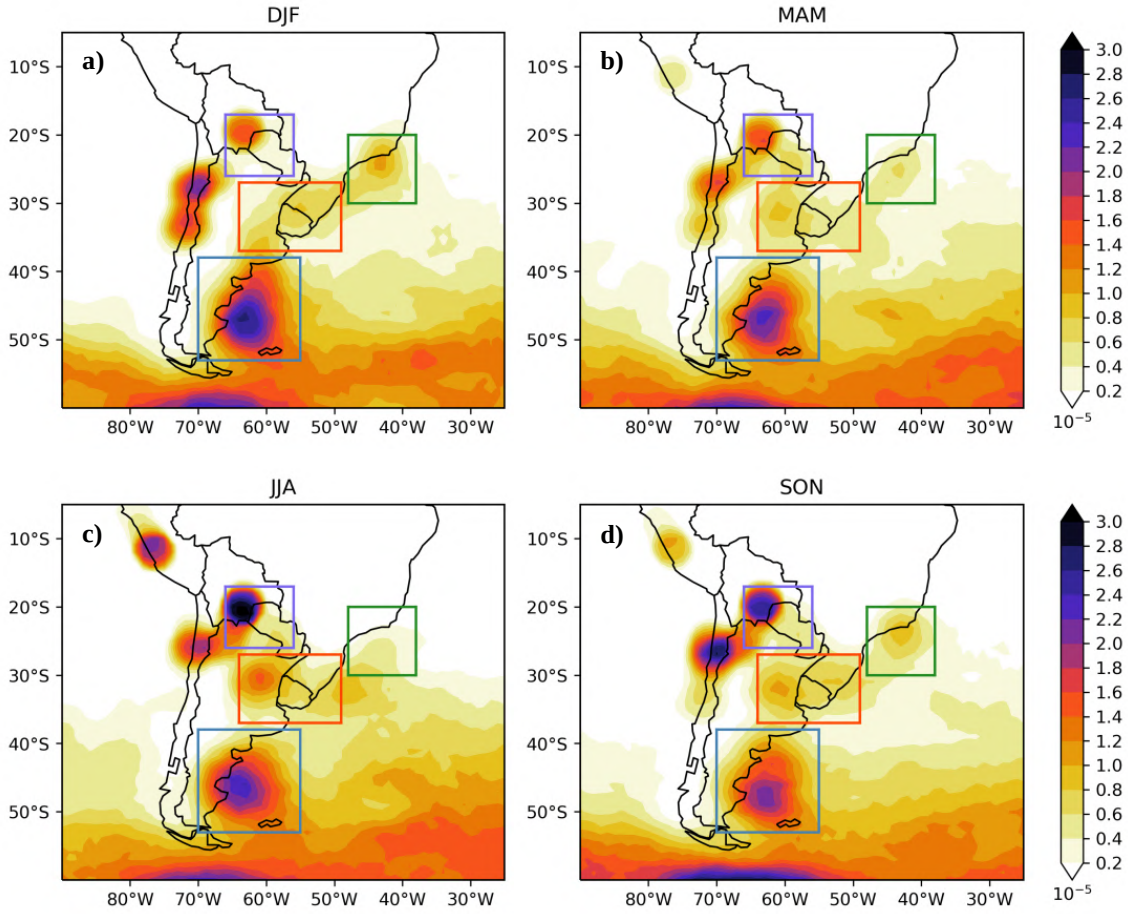

Figure 4.2 Seasonal cyclogenetic density (1979-2017) with boxes indicating the four main cyclogenetic regions: *Argentina* (blue line), *Uruguay* (red line), *SEBrazil* (green line) and *Andes* (purple line). a) DJF – austral summer, b) MAM – austral autumn, c) JJA – austral winter, and d) SON – austral spring. The unit is cyclogenesis per area (km^2) per season with the values multiplied by 10^5.

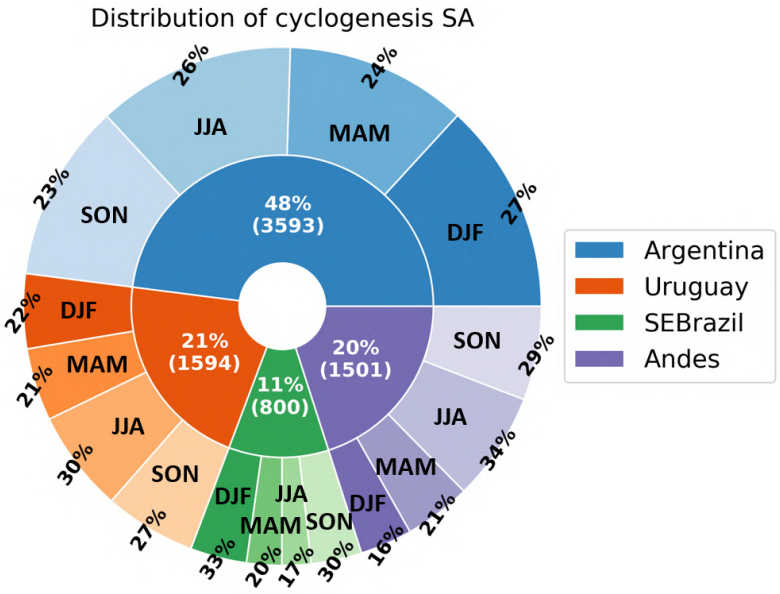

Figure 4.3 Seasonal absolute and relative frequencies (%) of cyclogenesis in the four regions. The inner pie represents the total number of cyclogenesis for the period 1979-2017 and the outer pie represents the seasonal distribution.

The annual density of cyclone trajectories from each region is shown in Figure 4.4. A common aspect, as expected, is the southeastward movement of cyclones starting from each genesis region. Cyclones from *Argentina* (Figure 4.4a) and *Uruguay* (Figure 4.4b) can achieve longer distances compared to *SEBrazil* (Figure 4.4c) and *Andes* (Figure 4.4d). *Argentina* and *Uruguay* present a second most dense spot close to Antarctica (near 60°S belt), respectively, in approximately 25°E and 40°E. Some cyclones from *SEBrazil* and *Andes* are also able to move towards these regions but less frequently. *Andes* presents a second very dense trajectory region located downstream of the genesis region, meaning that a higher percentage of cyclones have cyclolysis not far from their genesis region. Aspects as traveled distance, intensity and lifetime for each region will be discussed in the next section.

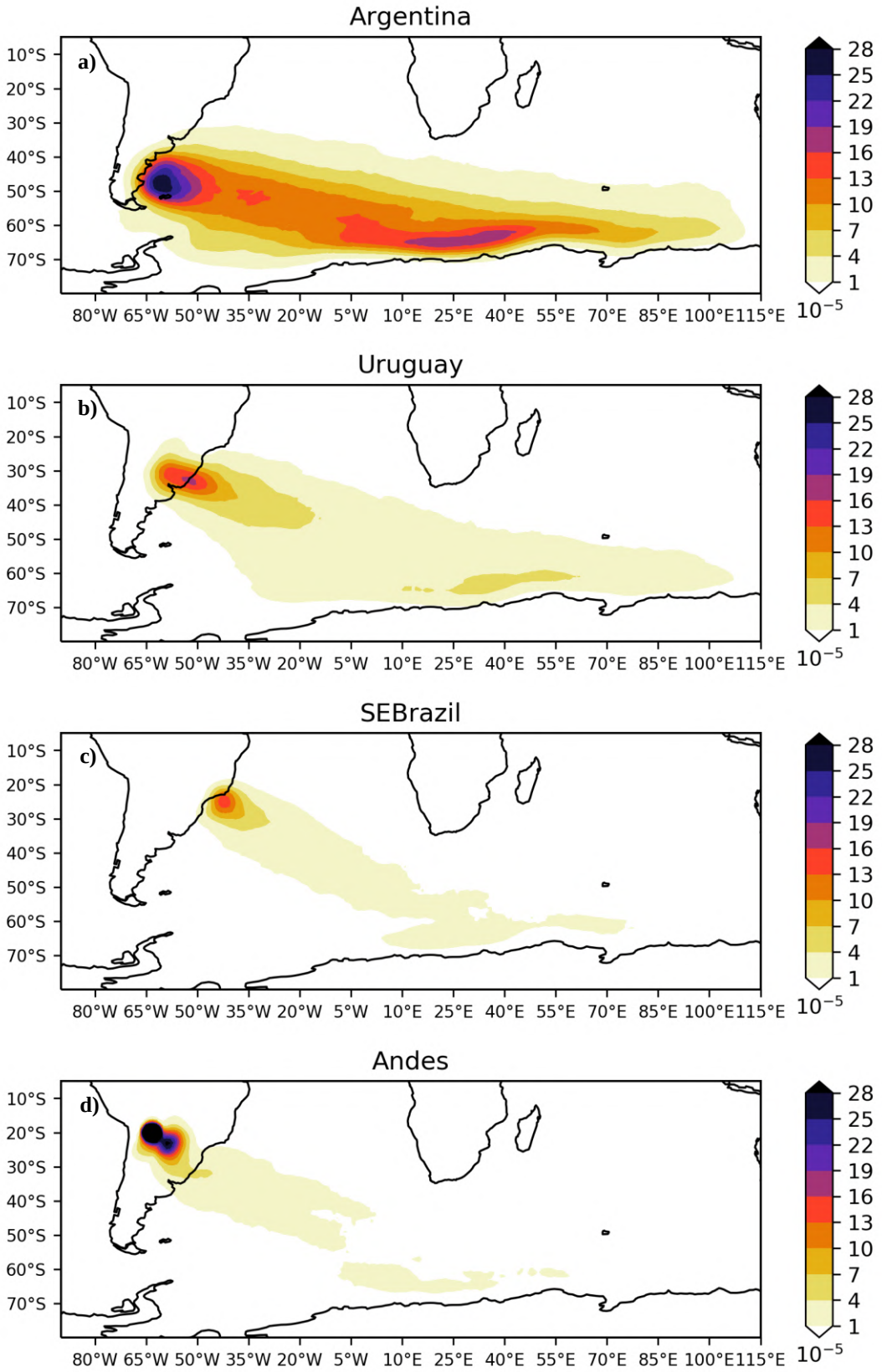

Figure 4.4 Annual mean tracking density (1979-2017) for a) *Argentina*, b) *Uruguay*, c) *SEBrazil*, and d) *Andes*. The unit is cyclone per area (km^2) per year with the values multiplied by 10^5.

4.2 Traveled distance, lifetime and intensity

This section presents results of the mean features of cyclones forming in each cyclogenetic region (*Argentina*, *Uruguay*, *SEBrazil* and *Andes*) and season (austral summer, autumn, winter and spring). The analyzed variables correspond to frequency distribution of: a) the total traveled distance, calculated as the sum of all distances between cyclone positions every 6 hours; b) the distance between the first and last positions of the cyclone (initial-final), i.e., cyclogenesis – cyclolysis locations; c) lifetime; d) minimum relative vorticity (maximum intensity) at 925 hPa, which is the smallest cyclonic vorticity value considering all of the cyclone's lifecycle.

In *Argentina* there are two distinct peaks of frequency for both distances (Figures 4.5a,b); the first peak (~ 2000 km) is similar for the two types of distances, indicating that cyclones traveling smaller distances have quite linear trajectory. However, the second peak of frequency (~12000 km for total traveled distance and ~ 7500 km for initial-final distance) is not similar for the two types of distances, which means that cyclones traveling larger distances present some stationary periods along their trajectories or they can assume irregular trajectories as they move to different directions throughout their lifecycle, resulting, for example, that the genesis is closer to lysis (Figures 4.5a,b). For both distances, the first peak indicates more cases in winter and less in autumn while the opposite occurs for the second peak. In summer, cyclones developing in *Argentina* travel more often intermediary distances, i.e., from 6000 to 10000 km (Figures 4.5a,b). There is also a third peak to lower distances observed only in summer (Figure 4.5a,b), compared to other seasons.

Regarding cyclone lifetime, in *Argentina* the four seasons have similar frequencies of occurrence, with the highest frequency being ~ 10 days, i.e., most of the cyclones are long-lived (Figure 4.5c). During winter, there is a secondary and much weaker peak of frequency for cyclones lasting between 1-2 days, mainly (Figure 4.5c). In all seasons, the vorticity distribution shows a main peak of frequency for intense cyclones (~ $-$ 8 x 10^{-5} s^{-1}) and a secondary peak for weaker cyclones (~ $-$ 3 x 10^{-5} s^{-1}), which is more frequent in summer (Figure 4.5d). Considering extreme events (left side of the distribution in Figure 4.5d), the cyclones during autumn are slightly stronger when compared to the other seasons.

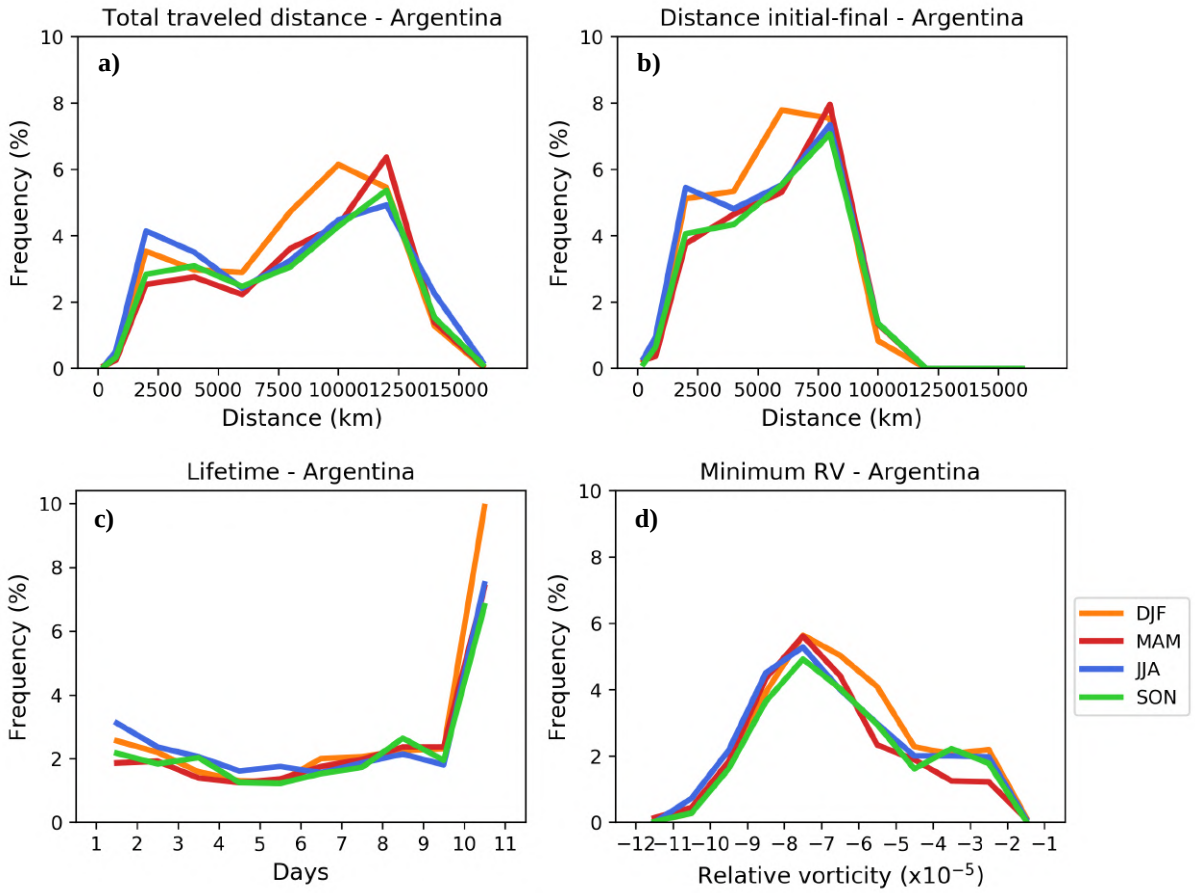

Figure 4.5 Seasonal relative frequency (%) for the period of 1979-2017 of: a) total traveled distance (km), b) distance between initial-final positions (km), c) lifetime (days), and d) cyclonic relative vorticity (x10^{-5} s^{-1}) for cyclones in *Argentina*.

Similarly to *Argentina*, *Uruguay* also has two peaks of total traveled distance: one around 2000 km and the other around 12000 km (Figure 4.6a). Differently from *Argentina*, however, these peaks have similar frequencies, and are comparatively higher in winter, followed by spring (Figures 4.6a). For the distance between cyclogenesis and cyclolysis, the greater frequencies are displaced to higher values of distances compared with *Argentina*, which means that cyclones from *Uruguay* have cyclolysis farther away from their cyclogenesis region, i.e., they have fewer stationary phases during their lifecycle (Figure 4.6b). Similarly to *Argentina*, *Uruguay* (Figure 4.6c) also has two frequency peaks of lifetime duration: one for the short-lived (~ 2 days) and other for the long-lived cyclones (~10 days). The short-lived cyclones occur more often in summer and winter, while the long-lived ones occur more in winter and spring. While in *Argentina* there is one most pronounced peak of minimum RV (Figure 4.5d), *Uruguay* has two peaks, one around – 9 x 10^{-5} s^{-1} and another

around – 4 x 10^{-5} s^{-1} (Figure 4.6d). While in summer these two peaks have similar frequencies, in the other seasons the RV minimum presents a higher frequency for the most intense cyclones (– 9 x 10^{-5} s^{-1}). In summary, similarly to *Argentina*, *Uruguay* also has two distinct types of cyclones (especially in summer). Comparatively, cyclones developing in *Uruguay* reach stronger intensities during their lifetime compared to those developing in *Argentina* (mostly in winter and spring).

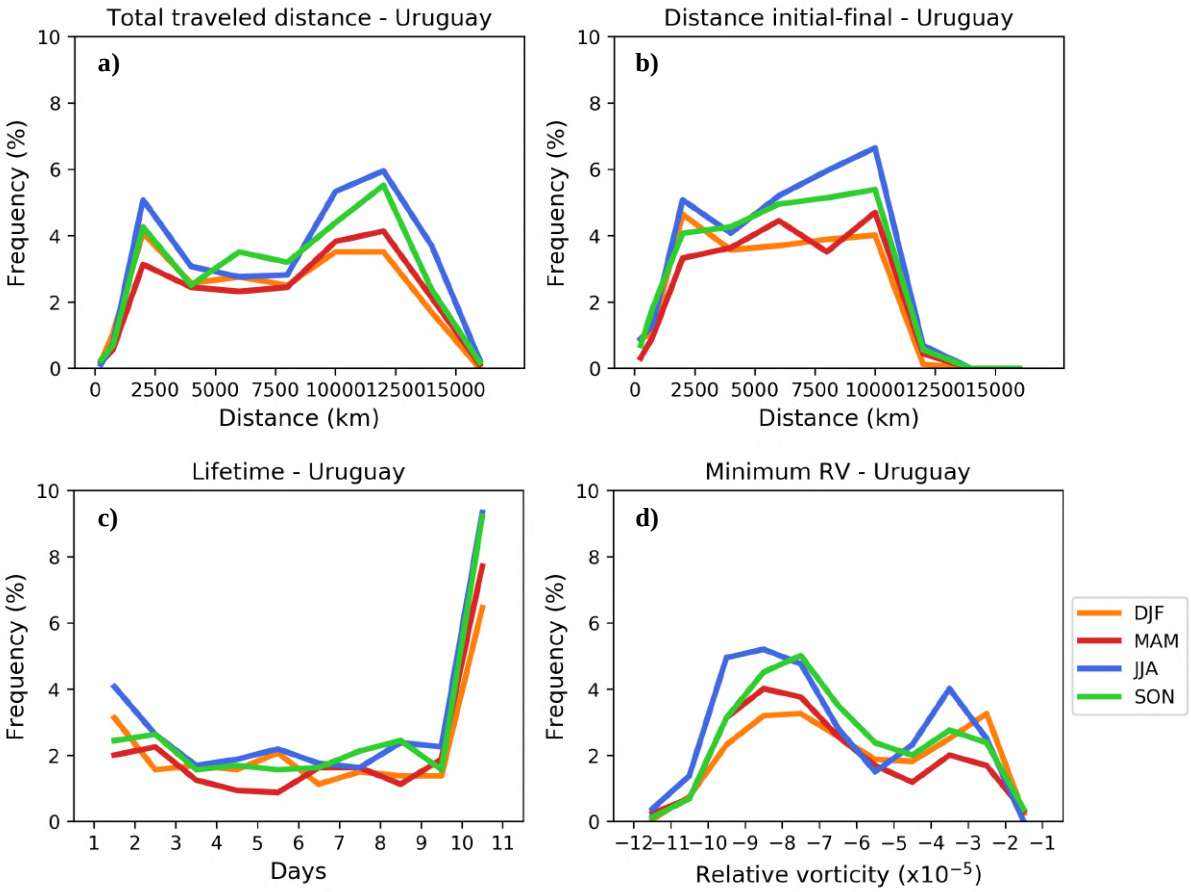

Figure 4.6 Seasonal relative frequency (%) for the period of 1979-2017 of: a) total traveled distance (km), b) distance between initial-final positions (km), c) lifetime (days), and d) cyclonic relative vorticity (x10^{-5} s^{-1}) for cyclones in *Uruguay*.

Differently from *Argentina* and *Uruguay*, cyclones from *SEBrazil* travel shorter distances in general (Figures 4.7a,b). Figure 4.7a shows two frequency peaks of total traveled distance, a strongest one around 2000 km and a secondary peak around 12000 km. There are also two peaks for the cyclogenesis-cyclolysis distance (Figure 4.7b), with the first peak coinciding with the first peak of Figure 4.7a and the second one around 10000 km. Again,

there are two types of cyclones, stationary and moving/mobile cyclones, with the former more frequent in summer (2000 km) and the latter in spring (10000 km) (Figures 4.7a.b). Regarding cyclones lifetime (Figure 4.7c), there are two well-distinct peaks for all seasons, as in other regions, one peak in about 1-2 days and the other in 10 days. In spring, however, there are three peaks, with the third around 7 days. Regarding the intensity, as for the other regions there are two peaks, but in *SEBrazil* the dominating frequencies are for weaker cyclones (between - 2 and - 3 x 10^{-5} s^{-1}) in most part of the year, except in winter when it presents similar frequencies for both weaker (between – 2 and – 3 x 10^{-5} s^{-1}) and more intense (– 8 and -9 x $10^{-5}s^{-1}$) cyclones (Figure 4.7d).

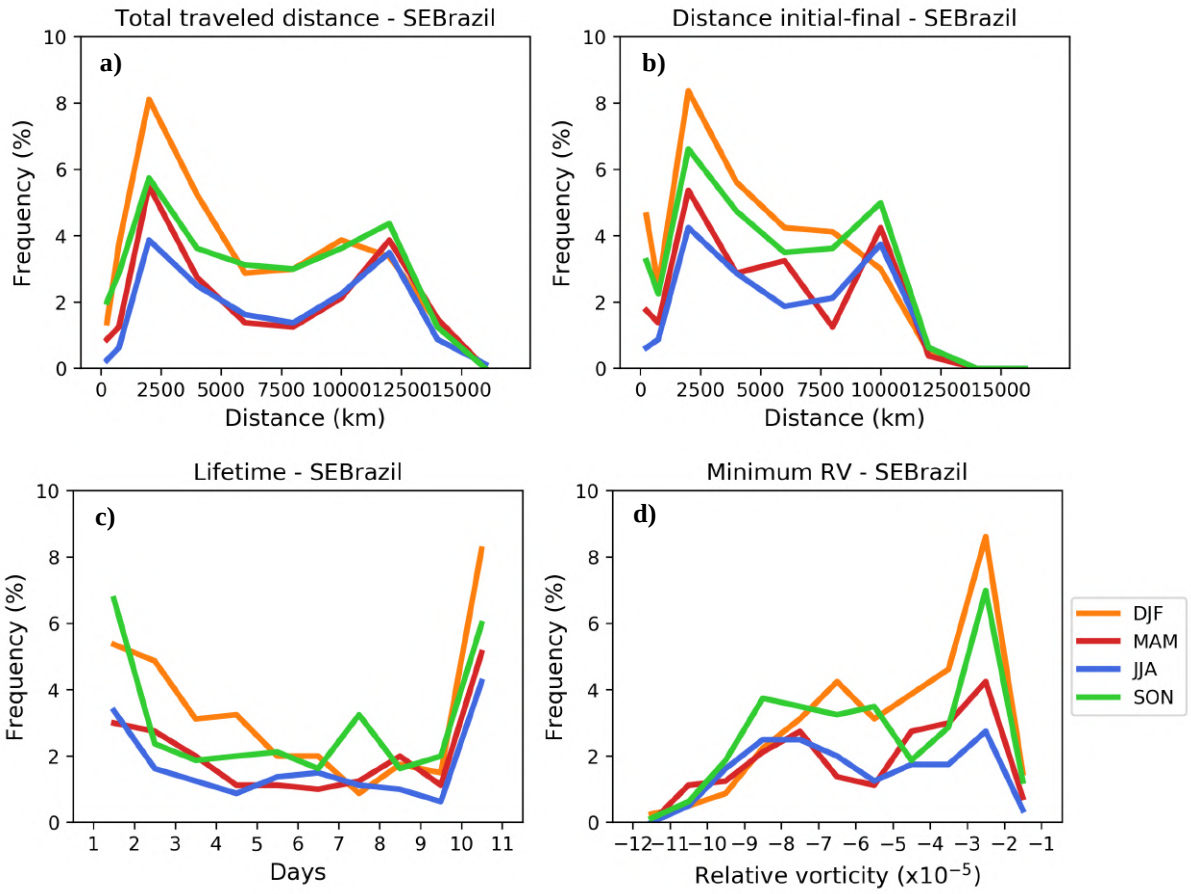

Figure 4.7 Seasonal relative frequency (%) for the period of 1979-2017 of: a) total traveled distance (km), b) distance between initial-final positions (km), c) lifetime (days), and d) cyclonic relative vorticity (x10^{-5} s^{-1}) for cyclones in *SEBrazil*.

The *Andes* region is located over the continent in subtropical latitudes (20-30ºS). It contains approximately the same number of cyclones as the *Uruguay* region and it is more

active during winter and spring. There is one pronounced frequency peak for cyclones traveling shorter distances (Figure 4.8a) with the other traveled distance classes presenting frequencies below 3%. An interesting feature is the frequency peak related to summer, where both total traveled and distance between initial-final locations (Figures 4.8a,b) are very close, meaning that during summer cyclogenesis and cyclolysis occur basically in the same place. This also occurs in other seasons; however, they present frequencies above zero in other distance classes, indicating that in these seasons cyclones can travel longer distances than in summer (where the frequency in other classes are close to zero). In general, cyclones in winter and spring travel longer distances (peak around 10000 km).

Differently from *Argentina* and *Uruguay*, most cyclones in *Andes* last about 1-2 days. In summer, most cyclones present only a few timesteps after the minimum lifetime threshold (24h) imposed by the tracking algorithm, while for the other seasons two frequency peaks occur: one of 1-2 days and another of 10 days. The stationary short-lived (1-2 days) cyclones (Figures 4.8a,b) correspond to thermal lows which develop in the lee side of the Andes Mountain, especially in summer (Salio et al., 2002; Salio et al., 2004). Cyclones in summer have weaker intensities (RV between -3 and -2 x 10^{-5} s^{-1}), but other seasons also present a small frequency peak around - 8 x 10^{-5} s^{-1}.

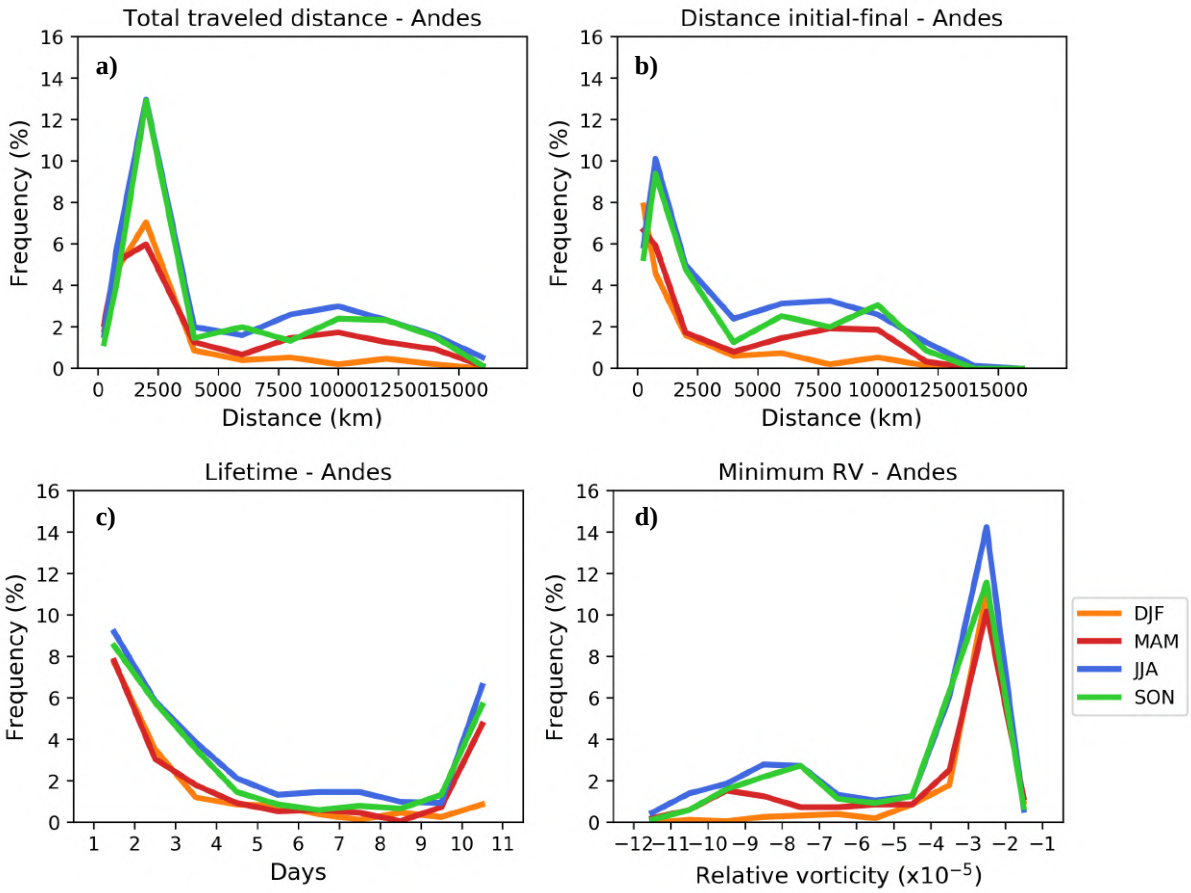

Figure 4.8 Seasonal relative frequency (%) for the period of 1979-2017 of: a) total traveled distance (km), b) distance between initial-final positions (km), c) lifetime (days), and d) cyclonic relative vorticity (x10^{-5} s^{-1}) for cyclones in *Andes*.

A common feature in *Argentina*, *Uruguay* and *SEBrazil* is the bi-modal frequency distribution in traveled distances and intensity (Figures 4.5, 4.6 and 4.7), where *Argentina* and *Uruguay* have stronger cyclones in the highest peak (Figures 4.5d and 4.6d), while the opposite is observed in *SEBrazil* (Figure 4.7d). In general, cyclones from *Argentina*, *Uruguay* and *SEBrazil* live longer and travel longer distances compared to *Andes*. Cyclones in *Argentina* and *Uruguay* are the most intense and in *Andes* they are less intense. In summary, cyclones from *Argentina* and *Uruguay* are the most intense, fast and long-lived, which in theory makes them travel longer distances; these are also formed and developed close to the coast. On the other hand, cyclones from *Andes* are more stationary and less intense while in *SEBrazil* they have intermediary characteristics.

4.3 Time lags

In order to explore a possible relation between cyclones in each cyclogenetic region, a first approach relating the time lag between cyclogenesis in each region is presented. Table 1 shows the absolute number of days from the whole series of cyclogenesis from each region occurring related to the other respective region. There is a larger number of cyclogenesis occurring in *Argentina* one day before cyclogenesis in *Uruguay* and *Andes*, while it occurs mostly two days after cyclogenesis in *SEBrazil*. In *Uruguay*, cyclogenesis occurs most likely one day after cyclogenesis in *Andes*, however, it occurs mostly two days prior than in *SEBrazil*. Cyclogenesis in *Andes* is most likely to occur two days before than in *SEBrazil*.

Table 1 Absolute number of days in which cyclogenesis occurs in each region (start at) related to other regions for different time lags (from -2 until +2 day). Red numbers highlight the greater values.

	-2 days	*-1 day*	*Same day*	*+1 day*	*+2 days*
Argentina (starts at), Andes	402	473	409	309	373
Argentina (starts at), Uruguay	436	487	318	301	413
Argentina (starts at), SEBrazil	181	162	194	211	225
Uruguay (starts at), Andes	161	134	282	302	169
Uruguay (starts at), SEBrazil	113	85	43	36	41
Andes (starts at), SEBrazil	101	89	41	43	65

These aspects are in accordance with the latitude position of each region. For instance, *Argentina*, the most southern region, is influenced by baroclinic waves during the whole year. Hence, cyclones are able to influence cyclogenesis as/or secondary cyclogenesis, or organizing favorable conditions in the northern regions as they travel northeastward during their development. Table 1 indicates that cyclogenesis in *Uruguay* occurs mostly at the same day or one day after cyclogenesis in *Andes* (this will be also shown in section 5 in the mean atmospheric fields). The opposite occurs in *SEBrazil*, where, in general, cyclogenesis occurs later than in *Uruguay* and *Andes*.

Figure 4.9 shows in details the seasonal relationship between cyclogenesis in time spans of 6 hours. Figure 4.9a presents the frequency of time genesis as a function of cyclogenesis in *Argentina*, and spring is the season with less frequencies of genesis in comparison with the other three regions. *Andes* present a higher peak in summer prior to genesis in *Argentina* (Figures 4.9a,d), which is also noticed in *Uruguay* but for all seasons

(Figure 4.9b). This is possibly related with the moisture transport by the low-level jet during this season, supporting the development of cyclones to the south. As Salio et al. (2002) pointed out, during an event of Chaco Jet, the flux of moisture and its convergence at low and mid-levels is about 10 times greater than the summer mean. *SEBrazil* has least relation with other cyclogenetic regions, but when it occurs it is during summer (Figure 4.9c).

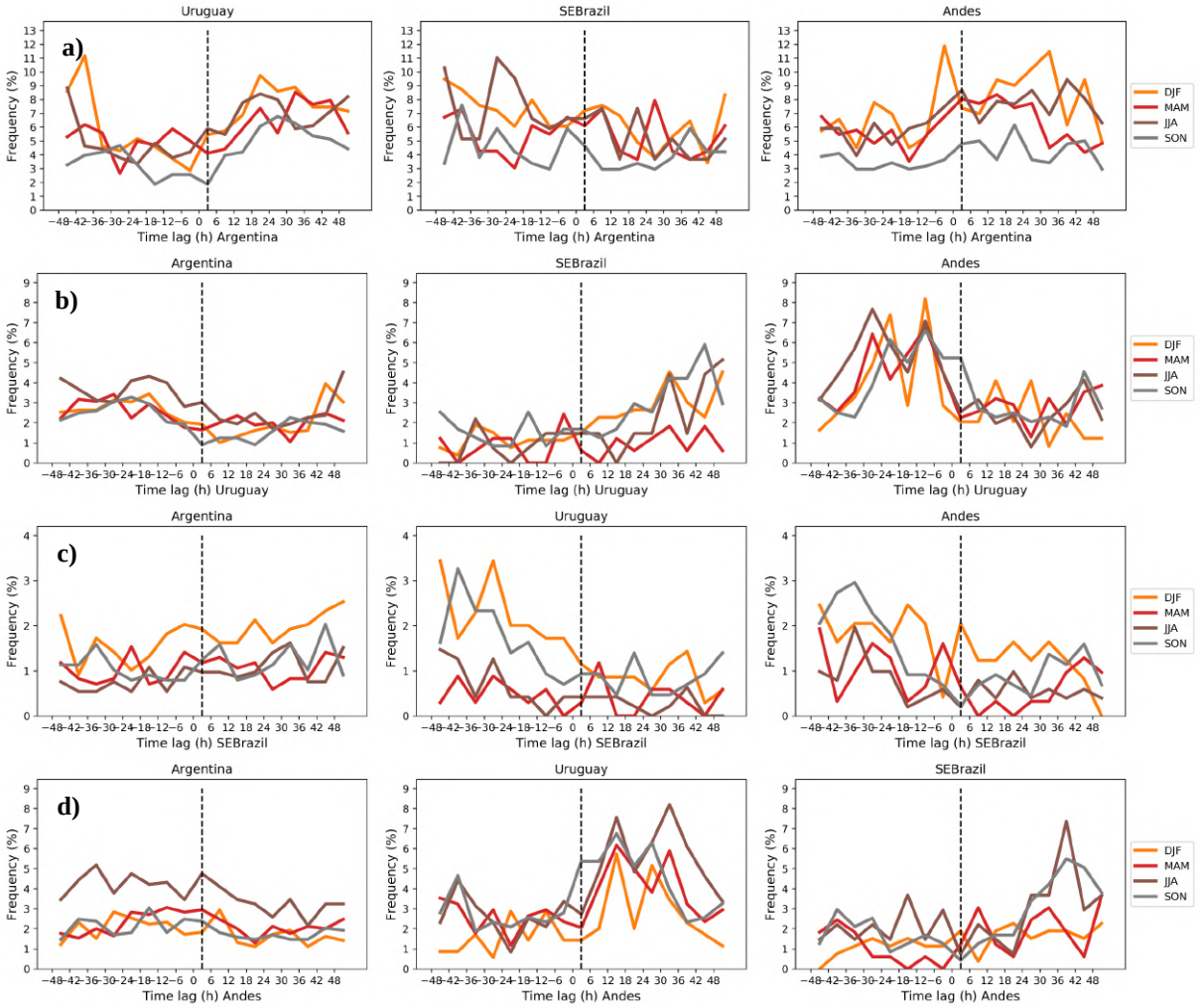

Figure 4.9 Seasonal relative frequency (%) (1979-2017) of the time lag (hours) between cyclogenesis in respect to other regions; a) *Argentina*, b) *Uruguay*, c) *SEBrazil*, and d) *Andes*.

Chapter 5

5 Results 2 – Atmospheric patterns

Here we present characteristics of the environment during cyclones genesis and development in the following order: i) climatological aspects of the tropopause and means of the meteorological variables/parameters in summer vs. winter, irrespective of whether cyclogenesis occurs or not; ii) a quantitative analysis of occurrence of stratospheric PV streamers and cutoffs in different isentropic levels near the four cyclogenetic regions; and, then, a final discussion of the spatial pattern of these PV structures and their association with dynamical forcing for iii) cyclogenesis and iv) the cyclone lifecycle.

5.1 Climatological aspects over SA and its surroundings

To further discuss the atmospheric patterns related to cyclogenesis on each region, this section presents a general overview of specific variables over SA and adjacent oceans. Figure 5.1 shows the seasonal mean pressure level of the tropopause (- 2 PVU) (Figures 5.1a-d) and the seasonal mean frequency of the tropopause (- 2 PVU contour) as a function of different isentropic levels (Figures 5.1e-h), i.e., the dynamical tropopause over South America and adjacent oceans. The isentropic levels shown are 320 K, 340 K and 360 K since they are more frequently associated with upper-level PV structures over the cyclogenetic regions.

The tropopause spatial pattern exhibits a great change throughout the year (Figure 5.1), i.e., it changes from a very undulated pattern in summer (Figures 5.1a,e) to a very zonal organized pattern in winter (Figures 5.1c,g). This undulation is strongly associated with the continental diabatic heat source (Hoerling, 1992) and the vorticity conservation in summer. There is a clear northward (or equatorward) displacement of the tropopause to upper isentropic levels from winter to summer (Figures 5.1e-h). By analyzing the pressure and isentropic mean fields, we can see the equivalence of the tropopause in both surfaces regarding the latitude and its dependence on the season. For instance, over the South Atlantic, northward of 30°S, the tropopause in 360 K is frequently equivalent to the 150 hPa level in summer (DJF) (Figures 5.1a,e). However, for tropopause locations between 30°S and 40°S

there is a transition between 360 K and 340 K isentropic levels and also a strong gradient in pressure levels, from 225 to 150 hPa (Figures 5.1a,e). On the other hand, southward of 45°S the tropopause is predominantly located at 320 K, equivalent to pressure levels of up to 225 hPa. This climatology is in agreement with the seasonal tropopause features in the Northern Hemisphere, as discussed in Wernli and Sprenger (2007), where during winter the tropopause level fluctuates between 305-335 K levels at mid-latitudes (30-60°N), while in summer it fluctuates between 325-350 K levels.

In autumn (MAM) (Figures 5.1b,f) the mean tropopause has a more zonal pattern, which accentuates in winter (JJA) when the isentropes and pressure levels are almost parallel to latitudinal lines (Figures 5.1c,g). In winter, the tropopause located southward of 45°S is at a maximum pressure level of 300 hPa. In spring (SON) (Figures 5.1d,h) the tropopause starts to undulate again. In general, the transition seasons (autumn and spring) have the most similar mean tropopauses (Figures 5.1b,d,f,h).

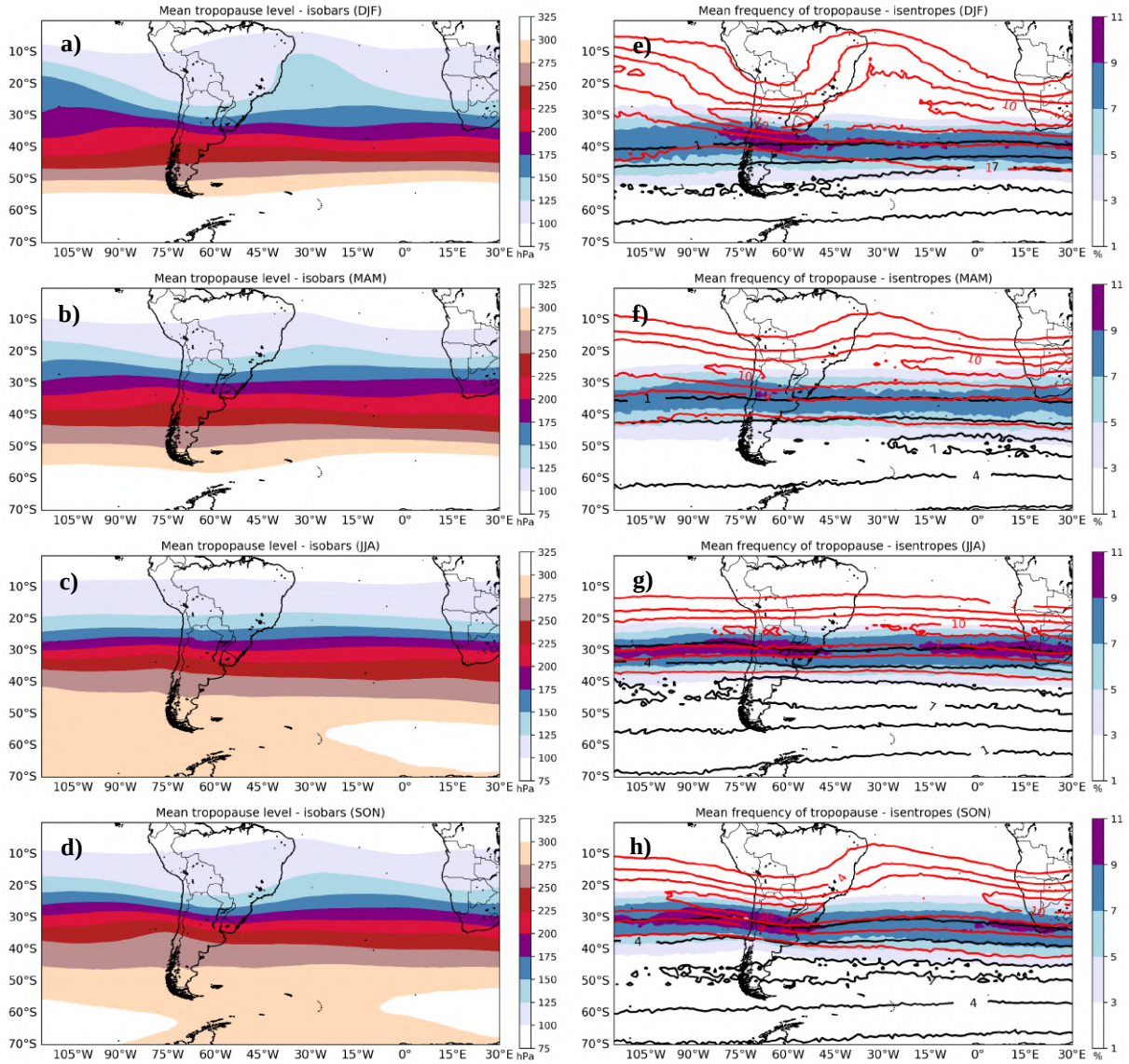

Figure 5.1 Seasonal mean (1979-2017) of: a-d) pressure level (hPa) of the tropopause (- 2 PVU) and e-h) frequency (%, intervals of 3) of the tropopause as a function of different isentropic surfaces: 320 K (black lines), 340 K (shaded), and 360 K (red lines).

Since autumn and spring are very similar in terms of tropopause levels (Figure 5.1), we will focus our next discussions in summer and winter. The mean fields in Figures 5.2a,b present the seasonal climatology (austral summer and winter) of the jet stream at 300 hPa and the upper-level PV at 320 K, 340 K and 360 K. The upper-level jet is further north in winter (Figure 5.2b) compared to summer (Figure 5.2a), with a mean jet streak maximum over the South Atlantic closer to SA in winter (Figure 5.2b). The PV distribution follows the latitudinal location of the dynamical tropopause over SA to be determined for the different seasons. In fact, during winter (Figure 5.2b) the PV distribution at 360 K, 340 K and 320 K is

rather zonal (as seen in Figures 5.1c,g) over the continent and the dynamical tropopause (-2 PVU isoline) is found at, respectively, about 23°S, 27°S and 40°S. However, over the ocean and in summer (Figure 5.2a) the dynamical tropopause at 360 K is located at lower latitudes (15°S), which follows from the SA monsoon configuration (Zhou and Lau, 1998) with two upper level troughs, one over the Pacific Ocean and the other close to northeastern Brazil. The undulation of the dynamical tropopause during summer is also discernible over the continent, where it is shifted southward reaching about 30°S. This north-south migration of the dynamical tropopause, and its undulation over the South Pacific and South Atlantic, is only apparent here at 360 K, but not at 350 K in the climatology of the dynamical tropopause by Ndarana and Waugh (2010). This seasonal cycle of the dynamical tropopause in Figures 5.2a,b influences the level on which PV streamers and cutoffs will be found in different seasons.

The seasonal mean EGR is shown in Figures 5.2c,d. The EGR gives a measure of the environmental baroclinicity and the importance of baroclinic instability, taking into account the vertical wind shear, static stability and the Coriolis parameter. The growth rate depends on the horizontal and meridional wavelength and the Rossby radius deformation. Generally, it increases towards the poles and over the continent, reaching values above 0.7 day^{-1} in *Argentina* and *Uruguay* regions (Figures 5.2c,d). The EGR in winter reaches a maximum value of ~ 1.0 day^{-1} near the Andes in the central part of Chile and Argentina (Figure 5.2d). These values are higher than the ones in the winter and summer climatologies by Lim and Simmonds (2007) and Yanase et al. (2014), respectively. However, this might be because these authors used the ERA-40 dataset (Uppala et al., 2005) and the Japanese 25-year Reanalysis (JRA-25; Onogi et al., 2007) and a single 850-hPa level for the EGR computation while in this study it is used ERA-Interim and a layer-averaged EGR. The EGR is constantly important for cyclogenesis in all cyclogenetic regions, especially in *Argentina* throughout the year and in *Uruguay* during winter and spring (Figures 5.2c,d, and Appendix A).

Finally, it is worthwhile to consider the near surface circulation pattern which predominates in SA climatology. To this aim, SLP fields and winds and specific humidity at 850 hPa are shown in Figures 5.2c-f. Over the year, the main circulation systems are the two subtropical anticyclones, one over the South Pacific and another over the South Atlantic. The anticyclone over the South Atlantic reaches the eastern part of SA, where it prevents convection in winter (Figures 5.2d,f) (Reboita et al., 2010, 2019). In summer, however, the

subtropical anticyclone is located far from the coast (Figures 5.2c,e), contributing to organize the moisture transport from the South Atlantic to subtropical latitudes over the continent, hence, favoring precipitation (Sun et al., 2017; Reboita et al., 2019). During summer (Figure 5.2c), a semi-permanent thermal low-pressure system occurs in the lee of the Andes (around 20°S), coinciding with the location of the aforementioned cyclogenetic region lee of the Andes. A semi-permanent low-level trough with weak amplitude is also a climatological feature along the coast of Argentina (centered in approximately 45^{o}S-65^{o}W) during summer (Figure 5.2c), whereas in winter (Figure 5.2d) it is displaced further to the north and hence acquires a more zonal characteristic.

The 850 hPa winds are stronger (weaker) over the South Pacific and southern SA in summer (winter), whereas over the South Atlantic and east coast of SA they are weaker (stronger) (Figures 5.2e,f). This is associated with east to west seasonal migration of the subtropical South Atlantic anticyclone (Figures 5.2c,d). Over the continent, the northerly winds eastward the Andes characterize the low-level jet (Sugahara et al., 1994; Marengo et al., 2004), which is stronger (weaker) during winter (summer). This jet exerts an important control of rainfall in the subtropics of SA since it is important to transport moisture from lower latitudes to the subtropics affecting the cyclogenetic regions identified in Figure 4.2. In summer the specific humidity is higher than in winter, which is associated to the establishment of the rainy season over tropics-subtropics SA during summer (Figures 5.2e,f).

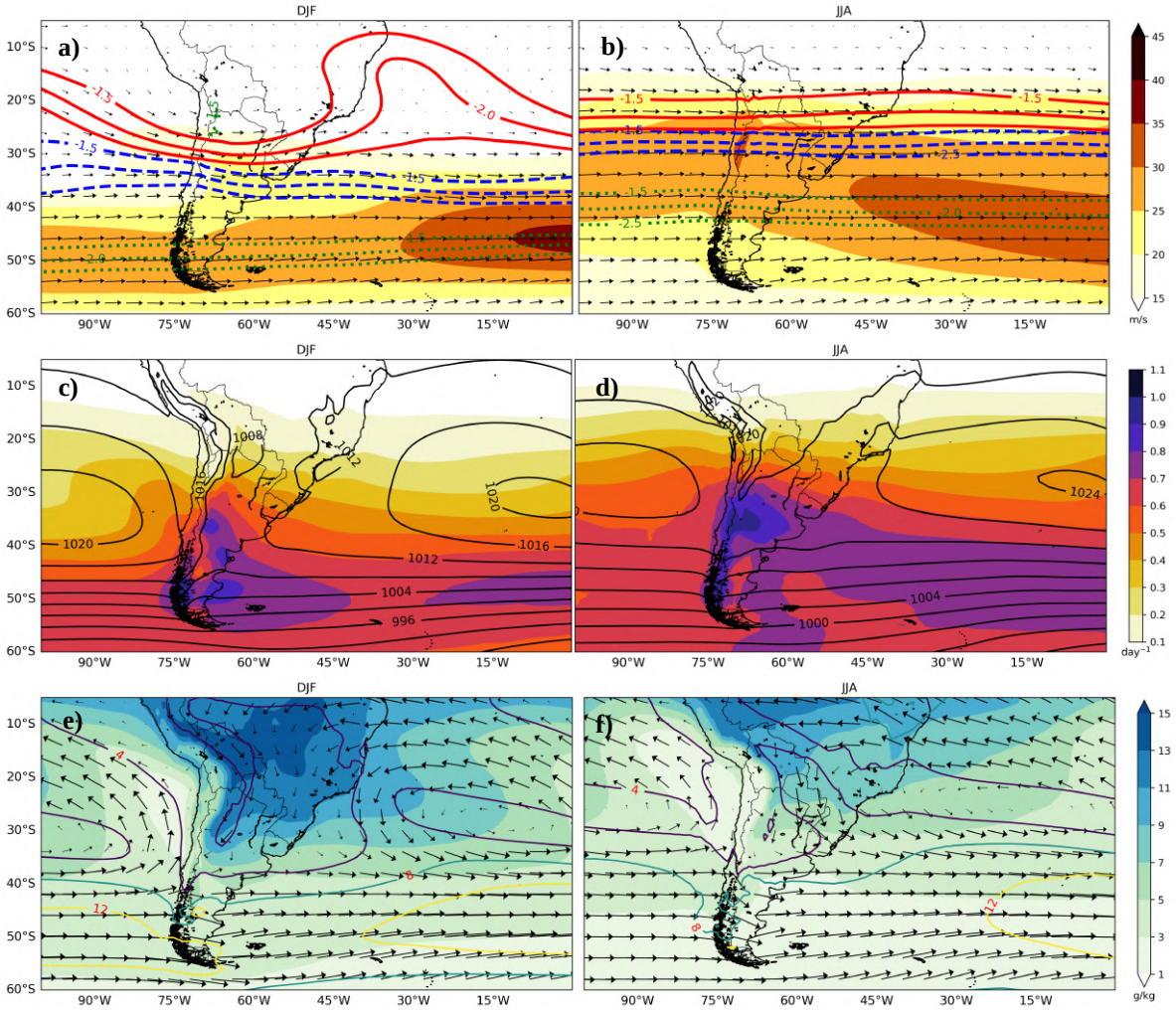

Figure 5.2 Seasonal climatology (1979-2017) of a,b) horizontal wind vectors and magnitude (m s^{-1}, shaded) at 300 hPa, PV (PVU) at 320 K (dotted green lines), 340 K (dashed blue lines) and 360 K (solid red lines) in austral a) summer and b) winter; c,d) EGR (day^{-1}, shaded) and SLP (hPa, solid lines, interval of 4 hPa) in austral c) summer and d) winter; and e,f) wind vectors and magnitude (m s^{-1}, lines) and specific humidity (g kg^{-1}, shaded) at 850 hPa in austral e) summer and f) winter.

As a final analysis, Figure 5.3 presents the seasonal climatology of PV streamers and PV cutoffs over SA in three different isentropic levels. This analysis will also be important to discuss the anomalies regarding each cyclogenetic region. From Figure 5.3 we can infer the approximate location of PV streamers by the -2 PVU contour.

In SA, isentropic surfaces are intersected by the high elevations of the Andes, which results in the stationary pattern of high frequency of PV cutoffs at 320K from 15ºS to 30°S over the Andes (Figures 5.3a,b). Hence, it is important to carefully select the adequate isentropic level for the analysis of PV streamers, and especially PV cutoffs in each of the cyclogenetic region, since the elevated topography leads to spurious signals. In general, PV

streamers and cutoffs occur more often in summer than in winter (Figure 5.3). There is a clear shift towards the equator of both PV features as moving to higher isentropic levels, however, the more equatorward this shift is, the lesser is the frequency during winter.

Argentina and *Uruguay* present signals of PV cutoffs especially in summer at 320 K and 340 K (Figures 5.3a,c), and *SEBrazil* at 360 K. In winter, *Uruguay* is the region most affected by PV cutoffs at 320 K (Figure 5.3b), followed by *SEBrazil* and *Andes* at 360 K (Figures 5.3f). During summer at 340 K (Figure 5.3c) there is already a signal of the northeast Brazilian trough over the South Atlantic, more evident at 360 K (10°S) (Figure 5.3e), which is related to the northeast trough downstream the Bolivia high, that is part of the South America monsoon system (Zhou and Lau, 1998). This is in agreement with the climatology of COLs (obtained from geopotential height) for the Southern Hemisphere performed by Reboita et al. (2010), where the COLs in the eastern part of northeast of Brazil were found only at higher levels, i.e., 200 hPa and 300 hPa levels.

PV streamers at 320K are very frequent southward of 55°S in summer (Figure 5.3a) and between 40°S-50°S in winter (Figure 5.3b). In both seasons they affect mainly the *Argentina* cyclogenetic region. At the intermediate level of 340K the most frequent region with PV streamers has a shift from 40°S in summer to 30°S in winter, most likely influencing cyclogenesis in *Uruguay* (Figures 5.3c,d). Finally, PV streamers at 360K occur near 20°S over the South Pacific and from 30°S to 10°S over the South Atlantic during summer (Figure 5.3e), which is also related to the monsoon season. *SEBrazil* cyclogenetic region is most likely to be affected by this 360K level in summer-winter and by 340K in winter (Figures 5.3c-e). However, this is the level with less frequent PV streamers in winter (Figure 5.3f).

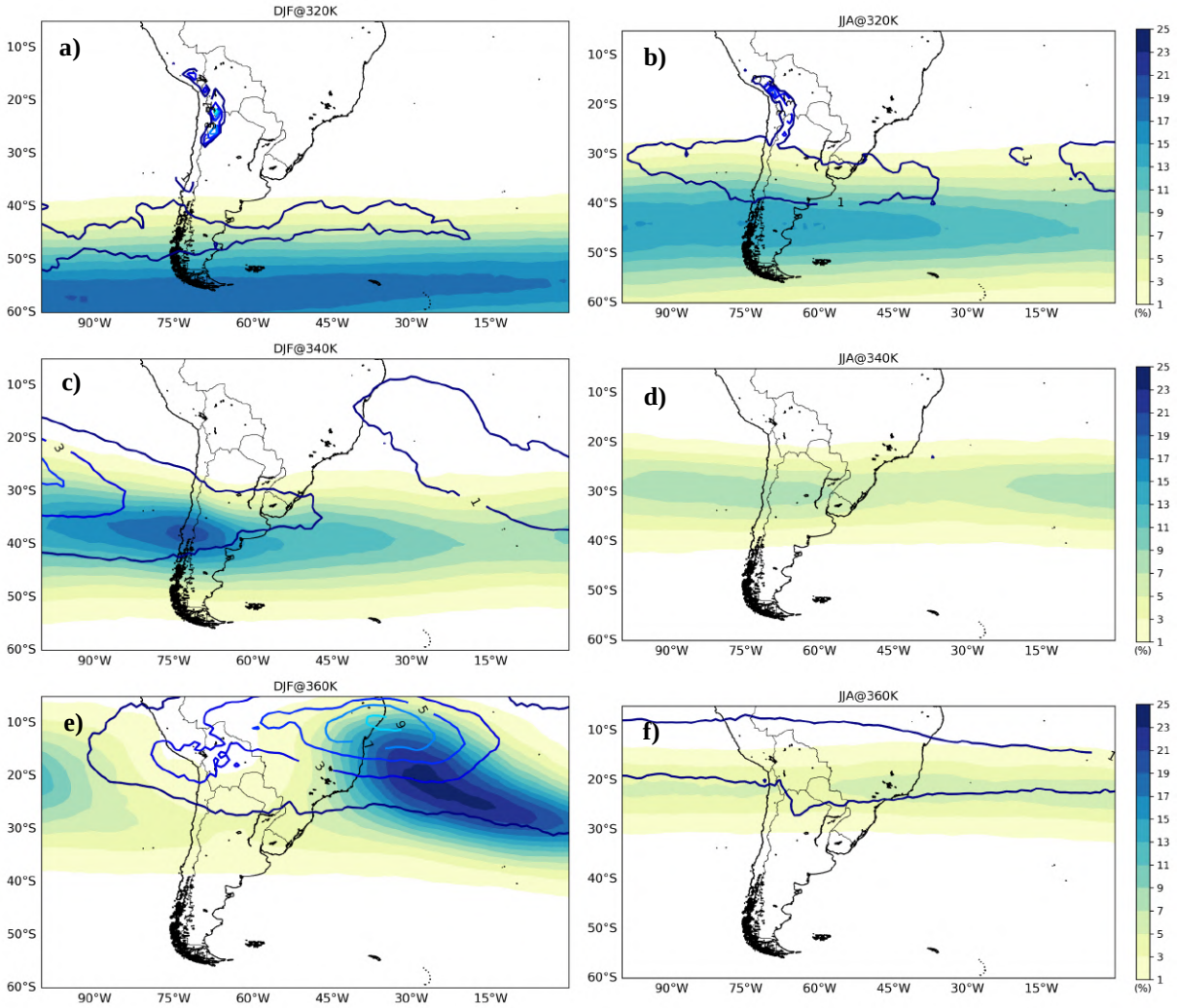

Figure 5.3 Seasonal climatology (1979-2017) of the mean frequency (%) of PV streamers (shaded) and PV cutoffs (lines) for austral summer and winter, respectively, for the isentropic levels: a,b) 320 K, c,d) 340 K and e,f) 360 K isentropic levels.

Table 2 summarizes the main information of the climatological variables previously discussed in relation to each cyclogenetic region.

Table 2 Summary of the climatological position and strength of the, jet stream, EGR, PV streamer and PV cutoff for the regions *Argentina*, *Uruguay*, *SEBrazil*, and *Andes*.

	Argentina	*Uruguay*	*SEBrazil*	*Andes*
Tropopause	320 K above and south (north) of cyclogenesis in summer (winter)	340 K above in summer; 340K to the north and 320 K close/to the south in winter	360 K above in summer; 340 K and 360 K above in winter	360 K to the south (above) the region in summer (winter)
Jet Stream	Stronger and above the region in summer; displaced northward in winter	Stronger in winter; close to the jet streak entrance	Further south in summer; closer to the jet streak in winter	Further south in summer; southward in winter
EGR	Larger maxima close to the coast in summer	Stronger in winter	Slightly stronger in winter	Slightly stronger in winter
PV streamer	320 K in summer and winter	340 K in summer; 320 and 340 K in winter	360 K in summer; 340 K and 360 K in winter	360 K in winter
PV cutoff	320 K in summer	340 K in summer; 320 K in winter	360 K in summer (most frequent) and winter	360 K in summer (most frequent) and winter
Low-level winds	Stronger westerly winds in summer	Stronger northerly winds in winter	Stronger northwesterly winds in winter	Stronger northwesterly winds in summer

5.2 PV streamers and cutoffs during cyclogenesis

The aim of this section is to quantify the occurrence of stratospheric PV streamers and cutoffs near the four cyclogenetic regions for summer and winter. For this, and considering several isentropic levels, Figures 5.4 and 5.5 show the frequency of PV streamers and PV cutoffs, respectively, as a function of the distance between the location of the surface cyclogenesis and the upper-level PV features (PV streamer and cutoff) for *Argentina*, *Uruguay*, *SEBrazil*, and *Andes*. Negative (positive) distances indicate that the PV structures are eastward (westward) of the cyclone center.

PV streamers occurs at all isentropic levels for both seasons and each region. They are located frequently at positive distances, meaning their occurrence to the west of the surface

cyclogenesis. However, there is clearly a shift to higher isentropic levels of PV streamers associated with cyclogenesis for more equatorward cyclogenetic regions. The frequency of PV streamers (Figure 5.4), especially very close to the genesis region, is higher in *Argentina* (Figures 5.4a,e) than in other regions (Figures 5.4b-d, f-h). In *Argentina*, PV streamers are most frequent at 320 K (Figures 5.4a,e) especially in summer, and tend to be vertically co-located with streamers at higher levels in both seasons. In contrast, in the other regions (Figures 5.4b-d, f-h), PV streamers at higher levels occur far from the surface cyclogenesis.

On the other hand, in *Uruguay* PV streamers on 330 and 340 K levels have a greater influence on cyclogenesis in summer (Figures 5.4b). They typically occur about 600 km west of genesis in summer (Figure 5.4b), and about 800 km west of genesis at 320 K in winter (Figure 5.4f). In *SEBrazil* the main peaks occur about 600-1000 km west of genesis at 340 and 360 K levels in summer (Figure 5.4c), i.e., at higher levels than for *Uruguay* and *Argentina*, and 320 and 330 K (Figure 5.4g) in winter. *Andes* is the region with lower frequency of PV streamers near cyclogenesis (Figures 5.4d,h), especially in summer (Figure 5.4d); the main peaks occur far from 1200 km west of genesis at 330 and 340 K in summer (Figure 5.4d) and at 320 and 330 K in winter (Figure 5.4h), comparable to *SEBrazil*.

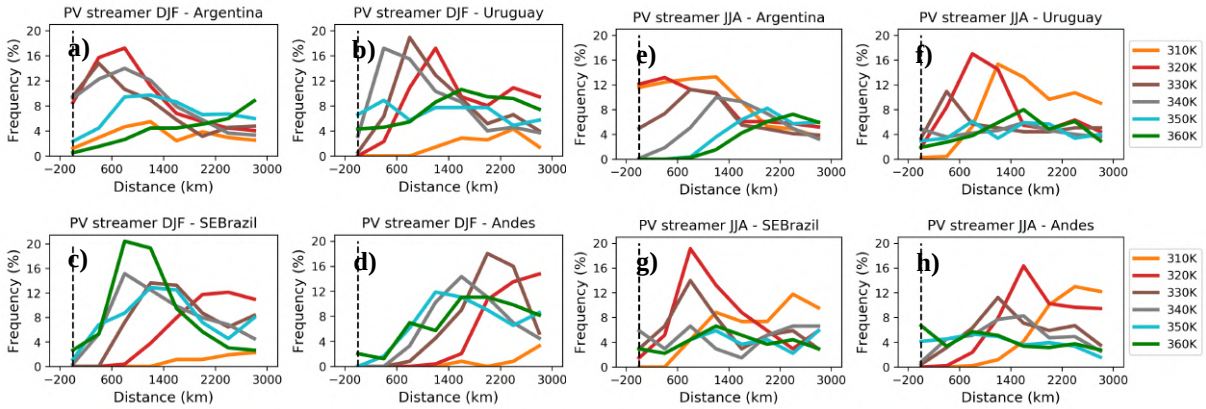

Figure 5.4 Frequency (%) of the distance (km) between the surface cyclogenesis and the nearest PV streamer in summer and winter, respectively, for a,e) *Argentina*, b,f) *Uruguay*, c,g) *SEBrazil*, and d,h) *Andes* detected in six different isentropic levels (lines): 310K (orange), 320K (red), 330K (brown), 340K (grey), 350K (turquoise), and 360K (green). The black dashed line indicates the distance 0 km, i.e., the surface cyclogenesis location. The period is 1979-2017.

PV cutoffs, in general, are less frequent than PV streamers near cyclogenesis, especially in winter (Figures 5.5e-h) for the four regions. They occur most frequently on 310 K for *Argentina* (Figures 5.5a,e) and on 360 K for *SEBrazil* in summer (Figure 5.5c). In

Uruguay (Figures 5.5b,f) the frequencies are similar at 310 K, 320 K, and 330 K in summer (Figure 5.5b) until 800 km to west, while in winter the frequencies for PV cutoffs in all levels are similar in a radius of 200 km and more frequent at 310 and 320 K western of 200 km (Figure 5.5f). Note that the highest peak in *Andes* at 320 K is related to spurious signals due topography, and the most prominent level is 360 K in both seasons (Figures 5.5d,h). In general, the frequency of PV cutoffs is lower than PV streamers in *Argentina* and *Uruguay*, comparable in summer for *SEBrazil*, and comparable in *Andes*.

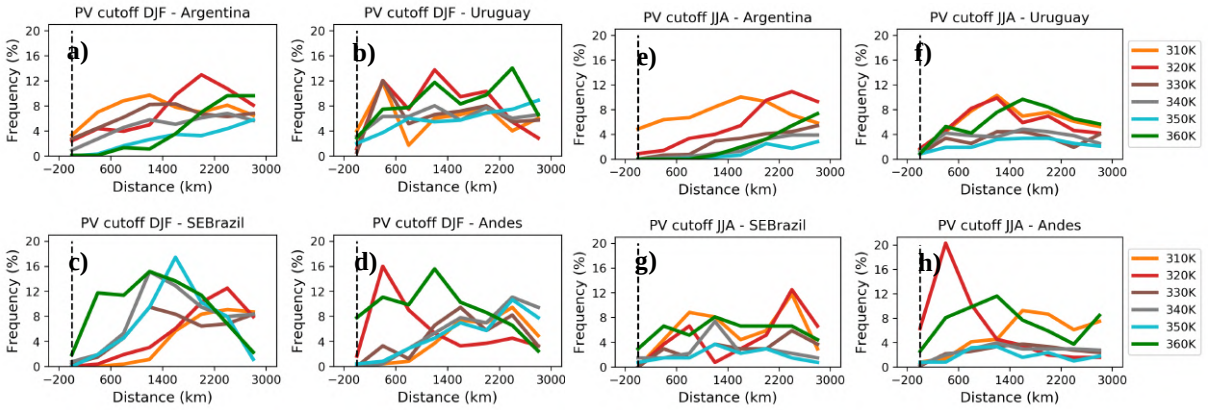

Figure 5.5 As in Figure 5.4, but for PV cutoffs.

5.3 Patterns during cyclogenesis

The previous section discussed the seasonal characteristics of the distance between PV streamers and cutoffs with respect to surface cyclogenesis. In this section, we will analyze the spatial pattern of these PV structures and how they are associated with dynamical forcing during cyclogenesis for *Argentina*, *Uruguay*, *SEBrazil* and *Andes*. The analysis is conduced to austral summer and winter in terms of anomalies, i.e., “mean of events” minus “seasonal climatology”. The isentropic level to access PV structures is defined based on the previous analysis (section 5.2).

5.3.1 *Argentina*

In *Argentina* region, the jet streak at 300 hPa over the continent presents a breaking around 45°S-73°W in summer (Figure 5.6a), whereas in winter it is continuous and wider in

the meridional direction (Figure 5.6b). Besides, QG-omega at 500 hPa fields are similar for both seasons, with stronger center of upward motion located over the South Atlantic (50°S-64°W), close to the continental coast. In both seasons, PV anomalies at 320 K are located southwestward *Argentina*, but in summer they are stronger, and concentrated in a smaller area closer to the genesis region compared to winter (Figures 5.6a,b). While in winter the stronger ascent is located in the polar side of the jet streak exit, during summer it is located in the entrance sector, closer to the PV anomaly core. This suggests greater contribution of PV anomaly inducing intensification of the upward motion and cyclogenesis at surface during summer than in winter.

The main features of the spatial patterns of geopotential height at 500 hPa, SLP and EGR anomalies have some similarities in summer and winter, but differences in intensity and size of the anomalies are noted (Figures 5.6c,d). In summer the SLP anomaly related to the cyclone center is located to the east and occupies smaller area over the southern SA (Figure 5.6c), while in winter these anomalies are wider, reaching lower latitudes (Figure 5.6d). The minimum anomalous central pressure is slightly stronger in winter (-6 hPa) than in summer (-5 hPa) and the wave train, in both surface and mid-levels, reaches lower latitudes in winter. However, the environment in summer seems to be slightly more baroclinic since the EGR anomalies are stronger and the vertical tilt from the low-pressure center from surface to mid-levels is greater (Figure 5.6c). Nevertheless, the anomalous PV structure is probably acting to induce the breaking in the jet streak, which is not evident in winter.

For both seasons, the specific humidity has the same intensity (Figures 5.6g,h) and locates directly over the minimum anomalous SLP and the positive EGR anomaly. The stronger low-level winds at 850 hPa locate at the western part of *Argentina* during summer (Figure 5.6g), over the continent, while in winter is displaced northward and to the coast. In general, the main difference between both seasons is the wave pattern, where the negative/positive SLP and geopotential anomalies are wider and slightly stronger in winter than in summer (Figures 5.6c,d). However, EGR and the frequency of PV streamers (and cutoffs) anomalies are higher over the genesis region in summer. Therefore, PV streamers seem to be most important to intensify upward motions with consequent contribution to the surface cyclone development in summer.

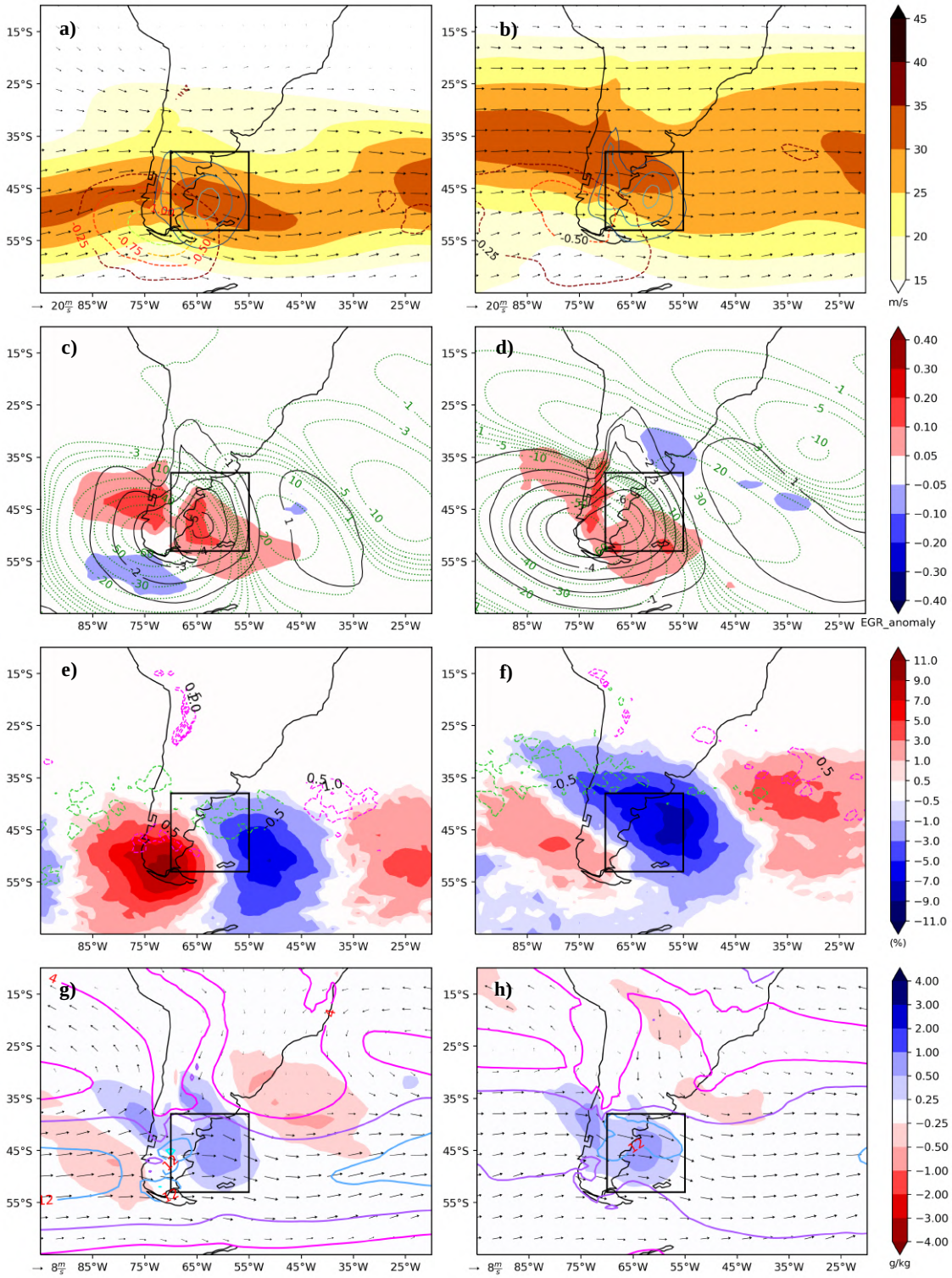

Figure 5.6 Austral summer (left panels) and winter (right panels) composites (for the period 1979-2017) for cyclogenesis in Argentina: a)-b) Horizontal wind (vectors) and magnitude (m s^{-1}, shaded) at 300 hPa, anomalies of PV (PVU) at 320 K (dashed lines) and QG-omega at 500 hPa (Pa s^{-1}, solid lines, the outer contour is -0.01, interval of 0.01); c)-d) anomalies of EGR (day^{-1}, shaded), SLP (hPa, solid lines) and geopotential height (m, dashed lines) at 500 hPa; e)-f) frequency (%) anomalies of PV streamers (shaded) and PV cutoffs (dashed lines) at 320 K; g)-h) horizontal wind (vectors) and magnitude (m s^{-1}, lines) and anomalies of specific humidity (g kg^{-1}, shaded) at 850 hPa.

5.3.2 *Uruguay*

Analyzing the same fields of *Argentina* but for *Uruguay*, in winter compared to summer the jet stream is stronger, which also occurs with PV and QG-omega anomalies (Figures 5.7a,b). The stronger jet stream is disturbed by Andes in winter leading to a curvature to south of the zonal westerly flow over the South Pacific, as a result of cyclonic vorticity induced by the mountain after crossing to its eastern side (Figure 5.7b). As a consequence, at lee Andes a strong ascent (~ 30°S;70°W) and a new spot for cyclogenesis is observed (Figure 5.7b), which also occurs in *Argentina* but less intense and further south (~ 45°S;70°W) (Figures 5.6a,b). Differently from *Argentina*, *Uruguay* presents stronger PV anomalies in winter mainly due to the position of the jet stream, which is displaced to the north in winter (Figure 5.2b), affecting lower latitudes.

The intensity of EGR anomalies reflects the strength of the jet stream, which is stronger in winter (Figure 5.7d) than in summer (Figure 5.7c). Also, SLP, geopotential and specific humidity anomalies are much stronger in winter than in summer, with anomalies elongating towards the equator. The minimum SLP anomaly in winter (-6 hPa) is located at the northwest sector of *Uruguay*, while it is weaker (-3 hPa) but located inside the box in summer (Figures 5.7c,d). The magnitude of low-level winds at 850 hPa has the double intensity northward *Uruguay* in winter (Figure 5.7h), presenting a strong confluence over *Uruguay*. However, at southwestern *Uruguay* there is a center of negative specific humidity anomalies in summer (Figure 5.7g), which is not present in winter. This is related with the anomalous SLP over the continent at the rear of cyclogenesis in summer (Figure 5.7c), whereas in winter is located over the South Pacific (Figure 5.7d). What is more evident for this region, different from *Argentina*, is that cyclogenesis is located northward (southward) of the positive (negative) EGR anomalies, i.e., between different anomaly signals (Figures 5.7c,d).

The positive anomaly center of SLP at the rear of *Uruguay* is closer to the genesis in summer (Figure 5.7c) than in winter (Figure 5.7d), which might be explained by the position of PV streamers in these two seasons (Figures 5.7e,f). For winter (Figure 5.7f), PV streamers are displaced northward and closer to *Uruguay* compared with summer (Figure 5.7e), and as noted in *Argentina*, the vertical alignment between PV streamers and geopotential anomalies also reflects in the SLP field. For summer the positive anomaly of PV streamer is already over

the South Atlantic, while in winter it is located in the western coast of SA. In terms of PV cutoffs, positive anomalies are seen in summer at the rear and closer to *Uruguay*, in opposition to negative anomalies observed in winter (Figures 5.7e,f). The weaker jet stream may explain the positive anomaly of PV cutoffs during summer (Figures 5.7a,e), since the weakening of the upper-level jet contributes to the detachment of PV anomalies from the main westerly flow.

In general, the baroclinic atmospheric coupling is stronger in winter during genesis in *Uruguay*, different from *Argentina*, where the difference between seasons is smaller. Although the PV streamer anomaly is greater during summer for both regions comparing with winter, the position of the jet stream seems to play an important role in *Uruguay* than in *Argentina*. In *Argentina*, the genesis in winter occurs more frequently at the polar jet exit sector (Figure 5.6b) while for *Uruguay*, at the equatorial entrance (Figure 5.7b), creating a more baroclinic environment and instability as the polar cold air moves towards warmer regions, and probably interacting with the Northwestern Argentinian Low (Seluchi et al., 2003; Seluchi and Saulo, 2012). Also, the southwestward inclination of pressure systems with height and stronger positive EGR anomalies indicate a more favorable environment for the systems to grow.

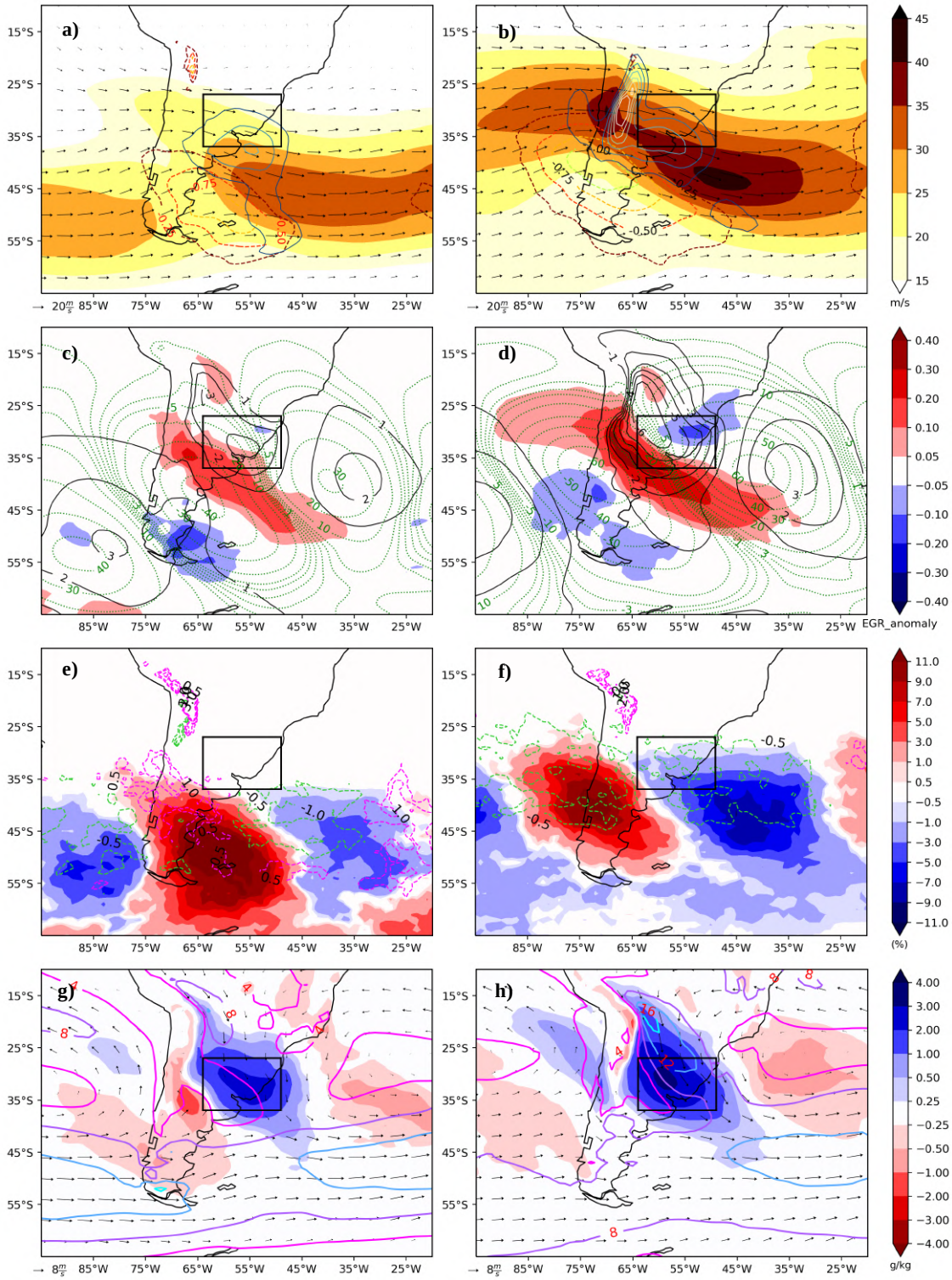

Figure 5.7 As in Figure 5.6, but for the region *Uruguay*.

5.3.3 *SEBrazil*

Figure 5.2a shows that the most prominent level to analyze PV for this region in summer is the 360 K isentropic level. Nevertheless, since this study focus on features prior and during genesis, it is expected that the forcing locates at the rear of the genesis region, most likely at westward/southwestward. As Figures 5.4 and 5.5 show, PV streamers (cutoffs) are more frequent at 340 and 360 K (360 K) in summer while in winter is at 320 K (310 and 360 K). In that sense, we will show the intermediate 340 K level for summer and 320 K for winter.

The level of the tropopause is clearly important for *SEBrazil*, where for summer (Figure 5.8a) the PV anomaly center is at 40°S;45°W, whereas in 320 K (not shown) it locates far from the genesis region. Since the jet stream at 300 hPa in summer (Figure 5.8a) is not directly affecting *SEBrazil* with the same intensity as in winter (Figure 5.8b), there is a very small signal of QG-omega, whereas in winter *SEBrazil* is under the equatorial entrance of the jet, resulting in stronger ascent (Figure 5.8b).

In winter EGR, SLP and geopotential height at 500 hPa anomalies (Figure 5.8d) are stronger compared to summer (Figure 5.8c). During winter, at the rear of the anomalous low-pressure at surface in *SEBrazil*, there is a strong anomalous transient high-pressure system which presents two centers, one over the continent (25°S;65°W) and the other southwestward from the former, over the west coast (43°S;77°W) of SA (Figure 5.8d), both associated with negative specific humidity anomalies at 850 hPa (Figure 5.8h). The latter is aligned with the positive geopotential anomaly in 500 hPa and the negative anomaly of PV streamer (Figures 5.8d,f). These features are not present in summer (Figures 5.8c,e), where although weaker, the anomalous low pressures at surface and at 500 hPa associated with *SEBrazil* are vertically aligned and elongated in the northwest-southeast direction, occupying a broad area over the South Atlantic (Figure 5.8c). Besides weak, the positive anomalous SLP center upstream *SEBrazil* in summer (Figure 5.8c) is associated with relatively strong negative specific humidity anomalies (Figure 5.8e), indicating a drier environment upstream genesis in summer. The vertical structure of anomalous pressure systems has a more barotropic structure in summer and a baroclinic one in winter. In the latter, the high frequency of PV streamers and cutoffs at the rear of cyclogenesis area are contributing to strengthen the baroclinic environment. And, as for *Argentina* and *Uruguay*, the same pattern of alignment occurs

between geopotential height and PV streamers in *SEBrazil* (Figures 5.8c-f), i.e., PV streamers are located to the southwest of the geopotential anomaly.

SEBrazil has a positive PV cutoff anomaly over the South Atlantic close to the northeast coast of SA (about 25°W) during summer (Figure 5.8e), which is related to the northeast trough in the monsoon season (Zhou and Lau, 1998), and at 360 K there is also a positive PV cutoff anomaly directly over *SEBrazil* in winter (Appendix B). The former is in agreement with the climatology of cutoff lows (COL) for the Southern Hemisphere by Reboita et al. (2010) who detected COLs along the northeast Brazilian coast at 200 hPa and 300 hPa during summer. However, the anomalies occurring in winter were not observed by Reboita et al. (2010).

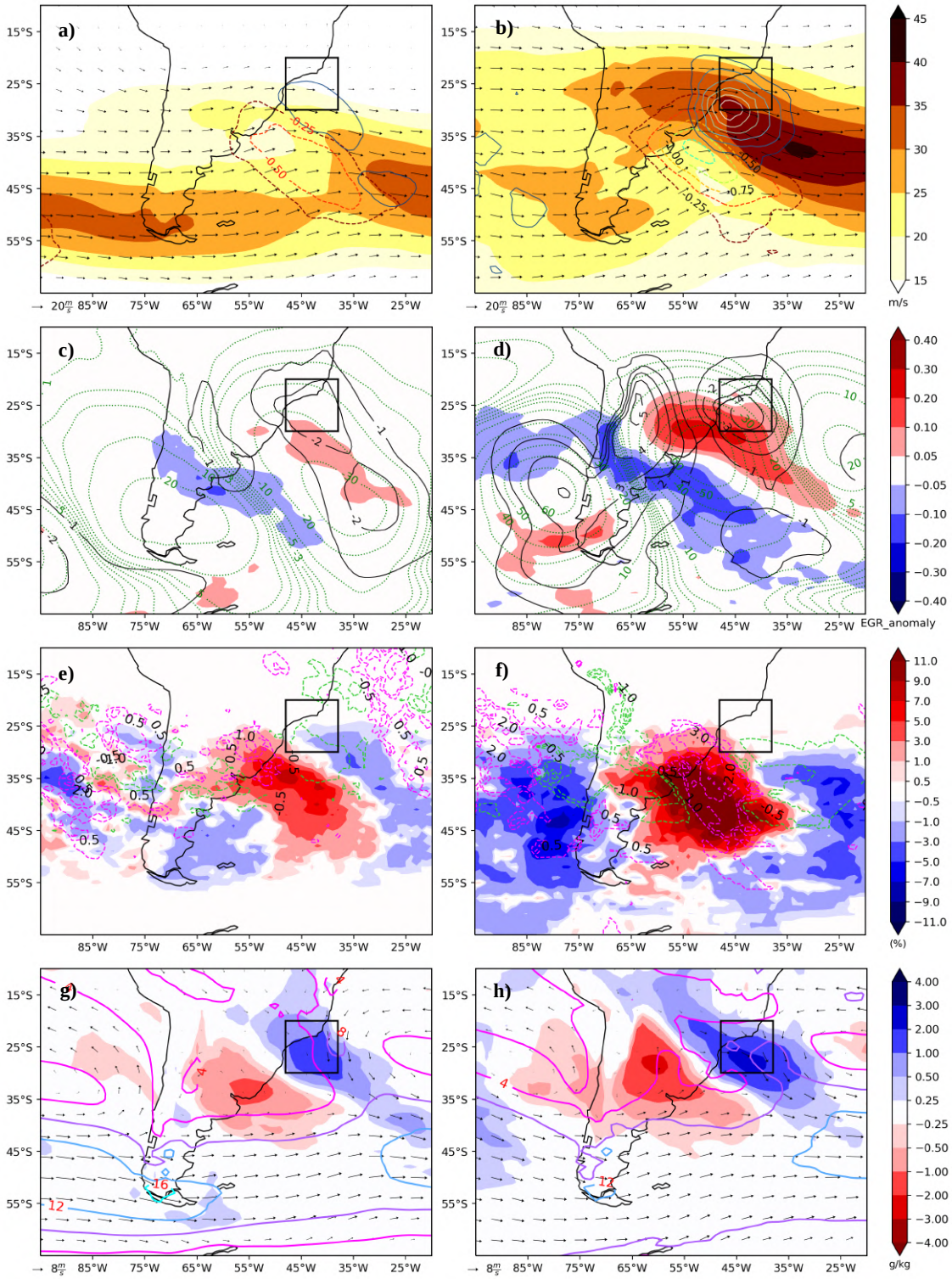

Figure 5.8 Similar as in Figures 5.6 and 5.7, but for the region *SEBrazil*, and in a) and e) the PV structures are shown for the 340 K level.

5.3.4 *Andes*

Over the *Andes* region, QG-omega anomaly at 500 hPa presents a very weak signal in summer (Figure 5.9a), similarly to the *SEBrazil* region (Figure 5.8a). There is also a weak QG-omega signal to the lee of the Andes about 40°S near the jet stream at 300 hPa, which is located to the south of the *Andes* box, far from the genesis location. Near 70°W, where the jet stream has a break, it is located the center of the PV anomaly at 340 K (Figure 5.9a), which is also present in other isentropic levels (not shown). On the other hand, in winter the upper-level jet, PV anomaly and QG-omega are stronger, with the anomalies to the south and closer to *Andes* than in summer (Figure 5.9b). Although with weaker intensity, these variables have similar spatial patterns to the ones in *Uruguay* (Figures 5.7a,b), which is in agreement with the previous discussion of time lags between genesis (section 4.3); in *Uruguay*, however, genesis is most likely to occur 12 hours after genesis in *Andes.*

The EGR anomaly fields show a strong positive anomaly southeast of the *Andes* composites for both seasons (Figures 5.9c,d), but in summer the anomaly is more widespread, reaching a larger area over Argentina, Chile and *Andes* (Figure 5.9c). Geopotential height and SLP anomalies in winter (Figure 5.9d) have a similar spatial pattern to that of *SEBrazil* in winter (Figure 5.8d) upstream genesis in *SEBrazil* but with opposite signals, i.e., two centers of anomalous low-pressure at the surface, one over *Andes* and the other to the west coast of SA. This pattern is more baroclinic (i.e., greater westward tilt with height of pressure anomalies) over the continent and South Atlantic, whereas over South Pacific is more barotropic. However, in summer there is one large pressure system with a baroclinic vertical structure, where the surface anomalous low elongates from northwest to southeast, reaching from the *Andes* region to *Uruguay* (Figure 5.9c). The spatial pattern of low-level anomalous specific humidity is very similar for both seasons (Figures 5.9g,h), while low-level winds are stronger in winter (Figure 5.9h). The most intense north-northwesterly winds are located inside the *Andes* region, reaching maximum speed of 8 and 12 m/s, respectively, in summer and winter. Finally, PV streamers seem to influence this region only during summer, where a positive PV streamer anomaly is centered in approximately 32°S, crossing the Andes at 340 K (Figure 5.9e). On the other hand, there is a weak signal of PV cutoffs over the region in winter (Figure 5.9f). From these analyses, and as discussed before, *Andes* presents a mix of systems, which needs to be studied separately depending on if they are mobile or stationary

systems, trying to highlight differences regarding the dynamic forcing between these two types of systems.

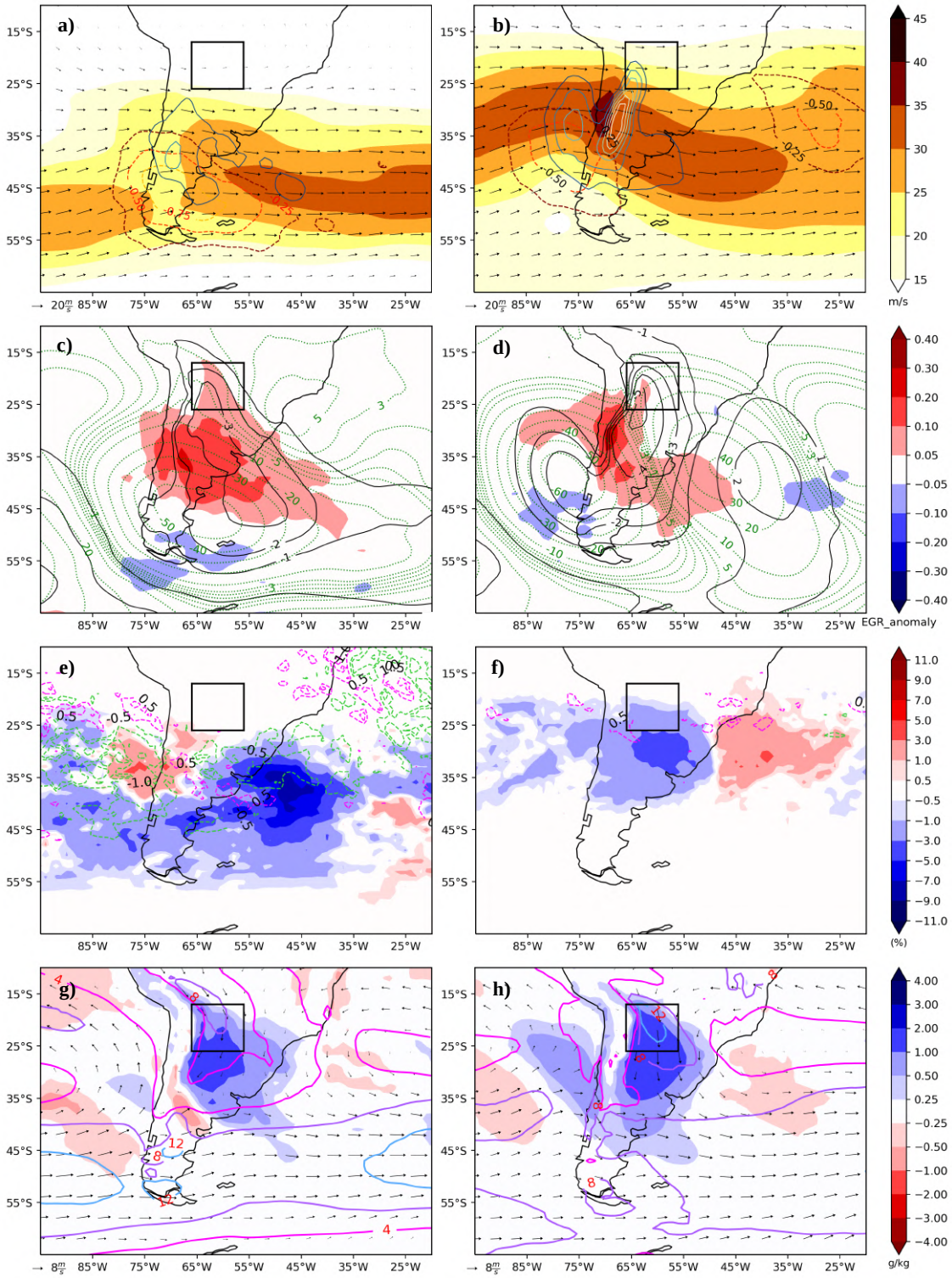

Figure 5.9 Similar as in Figures 5.6, 5.7 and 5.8, but for the region *Andes*, and in a)-b), e)-f) the PV structures are shown for the 340 K level.

5.4 Patterns prior and after cyclogenesis

In this section we discuss the composites anomalies for cyclogenesis but considering the time steps prior (-24h) and after (+24h) genesis. The aim is to explore the characteristics of the environment evolution from previous until one day after cyclogenesis in each region.

5.4.1 *Argentina*

In winter, prior cyclogenesis (-24h), the jet streak at 300 hPa, centered in approximately 35°S, is approaching SA from the South Pacific, followed by QG-omega upward motion and PV anomalies in the polar sector of the jet (Figure 5.10b). A different pattern occurs in summer when the exit sector of the jet streak, in approximately 50°S, is already over southern *Argentina*, while PV anomaly and QG-omega upward motion are displaced to the west, still over the South Pacific (Figure 5.10a). The processes of cyclogenesis occur faster in winter than in summer, since during cyclogenesis the anomalies of QG-omega and PV are relatively at the same location in summer (Figure 5.6a) and in -24 h (Figure 5.10a), different from winter.

Prior cyclogenesis, PV and QG-omega anomalies are weaker than in genesis (Figure 5.6a,b) and still over South Pacific (Figure 5.10a,b). For both winter and summer, the environment prior genesis shows relatively the same intensity as during genesis regarding the upward motion located to the northeast of PV anomalies, but in different locations in relation to the jet streak. In summer, QG-omega is positioned in the central part of the jet streak, while in winter it is in the polar exit sector.

The anomalous low pressure at surface and mid-troposphere are situated to the west of *Argentina* in winter and summer prior cyclogenesis (Figure 5.10c,d). Geopotential and SLP anomalies are more elongated northwest-southeast in winter whereas in summer these structures are more zonal, and this occurs prior and after cyclogenesis (Figures 5.10d and 5.11d). Prior genesis, positive EGR anomalies are weaker, but slightly more intense near the jet streak. In both seasons, the vertical alignment of the low-pressure systems to the west is small, indicating a weak baroclinic structure. In summer, an additional feature in the environment prior genesis is the high frequency of PV streamers and some events of PV

cutoffs at 320 K westward *Argentina* (Figure 5.10e). Both PV structures act as an additional forcing to cyclogenesis, inducing cyclonic vorticity and upward motion in a weaker baroclinic environment from a climatological point of view (Figure 5.10c). At west of *Argentina* there is positive anomaly of specific humidity with similar intensity in both seasons. Also, near and over *Argentina* the west-northwest low-level winds are intense (greater than 12 m/s) (Figures 5.10g,h).

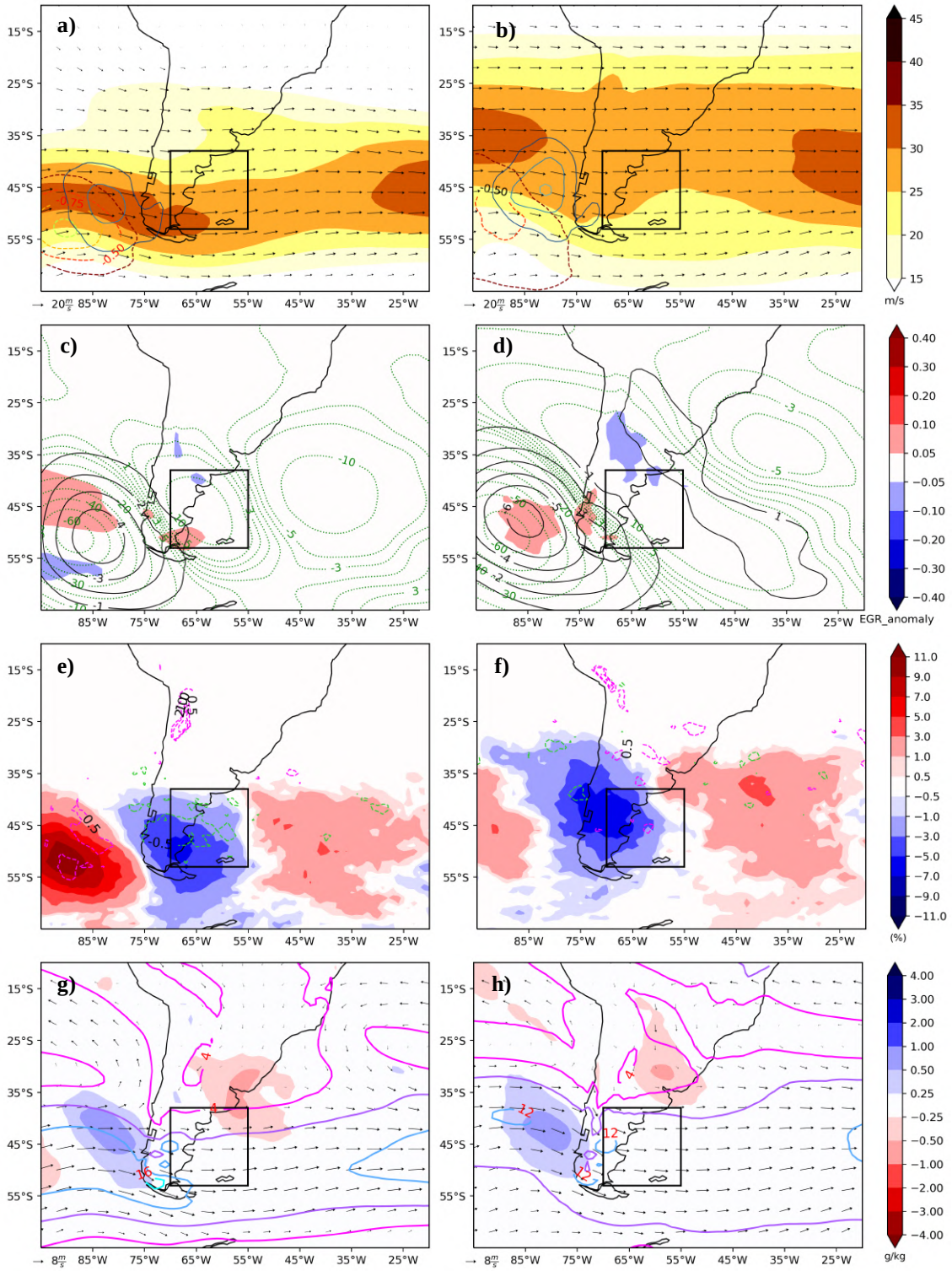

Figure 5.10 As in Figure 5.6, but for 24 hours prior cyclogenesis.

One day after genesis, PV anomalies are over the cyclogenetic region and still stronger in summer than in winter; the upper-level jet stream weakens in summer but continues intense in winter (Figures 5.11a,b). The anomalous low pressure presents a greater vertical inclination

to southwest (more baroclinic) in summer than in winter, and EGR is mostly positive over the center-north sector of the region in both seasons (Figures 5.11c,d). At surface, a wider anomalous low-pressure system is still over *Argentina* in winter, while in summer it occupies a smaller area and has moved to the east, found completely over the South Atlantic (Figures 5.11c,d). In summer, the stronger PV anomaly is in agreement with the higher frequency of PV streamers (and with PV cutoffs) over the region, while in winter it weakens considerably compared with the genesis phase (Figures 5.11c-f). In summer, positive anomalies of specific humidity are still relatively large and are located to northeast of *Argentina*, whereas the drier air upstream is occupying the cyclogenetic region (Figure 5.11g). This spatial pattern differs from winter (Figure 5.11h), where only weak positive anomalies are noted to the northeast, with no contrast between dry and moist air.

As for genesis time, the cyclone is more intense and baroclinic in summer than in winter. This is probably explained by the greater frequency of upper-level PV structures (PV streamers and cutoffs) to reinforce the baroclinic environment, contributing to the cyclone genesis and intensification. A secondary feature is the slightly greater contribution of moisture in summer than in winter, where there is a greater area of positive specific humidity anomaly during and after genesis (Figures 5.6g,h, 5.11g,h), especially the stronger contrast between the downstream moist and upstream dry sectors of the cyclone.

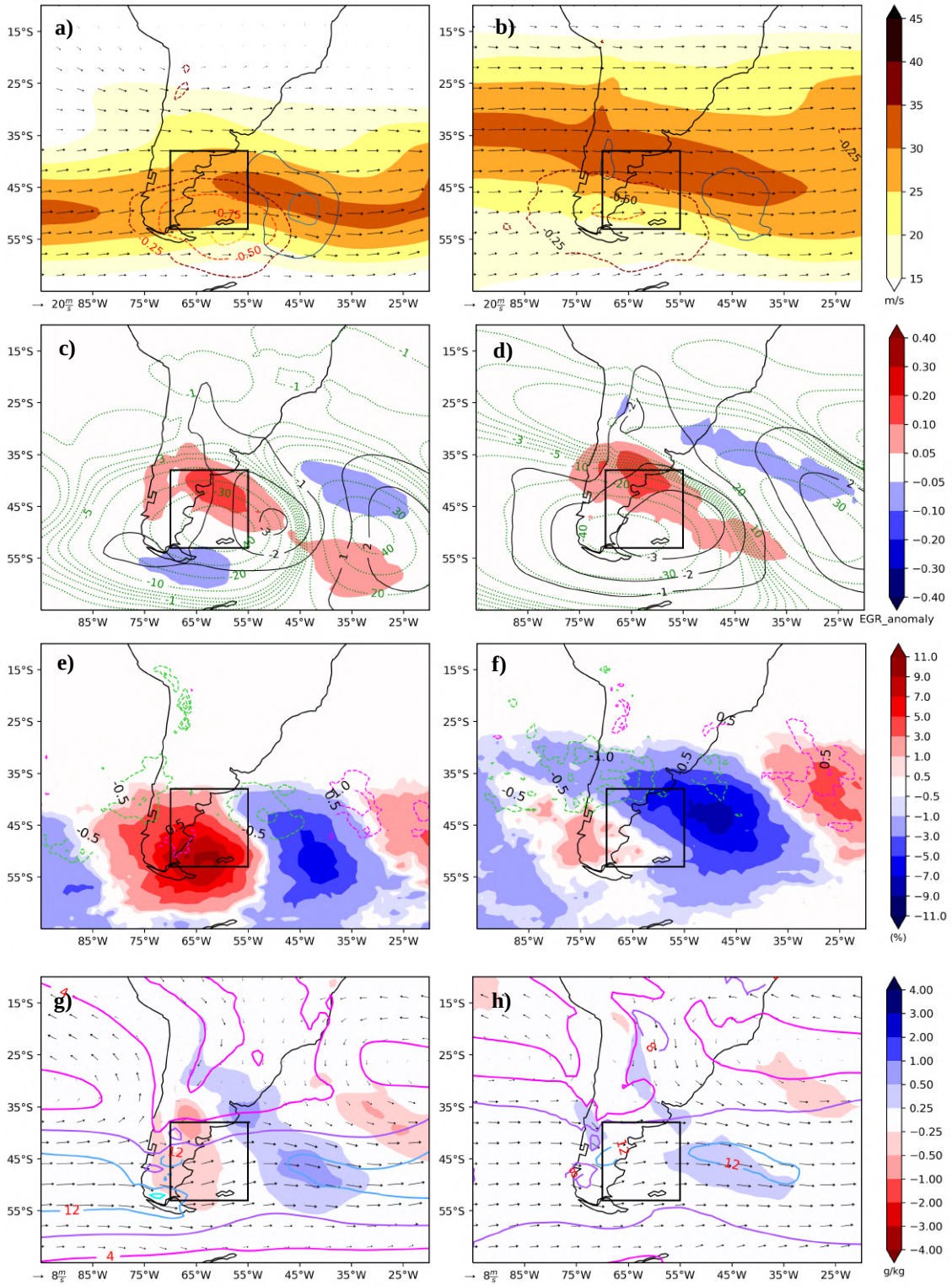

Figure 5.11 As in Figures 5.6 and 5.10, but for 24 hours after cyclogenesis.

5.4.2 *Uruguay*

Figures 5.12 shows the 24 hours previous environment for *Uruguay*. In winter, a very strong jet streak is crossing the Andes, between 25°S-40°S, accompanied by intense PV anomaly still in western side of Andes (Figure 5.12b). QG-omega splits in two different regions of upward motion, one center is over the western SA coast (35°S) and the other eastward at lee side of the Andes. In summer, a different pattern occurs since a weaker jet stream is already located to the south of the genesis region, with QG-omega indicating ascent under equatorial jet entrance and weaker PV anomaly far from *Uruguay* (Figure 5.12a). PV anomalies are closer to *Uruguay* in winter than in summer, as also are the jet stream, which provides a more baroclinic environment since prior genesis.

EGR for *Uruguay* presents an elongated band coming from the South Pacific/south Argentina and reaching the South Atlantic, especially in winter (Figures 5.12c,d and 5.13c,d). The positive EGR anomalies are widespread in winter (Figures 5.12d, 5.13d), which synthetizes the baroclinic support for cyclone development. This strong positive EGR anomaly band has a strong negative signal up and downstream *Uruguay*, and, as for *Argentina*, cyclones from *Uruguay* form and develop on the edge of two opposite anomalous signals of EGR (Figures 5.12c,d, 5.13c,d). As the cyclone develop, the positive EGR anomalies displace to the northeast until they reach *Uruguay* region one day after the cyclogenesis (Figure 5.13c,d).

A broad area with anomalous positive specific humidity is present in *Uruguay* since one day before the cyclogenesis, where the moist air is widespread in a larger area in winter than summer (Figures 5.12g,h). The stronger northerly winds (with velocities of ~12 m/s, characterizing a low-level jet) at 850 hPa located to the north of *Uruguay* contributes to explain the moister environment to cyclogenesis in winter. Furthermore, the environment in *Uruguay* is moister in winter prior and during cyclogenesis, while in summer this occurs during and after genesis (Figures 5.7g,h, 5.12g,h and 5.13g,h).

From prior to after genesis, it is evident the displacement from the positive anomalies of PV streamers, however, as discussed in section 5.3.2, in winter the frequency of PV cutoffs is anomalously negative, while in summer it is positive. That becomes more evident after genesis (Figure 5.13e,f), where positive frequencies of PV cutoffs are over *Uruguay*.

Compared to *Argentina*, *Uruguay* is characterized by higher frequencies of PV cutoffs in summer (Figure 5.13e).

Comparing *Argentina* and *Uruguay*, some points are highlighted: i) the upper-level jet stream is wider (narrower) in summer (winter) in *Uruguay* (Figures 5.12a,b, 5.13a,b) than in *Argentina* (Figures 5.10a,b, 5.11a,b); ii) PV anomalies are stronger in winter than in summer in *Uruguay*, where the opposite occurs in *Argentina*; iii) positive EGR anomalies are stronger in *Uruguay* than in *Argentina* prior and after genesis, especially in winter (Figures 5.12c,d, 5.13c,d).

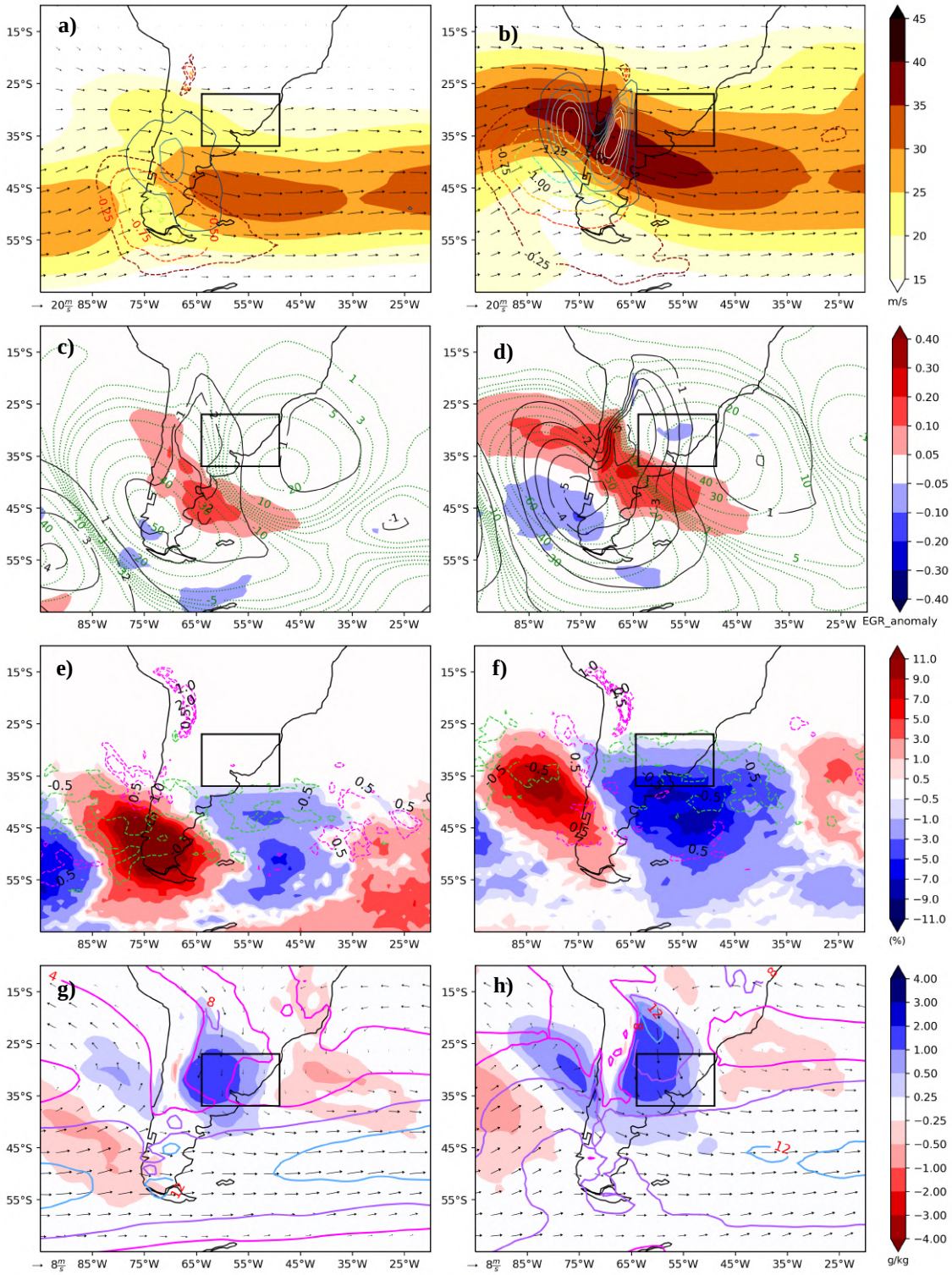

Figure 5.12 As in Figure 5.7, but for 24 hours prior cyclogenesis.

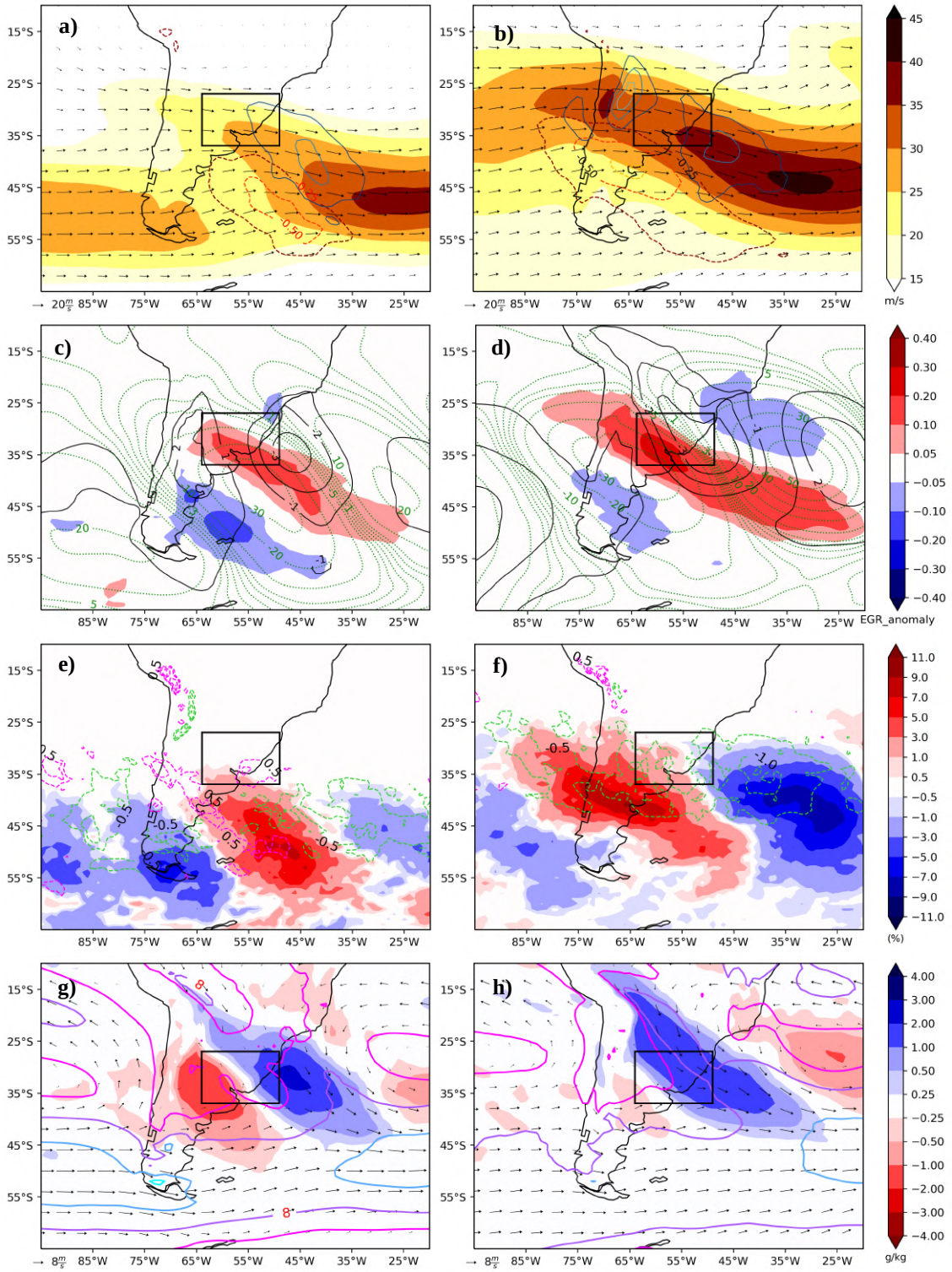

Figure 5.13 As in Figures 5.7 and 5.12, but for 24 hours after cyclogenesis.

5.4.3 *SEBrazil*

For summer, the upper-level wind field presents a jet stream with similar pattern and location to that of one day after the cyclogenesis in *Uruguay* (Figure 5.13a), but with differences in intensity (Figure 5.14a). For *SEBrazil* the branch of jet stream over the Atlantic (south Argentina) is weaker (stronger) than in *Uruguay*. Both jet stream and PV anomaly are located (~42^{o}S;55^{o}W), southward and away from the cyclogenetic region in summer. In winter, the jet stream and associated PV anomaly are closer to *Andes*, and QG-Omega upward motion occurs in the equatorial entrance of the jet to the west of *SEBrazil* (Figure 5.14b). The similarities between the spatial pattern of upper-level wind field and PV anomalies in *SEBrazil* and *Uruguay* occurs as a function of ~ 30 h lag (as presented in Figure 4.9c), e.g., prior genesis in *SEBrazil* the PV anomaly centered at ~ 42°S in summer (Figure 5.14a) is noted one day after genesis in *Uruguay* (Figure 5.13a).

The main feature in *SEBrazil* is a preexisting through over the continent, which has a PV anomaly associated in winter (Figure 5.14b). It seems that after cyclogenesis in *Uruguay* in winter, the perturbation existing at lee of the Andes (after the split of the QG-omega anomaly) moves towards *SEBrazil*, leading to cyclogenesis in winter (Figure 5.14b). These perturbations appear already in -48h (not shown). This is also confirmed in the time lag for *SEBrazil* (Figure 4.9c) that, besides weak, there is a peak for *Andes* in 36 h prior genesis in winter.

QG-omega anomaly is weaker in summer for *SEBrazil* but stronger than the other regions in winter, especially after genesis (Figure 5.15b). According to QG-omega, upward motions are always located at the equatorial jet entrance. In general, PV anomalies approaching *SEBrazil* from southwest, as a “residual” from cyclones formed in *Uruguay*, play an important role in forcing cyclogenesis and cyclone development in *SEBrazil*.

EGR anomalies in winter indicate a greater probability for the systems to grow, similar to *Uruguay*, while it is weak in summer (Figures 5.14c,d). As for the other regions, cyclones develop downstream the edge of the EGR positive anomaly, which strengthens during and after genesis in winter (Figures 5.8d and 5.15d). Even though PV streamers and PV cutoffs present positive frequency in both seasons near *SEBrazil*, these anomalies are slightly stronger after genesis in winter (Figure 5.15f), an opposite behavior from what is observed in

Argentina and *Uruguay*. One day after cyclogenesis, a positive anomaly of PV cutoffs is over *SEBrazil* in winter, which is probably developing during the cyclone lifecycle in the region.

Cyclones from *SEBrazil* travel shorter distances, as discussed in section 4.2 (Figures 4.7a,b), which is evident in the anomalous SLP in both seasons during the cyclone lifecycle (Figures 5.8c,d, 5.14c,d and 5.15c,d). The center of low pressure related to the cyclone has a small movement since prior (Figure 5.14c,d) to after (Figures 5.15c,d) genesis, especially in summer (traveled distance of approximately 7°), characterizing them as more stationary. In terms of vertical structure, prior cyclogenesis there is a considerable vertical inclination with height to the southwest of the low-pressure systems in both summer and winter seasons (Figures 5.14c,d). This inclination persists until the cyclogenesis day during winter, while in summer it decreases characterizing a barotropic equivalent vertical structure of the cyclone (Figures 5.8c,d). Similar to *Uruguay,* the anomalous moist air at 850 hPa occupies a large area upstream and over the region since prior until after cyclogenesis (Figures 5.14g,h, 5.15g,h). Different from *Uruguay,* where the contrast between moist and dry air is weak, cyclones in *SEBrazil* present a more intense gradient between moist and the dry air upstream since one day before cyclogenesis. This gradient intensifies from the cyclogenesis day until after it (Figures 5.8g,h and 5.15g,h). A very interesting result is the moister anomalous environment in winter than in summer during the cyclone lifecycle. This is explained by the low-level winds that are stronger in winter than in summer (Figures 5.14g,h). The direction of the low-level wind also helps to understand the differences; in winter, one day prior cyclogenesis the northwesterly jet (with mean velocity of 8 m/s) is transporting moist air of tropical origin to the cyclogenetic region (Figure 5.14h). Moreover, the absence of this low-level jet in summer explains the smaller moisture content in *SEBrazil* (Figure 5.14h).

Overall, cyclones in *SEBrazil* in winter present a more baroclinic structure, and this occurs due to the presence of the jet streak and PV structures (streamers and cutoffs) affecting the region. An additional ingredient in winter is the presence of a strong low-level jet transporting moist air to the cyclogenetic region. On the other hand, summer is also influenced by a weaker upper-level PV anomaly, however, although the prior cyclogenesis environment indicates a weak baroclinic vertical structure, it decreases during cyclogenesis when the cyclones acquire a more barotropic vertical.

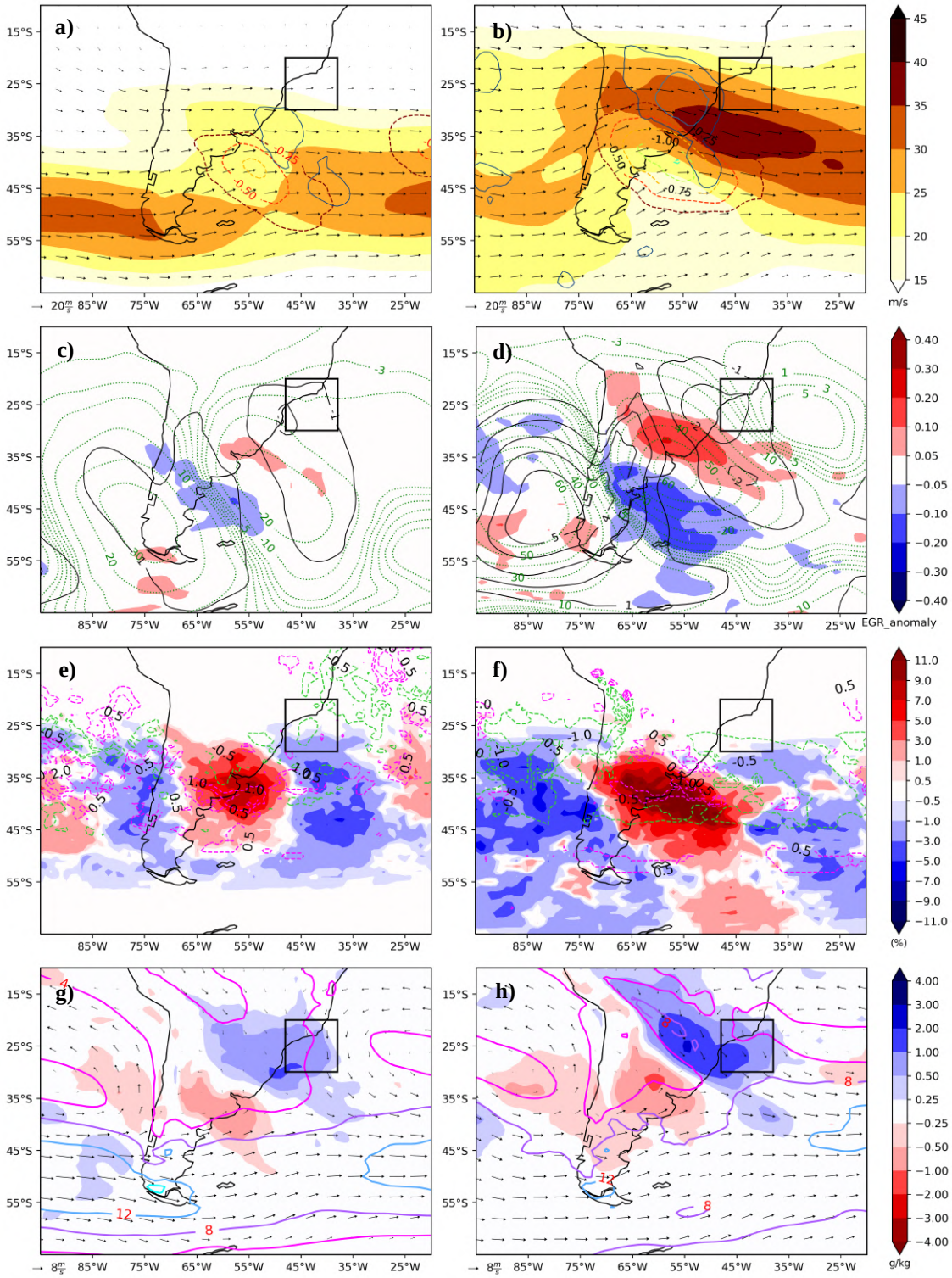

Figure 5.14 As in Figure 5.8, but for 24 hours prior cyclogenesis.

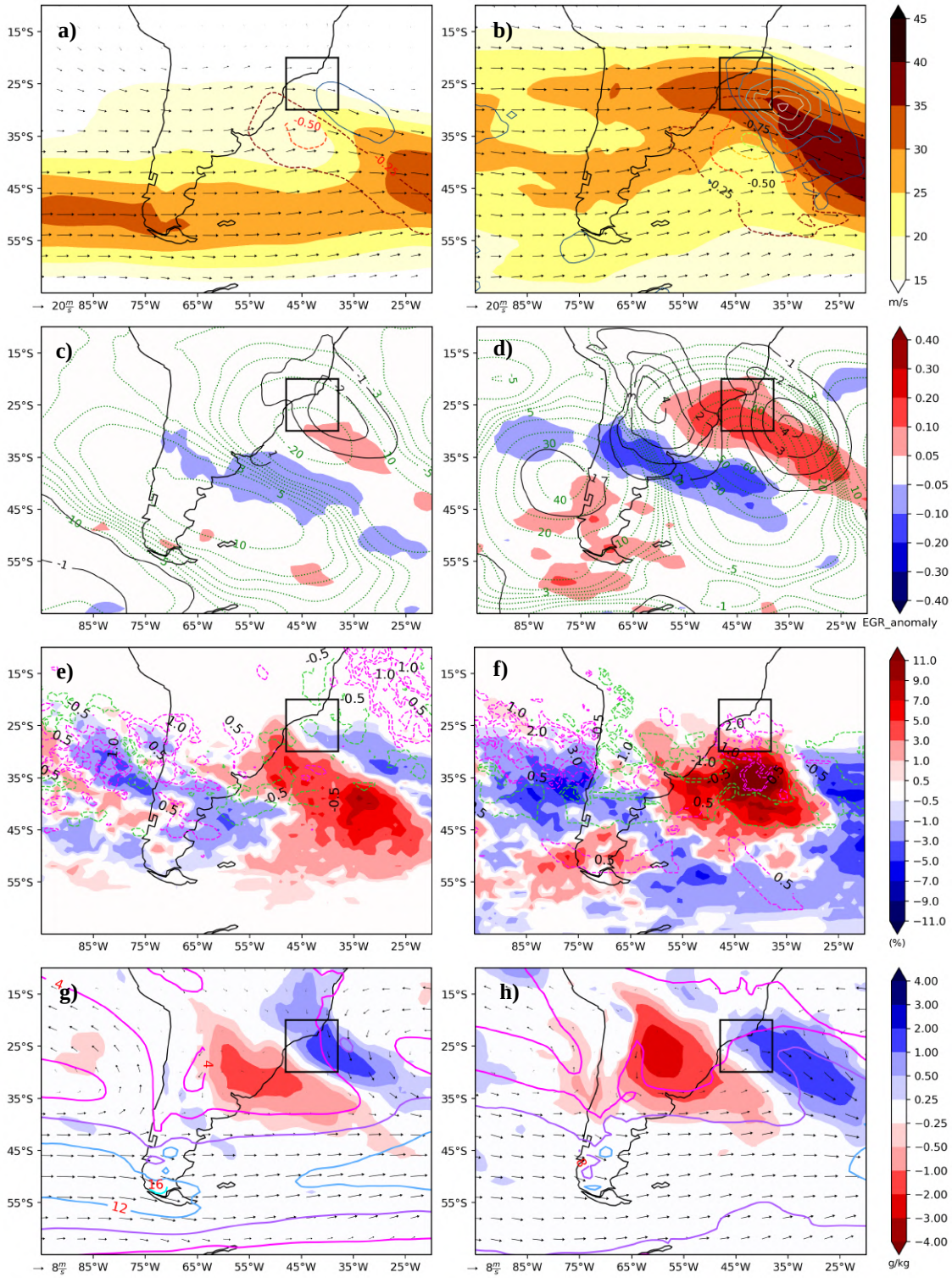

Figure 5.15 As in Figures 5.8 and 5.14, but for 24 hours after cyclogenesis.

5.4.4 *Andes*

In summer, the upper-level jet is very zonal and there is not a clear break prior cyclogenesis while PV anomalies at 340 K are coming from the South Pacific (Figure 5.16a). Both structures are located further south (centered ~ 45^{o}S) of the cyclogenetic region and the jet speed are higher in the South Atlantic sector of jet stream (Figure 5.16a). During cyclogenesis, the jet stream splits at same time that a weak anomaly of QG-omega develops near 40°S, which is still far from *Andes*. The hypothesis is that the jet crossing Andes, followed by PV anomalies, leads to a strong QG-omega anomaly lee Andes, especially because it is located at the jet stream equatorial entrance, creating a potential environment for cyclogenesis over that region in summer. Different from what occurs in other regions, the high frequency of PV streamers at 340 K is located to the north of the PV anomaly from prior to after genesis (Figures 5.16a,e, 5.9a,e and 5.17a,e). However, at 360 K (Appendix B) the presence of higher positive PV cutoffs frequency is contributing to force cyclogenesis in *Andes*.

EGR positive anomalies are stronger in summer than in winter for *Andes*, presenting a stronger signal since before cyclogenesis (Figure 5.16c). The positive EGR anomalies are located northward of the jet stream closer to *Andes* during and, especially, after genesis (Figure 5.17c). It is interesting also to point that the positive EGR anomalies are somehow associated with the positive frequency of PV streamers.

In summer, the vertical alignment of low-pressure systems before genesis has a barotropic equivalent structure (Figure 5.16c). On the other hand, during and after genesis the inclination to the southwest increases acquiring a vertical baroclinic structure (Figures 5.9c and 5.17c), where the anomalous SLP moves to the east and forms one center in about 45°S, elongating northward, reaching *Andes* (Figures 5.9c and 5.17c). From the low-level flow and specific humidity, the winds are mainly from north and a widespread area of moister air is over and to the south of the cyclogenetic region (Figure 5.16g). The northerly winds intensification during genesis remains until one day after, while the anomalous moister air observed during genesis weakens after cyclogenesis (Figures 5.9g and 5.17g).

In winter, the upper-level jet influences *Andes* while crossing SA prior, during and after genesis (Figures 5.16b, 5.9b and 5.17b). This jet stream is intensifying over the Andes Mountain and PV anomaly is covering the center of the jet, followed by QG-omega anomaly

to the northeast (Figure 5.16b). Different from summer, QG-omega is closer to the cyclogenetic region during and after genesis (Figures 5.9b and 5.17b), remaining relatively in the same position and weakening after genesis (Figure 5.17b).

As mentioned before, EGR anomalies are weaker in winter compared to summer, and the low-pressure systems before genesis present a barotropic equivalent vertical structure to the west of SA (Figure 5.16d). This pattern is quite similar to *Uruguay*'s before genesis (Figure 5.12d), where the system crossing the Andes Mountain develops a secondary anomalous low-pressure center around 25°S, over *Andes*, with a characteristic baroclinic vertical structure.

As for the other regions, the low-level winds are stronger in winter over the cyclogenetic region. However, in *Andes*, before genesis, the positive anomalies of specific humidity are stronger in summer than winter, even though in winter the anomalies cover a larger north-south area and extend to the west of Andes Mountain (Figures 5.16g,h). After genesis, as observed in *SEBrazil* and *Uruguay*, the positive moisture anomaly is more intense in winter than in summer (Figures 5.17g,h).

In general, *Andes* cyclone patterns are similar to the ones of *Uruguay* until genesis; the differences are basically the time lag and the intensity of the anomalies, as discussed in other sections.

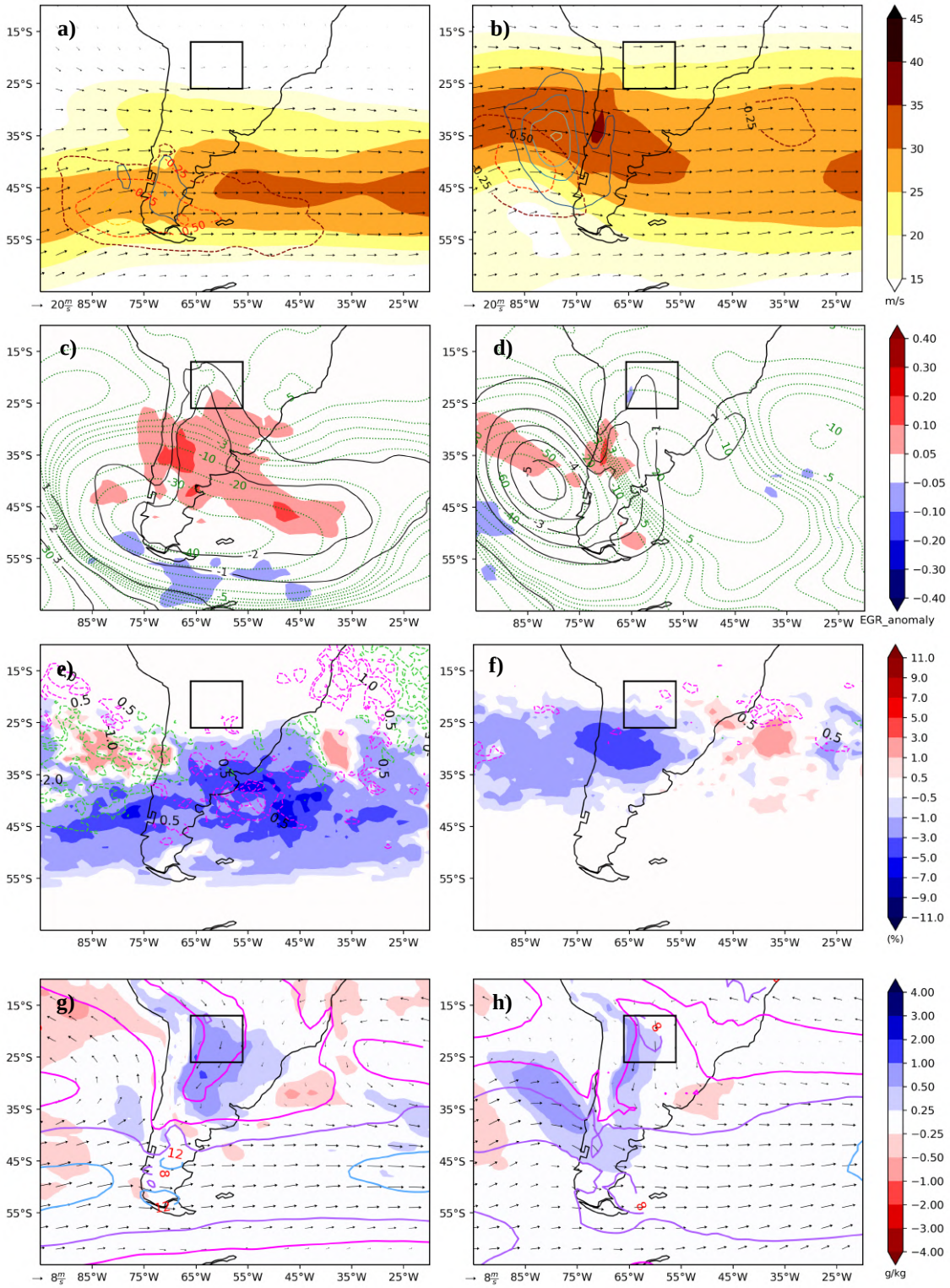

Figure 5.16 As in Figure 5.9, but for 24 hours prior cyclogenesis.

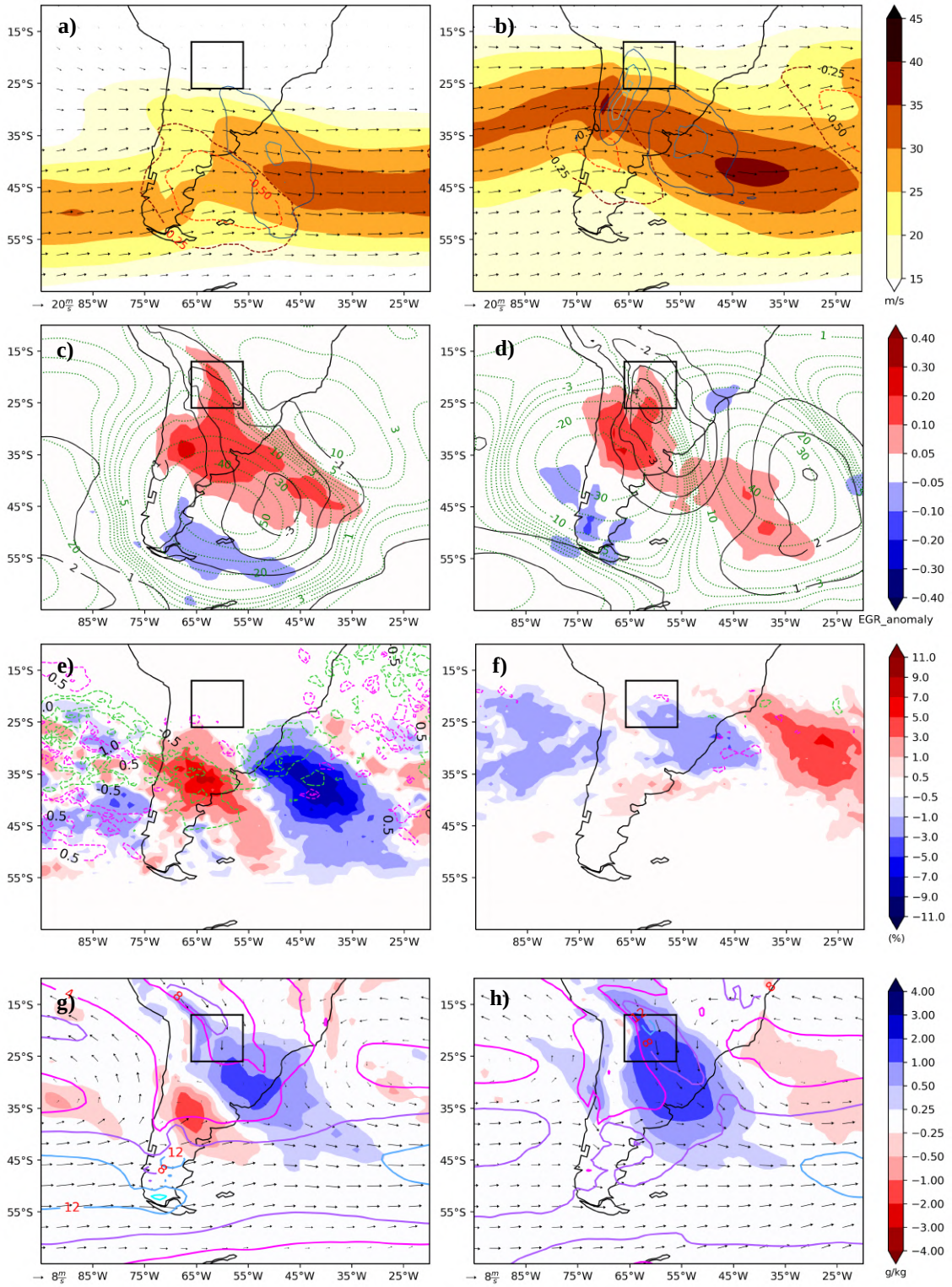

Figure 5.17 As in Figures 5.9 and 5.16, but for 24 hours after cyclogenesis.

5.5 Time evolution of the variables in each cyclogenetic regions

The time evolution of the atmospheric variables and parameters from prior until after cyclogenesis for *Argentina*, *Uruguay*, *SEBrazil* and *Andes* is presented in Figure 5.18. The values of the anomalies of each variable (QG-omega at 500 hPa, EGR, SLP, specific humidity at 850 hPa, and PV at 320, 340 and 360 K) represent the average over each cyclogenetic region (shown in Figure 4.2) since 48 h (-48) before until 48 h (+48) after genesis.

For all cyclogenetic regions, QG-omega shows a change from positive to negative from 48 until 12 h before the genesis, except for *Andes* in summer, which remains close to zero until 12 h after genesis (Figure 5.18a). This occurs since the weak QG-omega is far from the cyclogenetic region during the cyclone lifecycle (Figures 5.9a, 5.16a, 5.17a). Winter is the season with stronger ascent. *Argentina*, however, presents also stronger upward motion in summer, followed by *Uruguay* and *SEBrazil*. The maximum QG-omega, i.e., the most negative value, is achieved at the genesis in all regions and seasons, except for *SEBrazil* and *Andes*, where the minimum occurs, respectively, 12 h and 48 h after genesis in winter.

EGR anomalies (Figure 5.18b) for *Argentina* present the similar evolution for winter and summer, but with slightly higher values 12 h after genesis in summer. This is explained by the jet stream presence in *Argentina* during the whole year. In summer, *Uruguay* has EGR values similar to *Argentina*, however, the difference between two seasons in *Uruguay* is larger after genesis, with EGR presenting a higher peak 24 h after genesis in winter. This maximum peak is also present in *SEBrazil* during winter, where the EGR is increasing since 48 h prior until 24 h after cyclogenesis. This does not occur in summer since EGR rises until cyclogenesis and remains quasi-constant afterwards. The greater proximity of the upper-level jet stream to *Uruguay* and *SEBrazil* in winter explains the stronger EGR anomalies in this season. *Andes* presents a peculiar evolution of EGR, especially in summer (Figure 5.18b), where the evolution in time has a seesaw feature; achieving a minimum EGR value 12 h before cyclogenesis and increasing afterwards but following similar seesaw feature. In winter, EGR anomaly also achieves the minimum 12 h before genesis but increasing until 48 h after genesis in *Andes*. Considering all regions, in general, EGR anomalies reach maximum values 12 or 24 h after genesis (Figure 5.18b).

As for EGR, the low pressure is more intense during winter than summer (Figure 5.18c). The minimum SLP anomaly is observed at the time of genesis (0 h) in the four

cyclogenetic regions. After genesis, during winter, the anomalous low-pressure system has similar intensity in *Argentina* and *Uruguay*, while it is ~ 1 hPa weaker in *SEBrazil* and *Andes*. As discussed in section 5.1 and shown in Figure 5.18c, low pressure anomalies are stronger in winter, which was already identified in other studies over SA (Reboita et al., 2010; Gramcianinov et al., 2019).

The positive specific humidity anomalies are stronger in *Uruguay*, with maximum reaching 2 g kg^{-1} at cyclogenesis time (Figure 5.18d). The specific humidity anomaly increases since 48 h prior genesis achieving its maximum at genesis (0 h) in the four regions. *Argentina* presents smaller differences between winter and summer in terms of moisture anomaly. As previously discussed, in winter the stronger low-level jet acts transporting moist air to the cyclogenetic regions resulting in larger mean positive anomalies in *Uruguay-Andes* (after the genesis) and *SEBrazil* (since 24 h prior until genesis).

For the anomalies of PV at 320 K (Figure 5.18e), *Argentina* presents higher values (in module), with two distinct peaks in both seasons, one peak of minimum (maximum) PV 12 h (12 and 24 h) prior (after) genesis, which is in agreement with the fact that PV is in general located upstream of the surface cyclone from genesis until the cyclone reaches its maturity. *SEBrazil* and *Andes* presents a very small variability as the cyclone moves far from the region as function of the season, whereas *Uruguay* in winter presents a slightly higher variation, with the maximum occurring 48 h after genesis, while in summer the values are closer to zero and similar to *SEBrazil* and *Andes*.

A different pattern of PV is observed at upper isentropic levels (Figures 5.18f,g). *Argentina* is less sensitive to upper levels, especially in winter, where the amplitude variations decrease. The opposite occurs in *Uruguay* and *SEBrazil*, where from 12 h prior until 48 h after genesis the regions experience stronger variation of PV anomalies (e.g., in *Uruguay*, the averaged PV anomaly strengthens from 0.7 to -0.01 PVU in 60 hours in winter). This reinforces the vertical westward tilt, with a lag of 12 h from 320 to 340 K. In *SEBrazil*, the variation of the mean PV anomaly is noticeable at 340 K (360 K) in winter (summer).

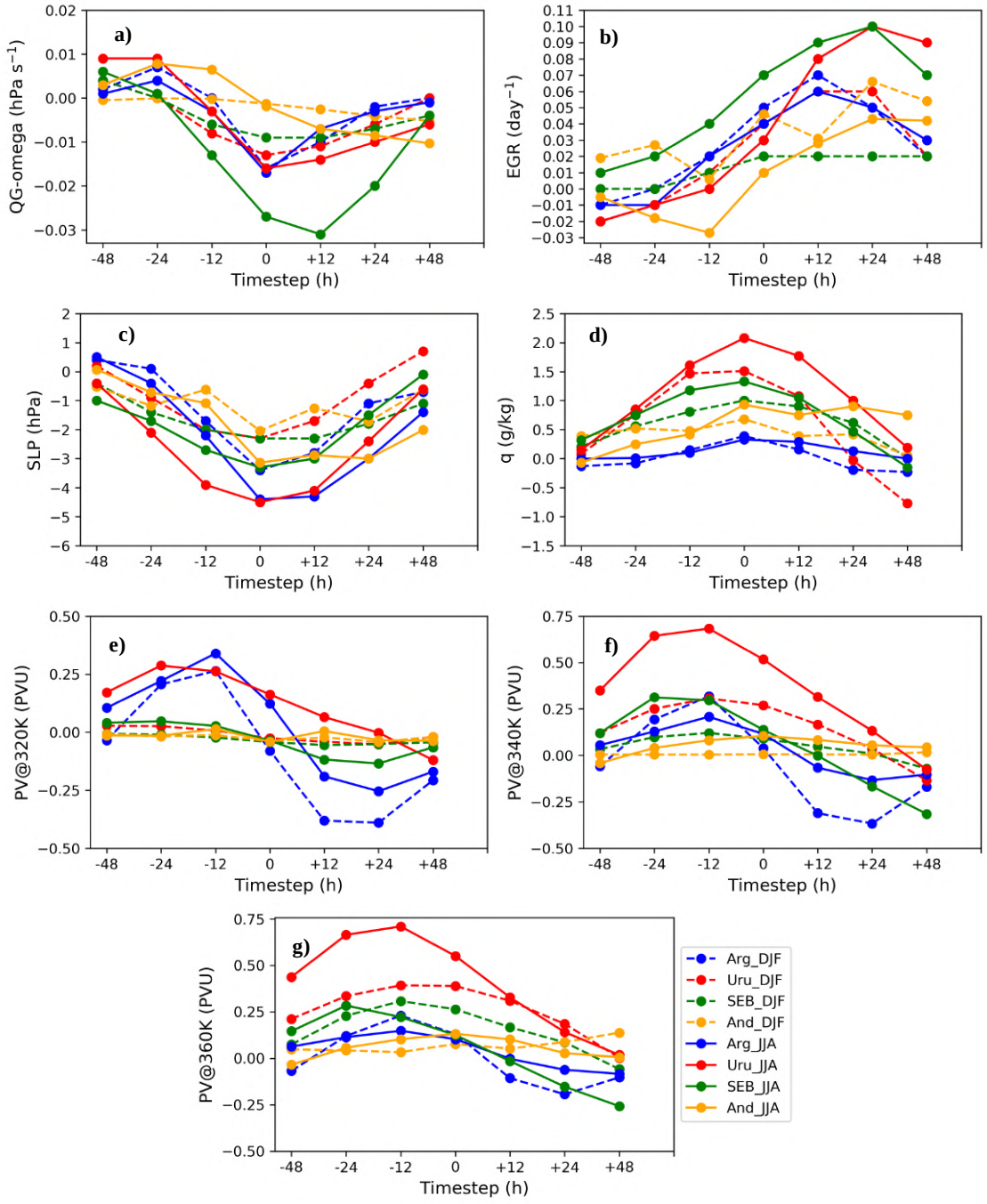

Figure 5.18 Mean of a) QG-omega (Pa s^{-1}), b) EGR (day^{-1}), c) SLP (hPa), d) specific humidity (g kg^{-1}) at 850 hPa, and PV (PVU) at e) 320 K, f) 340 K and g) 360 K anomalies inside the delimited area for *Argentina* (Arg, blue), *Uruguay* (Uru, red), *SEBrazil* (SEB, green) and *Andes* (And, yellow) for summer (dashed line) and winter (solid line). The timesteps represent genesis (0), and 48h, 24h, 12h before (-) and after (+) genesis.

Chapter 6

6 Conclusions

This study presents a general overview of the atmosphere from a potential vorticity (PV) perspective at upper levels, focusing on the upper-level PV structures and their influences on surface cyclones over South America. Surface cyclones and PV structures on isentropic surfaces (PV streamers and PV cutoffs) are identified using ERA-Interim reanalysis for the period 1979-2017. The following sections present a summary and the main conclusions of this work.

6.1 Tracking and cyclones characteristics

After identifying cyclones in four regions of South America (*Argentina, Uruguay, SEBrazil* and *Andes),* their traveled distance, intensity, lifetime, association with PV structures, and time lags are analyzed in different seasons. Since it is used a larger area to apply the tracking algorithm, the surface cyclones climatology provides higher number of events. This occurs since a larger domain allows to include in the climatology cyclones upstream Andes and, with the absent of boundaries close to the continent, the cyclone reaches at least 24 hours of lifecycle inside the domain.

The relationship between cyclogenesis in different regions shows that before cyclogenesis in *Uruguay* there is a high frequency of cyclogenesis in *Andes*. The bi-modal characteristics of frequency distributions of displacement, intensity and lifetime, indicate two different types of cyclones occurring in *Argentina, Uruguay* and *SEBrazil*. A general feature is that cyclones from *Argentina* and *Uruguay* travel longer distances and are more intense.

In the four regions, upper-level PV streamers occur frequently during cyclogenesis, typically located to the southwest. However, there are seasonal differences during genesis: in *Argentina* and *Andes*, PV streamers occur frequently in summer, in *Uruguay* in summer and winter, and in *SEBrazil* mainly in winter. The isentropic level with higher occurrence of PV streamers varies in function of the cyclogenetic region. In *Argentina* and *Uruguay*, they are

more frequent at 320 K throughout the year, while in *SEBrazil* and *Andes* at 340 K in summer.

PV cutoffs frequency is lower than PV streamers at cyclogenesis time, however, they tend to increase during the cyclone lifetime, which occurs more frequently in summer than in winter. PV cutoffs are also more frequent in function of the latitudinal location of each region, where the more equatorward, the higher probability of detachment of PV centers from the polar stratospheric reservoir. Therefore, the frequency of PV cutoffs is lower than PV streamers in *Argentina* and *Uruguay*, comparable in summer for *SEBrazil*, and comparable in *Andes*, and the most prominent levels of occurrence during cyclogenesis are 310, 320, 360 and 360 K for, respectively, *Argentina, Uruguay, SEBrazil* and *Andes*.

6.2 Spatial patterns of cyclones environment

Over South America, climatologies of the dynamical tropopause in isobaric and isentropic levels present a variation according to the season, e.g., in summer the 360 K (340 and 320 K) level is very representative for latitudes northward (southward) 25°S. Composites before, during and after cyclogenesis, for each region and for austral summer and winter, presented specific characteristics:

Argentina contains the highest number of cyclones with similar frequency in the four seasons, with a slightly higher occurrence in summer. In this region, cyclogenesis occurs under the equatorial entrance of the jet stream in summer, where PV anomalies are stronger and concentrated in a smaller area closer to the genesis region than in winter. This suggests that upper-level PV anomalies contribute more strongly to upward motion and cyclogenesis at the surface during summer than in winter. A secondary feature is the slightly greater contribution of moisture in summer than in winter, during and after genesis, especially the stronger contrast between the downstream moist and upstream dry sectors of the cyclone. In winter, the genesis region is under the polar exit sector of the jet streak; sea level pressure and geopotential at 500 hPa anomalies are slightly stronger and wider, reaching lower latitudes. Nevertheless, the environment in summer seems to be slightly more baroclinic since there is greater vertical tilting of the pressure centers and EGR positive anomaly is also stronger. The anomalous PV acts to induce the breaking in the jet streak which is not evident in winter.

Hence, PV streamers seem to be an important mechanism to intensify upward motion with consequent contribution to the surface cyclone development mainly in summer.

Uruguay is the second most cyclogenetic region, presenting higher frequency in winter followed by spring. All forcing factors are stronger in winter than in summer, but not specifically inside the region. The jet stream is significantly disturbed by the high-altitude Andes in both seasons, resulting in its latitudinal undulation and poleward shift when crossing the Andes during winter and a weaker equatorward shift during summer. The position of the jets characterizes two different regions of ascent in winter, one in the lee of the Andes and a second one over the cyclogenetic region, whereas in summer a weaker center of QG-omega is found over the cyclogenetic region. This region is characterized by a higher probability of detachment of PV streamers from the westerly flow, which is evident by the positive PV cutoff anomaly in summer. Specific humidity is present over the region since before cyclogenesis, where stronger low-level northerly winds contribute to enhance the moisture transport in a larger area prior and during cyclogenesis in winter, whereas in summer the winds are weaker since prior until after genesis. The cyclogenesis is located between different EGR anomalies signals (positive and negative, respectively, southward and northward) in summer and winter. Finally, cyclogenesis occurs, again in both seasons, at the equatorial entrance sector of a jet streak, in contrast to *Argentina* where this was the case only in summer.

SEBrazil is the region with less cyclones, with greater occurrence in summer and spring. The level of the tropopause is higher in summer for this region, being essential to select different isentropic levels for summer (340-360 K) and winter (320 K). The jet stream on 300 hPa is located far south of the cyclogenesis region in summer. On the other hand, in winter, cyclogenesis occurs beneath the equatorial entrance of a jet streak, which results in stronger forcing for upward motion during winter than in summer. EGR, sea level pressure, geopotential at 500 hPa and specific humidity at 850 hPa anomalies are stronger in winter than in summer. Furthermore, the weaker anomalous pressure and geopotential at 500 hPa are essentially vertically aligned during summer, which is characteristic for a more barotropic vertical structure. In winter, the high frequency of PV streamers and cutoffs upstream cyclogenesis area contributes to strengthen the baroclinic environment. Finally, summer cyclogenesis might be strongly influenced by PV cutoffs at high isentropic levels, whereas

winter cyclogenesis is more influenced by lower-isentropic PV streamers and the moister environment provided by the stronger low-level jet.

Andes has comparable number of cyclogenesis with *Uruguay*, also with higher frequency in winter followed by spring. This region present similar environment patterns to that of *Uruguay* but with a lag of 12 h prior in winter. On the other hand, in summer, the patterns in *Andes* are similar to *SEBrazil*. In winter, the upper-level jet stream, PV anomaly and QG-omega are stronger, with anomalies to the south and closer to *Andes* than in summer. Geopotential height and pressure anomalies are stronger in winter, presenting a more baroclinic vertical structure. However, EGR positive anomaly are widespread in summer. The spatial pattern of specific humidity is very similar for both seasons, but with stronger low-level winds in winter. PV streamers are found only in summer, upstream *Andes*, while there is a weak signal of PV cutoffs over the region in winter.

This study presented a novel dynamical discussion for surface cyclogenesis over the center-east of South America in the presence of upper-level PV forcing. It highlighted the importance of upper-level PV anomalies, PV streamers and PV cutoffs for a better understanding of cyclone development in the four regions *Argentina*, *Uruguay*, *SEBrazil* and *Andes.*

6.3 Suggestions for future study

The results open up five further lines of research that should be addressed in future studies:

1) To separate the two types of cyclones found in the bi-modal frequency distribution and study them separately;
2) To separate the moving from the stationary cyclones in *Andes* to characterize the dynamic processes acting in these two categories;
3) A study based on the analysis of vertical cross section would be needed for a better understanding on how the tropical features interact with PV structures in *SEBrazil*;
4) Instead of using the seasonal climatology to calculate the anomalies, a moving climatology according to the exact day of the year (e.g. Graf et al., 2017) would be an interesting option to compile all cases, since there are seasonal transition factors that not exactly follow the

current separation (e.g., the South America monsoon season starts at October and ends up in March);

5) To perform an analysis of the relationship between cyclones from the cyclogenetic regions with different large-scale low frequency patterns as, e.g., El Niño, SAM, Rossby wave patterns.

References[1]

Appenzeler, C., & Davies, H. C. (1992). Structure of stratospheric intrusions into the troposphere. *Letters to Nature*, 358, 570-572.

Appenzeler, C., Davies, H. C., & Norton, W. A. (1996). Fragmentation of stratospheric intrusions. *Journal of Geophysical Research*, 101, 1435-1456.

Aebischer, U., & Schär, C. (1998). Low-level Potential Vorticity and Cyclogenesis to the Lee of the Alps. *Journal of the Atmospheric Sciences*, 55, 186-207.

Avila, V. D. (2018) *Estudo de Ciclogêneses Explosivas no Atlântico Sul*, (Doctoral Dissertation). Rretrieved from Repositório Digital UFRGS (http://hdl.handle.net/10183/189064). Porto Alegre, RS: Universidade Federal do Rio Grande do Sul.

Bjerknes, J., & Solberg, H. (1922). Life cycle of Cyclones and the Polar Front Theory of Atmospheric Circulation. *Geophysisks Publikationer*, 3, 3-18.

Čampa, J., & Wernli, H. (2012). A PV Perspective on the Vertical Structure of Mature Midlatitude Cyclones in the Northern Hemisphere. *Journal of the Atmospheric Sciences*, 69, 725-740.

Campetella, C. M., & Possia, N. E. (2007). Upper-level cut-off lows in southern South America. *Meteorology and Atmospheric Physics*, 96, 181-191.

Crespo, N. M. (2015). *Contribuição da interação troposfera-estratosfera nas ciclogêneses em superfície sobre a América do Sul*, (Master thesis). Retrieved from Teses e Dissertações USP. (DOI: 10.11606/D.14.2015.tde-29052015-003758). São Paulo, SP: Universidade de São Paulo.

Cressman, G. P. (1959). An operational objective analysis system. *Monthly Weather Review*, 87, 10, 367-374.

Danielsen, E. F. (1959). The Laminar Structure of the Atmosphere and Its Relation to the Concept of a Tropopause. *Archiv für Meteorologie, Geophysik und Bioklimatologie*, Serie A, 11, 3, 293-332.

Davies, H. C. (2015). The Quasigeostrophic Omega Equation: Reappraisal, Refinements, and Relevance. *Monthly Weather Review*, 143, 3–25.

Dee, D. P., Uppala, S. M., Simmons, A. J., Berrisford, P., Poli, P., Kobayashi, S., et al. (2011). The ERA-Interim reanalysis: configuration and performance of the data assimilation system. *Quarterly Journal of the Royal Meteorological Society*, 137, 553–597.

[1] According to APA reference style (American Psychological Association)

Dias Pinto, J. R., Reboita, M. S., & da Rocha, R. P. (2013). Synoptic and dynamical analysis of subtropical cyclone Anita (2010) and its potential for tropical transition over the South Atlantic Ocean. *Journal of Geophysical Research*, 118, 10870–10883.

Eady, E. T. (1949). Long Waves and Cyclone Waves. *Tellus*, 1, 33-52.

Ertel, H. (1942). Ein neuer hydrodynamischer Erhaltungssatz. *Naturwissenschaften*, 30, 543-544.

Fuenzalida, H. A., Sánchez, R., & Garreaud, R. D. (2005). A climatology of cutoff lows in the Southern Hemisphere. *Journal of Geophysical Research*, 110, D18101.

Gan, M. A., & Rao, V. B. (1991). Surface cyclogenesis over South America. *Monthly Weather Review*, 119, 1293-1302.

Gan, M. A., & Rao, V. B. (1994). The Influence of the Andes Cordillera on Transient Disturbances. *Monthly Weather Review*, 122, 1141-1157.

Gozzo, L. F. (2014). *Ciclones Subtropicais Sobre o Sudoeste do Atlântico Sul: Climatologia e Fontes de Umidade* (Doctoral dissertation). Retrieved from IAG repository (https://www.iag.usp.br/pos/sites/default/files/t_luiz_f_gozzo_corrigida.pdf). São Paulo, SP: Universidade de São Paulo.

Graf, M. A., Wernli, H., & Sprenger, M. (2017). Objective classification of extratropical cyclogenesis. *Quarterly Journal of the Royal Meteorological Society*, 143, 1047-1061.

Gramcianinov, C. B., Hodges, K. I., & Camargo, R. (2019). The properties and genesis environments of South Atlantic cyclones. *Climate Dynamics*, DOI: 10.1007/s00382-019-04778-1.

Hirschberg, P. A., & Fritsch, J. M. (1991). Tropopause Undulations and the Development of Extratropical Cyclones. Part II: Diagnostic Analysis and Conceptual Model. *Monthly Weather Review*, 119, 518-550.

Hoerling, M. P. (1992). Diabatic Sources of Potential Vorticity in the General Circulation. *Journal of the Atmospheric Sciences*, 49, 2282-2292.

Hoerling, M. P., Schaack, T. D. & Lenzen, A. J. (1991). Global objective tropopause analysis. *Monthly Weather Review*, 119, 1816–183.

Hoinka, K. P (1998). Statistics of the Global Tropopause Pressure. *Monthly Weather Review*, 126, 3303-3325.

Holton, J. R. (2004). *An Introduction to Dynamic Meteorology*. Elsevier Academic Press, New York, 4th ed., 535p.

Hoskins, B. J., & Hodges, K. I. (2005). A New Perspective on Southern Hemisphere Storm Tracks. *Journal of Climate*, 18, 4108-4129.

Hoskins, B. J., & James, I. N. (2014). *Fluid Dynamics of the Midlatitude Atmosphere*. John Wiley & Sons, Ltd., West Sussex, 430p.

Hoskins, B. J., McIntyre, M. E., & Robertson, W. (1985). On the use and significance of isentropic potential vorticity maps. *Quarterly Journal of the Royal Meteorological Society*, 111, 877-946.

Iwabe, C. M. N. (2012). *Ciclones Secundários no Sudoeste do Atlântico Sul: Climatologia e Simulação Numérica*. (Doctoral dissertation). Retrieved from Teses e Dissertações USP. (DOI: 10.11606/T.14.2012.tde-08042013-180829). São Paulo, SP: Universidade de São Paulo.

Iwabe, C. M. N., & da Rocha, R. P. (2009). An event of stratospheric air intrusion and its associated secondary surface cyclogenesis over the South Atlantic Ocean. *Journal of Geophysical Research*, 114, DOI: 10.1029/2008JD011119.

James, I. N. (1995). *Introduction to Circulating Atmospheres*. Cambridge University Press, New York, 448 p.

Kunz, A., Konopka, P., Müller, R., & Pan, L. L. (2011). Dynamical tropopause based on isentropic potential vorticity gradients. *Journal of Geophysical Research*, 116, D01110, DOI:10.1029/2010JD014343.

Krüger, L. F., da Rocha, R. P., Reboita, M. S., & Ambrizzi, T. (2012). RegCM3 nested in HadAM3 scenarios A2 and B2: projected changes in extratropical cyclogenesis, temperature and precipitation over the South Atlantic Ocean. *Climatic Change*, 113, 599-621.

Lim, E. P., & Simmonds, I. (2007). Southern Hemisphere Winter Extratropical Cyclone Characteristics and Vertical Organization Observed with the ERA-40 Data in 1979–2001. *Journal of Climate*, 20, 2675-2690.

Marengo, J. A., Soares, W. R., Saulo, C., & Nicolini, M. (2004). Climatology of the Low-Level Jet East of the Andes as Derived from the NCEP-NCAR Reanalyses: Characteristics and Temporal Variability. *Journal of Climate*, 17, 2261-2280.

Martin, J. E. (2006). *Mid-Latitude Atmospheric Dynamics: A First Course*. John Wiley & Sons, Ltd., West Sussex, 336p.

McIntyre, M. E., & Palmer, T. N. (1983). Breaking planetary waves in the stratosphere. *Nature*, 305, 593-600.

Mendes, D., Souza, E. P., Trigo, I. F., & Miranda, P. M. A. (2007). On precursors of South American cyclogenesis. *Tellus*, 59A, 114–121.

Miky Funatsu, B., Gan, M. A., & Caetano, E. (2004). A case study of orographic cyclogenesis over South America. *Atmósfera*, 17, 91-113.

Ndarana, T., & Waugh, D. W. (2010). The link between cut-off lows and Rossby wave breaking in the Southern Hemisphere. *Quarterly Journal of the Royal Meteorological Society*, 136, 869-885.

Neu, U., Akperov, M.G., Bellenbaum, N., Benestad, R., Blender, R., Caballero, R., et al. (2013). IMILAST: A Community Effort to Intercompare Extratropical Cyclone Detection and Tracking Algorithms. *Bulletin of the American Meteorological Society*, 94, 529–547.

Nieto, R., Sprenger, M., Wernli, H., Trigo, R. M., & Gimeno, L. (2008). Identification and Climatology of Cut-off Lows near the Tropopause. *Annals of the New York Academy of Sciences*, 1146, 256-290.

Onogi, K., Tsutsui, J., Koide, H., Sakamoto, M., Kobayashi, S., Hatsushika, H., et al. (2007). The JRA-25 reanalysis. *Journal of the Meteorological Society of Japan*, 85, 369− 432.

Orlanski, I., & Katzfey, J. (1991). The Life Cycle of a Cyclone Wave in the Southern Hemisphere. Part I: Eddy Energy Budget. *Journal of the Atmospheric Sciences*, 48, 1972-1998.

Pinheiro, H. R., Hodges, K. I., Gan, M. A., & Ferreira, N. J. (2017). A new perspective of the climatological features of upper-level cut-off lows in the Southern Hemisphere. *Climate Dynamics*, 48, 541-559.

Pezza, A. B., & Simmonds, I. (2005). The first South Atlantic hurricane: Unprecedented blocking, low shear and climate change. *Geophysical Research Letters*, 32, doi:10.1029/2005GL023390.

Portmann, R., Crezee B., Quinting J., & Wernli, H. (2018). The complex life cycles of two long-lived potential vorticity cut-offs over Europe. *Quarterly Journal of the Royal Meteorological Society*, 144, 701–719.

Reboita, M. S., Ambrizzi, T., Silva, B. A., Pinheiro, R. F., & da Rocha, R. P. (2019). The South Atlantic Subtropical Anticyclone: Present and Future Climate. *Frontiers in Earth Science*, 7:8, 1-15.

Reboita, M. S., da Rocha, R. P. & Ambrizzi, T. (2012). Dynamic and climatological features of cyclonic developments over southwestern South Atlantic Ocean. In B. Veress and J. Szigethy (Eds.), *Horizons in Earth Science Research*, 6, 135-160. Nova Science Publishers, Inc.

Reboita, M. S., da Rocha, R. P., Ambrizzi, T., & Sugahara, S. (2010). South Atlantic Ocean cyclogenesis climatology simulated by regional climate model (RegCM3). *Climate Dynamics*, 35, 1331-1347.

Reboita, M. S., da Rocha R. P., de Souza M. R., & Llopart M. (2018). Extratropical cyclones over the southwestern South Atlantic Ocean: HadGEM2- ES and RegCM4 projections. *International Journal of Climatology*, 38, 2866 –2879.

Reboita, M. S., Gan, M. A., da Rocha, R. P., & Custódio, I. S. (2017). Ciclones em superfície nas Latitudes Austrais: Parte I Revisão Bibliográfica. *Revista Brasileira de Meteorologia*, 32, 171-186.

Reboita, M. S., Nieto, R., Gimeno, L., da Rocha, R. P., Ambrizzi, T., Garreaud, R., & Krüger, L. F. (2010). Climatological features of cutoff low systems in the Southern Hemisphere. *Journal of Geophysical Research*, 115, DOI: 10.1029/2009JD013251.

Reed, R. J. (1955). A study of a characteristic type of upper level frontogenesis. *Journal of Meteorology*, 12, 226–237.

Rossby, C. G. (1940). Planetary flow patterns in the atmosphere. *Quarterly Journal of the Royal Meteorological Society*, 66, 68-87.

Salio, P., Nicolini, M., & Saulo, A. C. (2002). Chaco low-level jet events characterization during the austral summer season. *Journal of Geophysical Research*, 107, DOI:10.1029/2001JD001315.

Saulo, A. C., Seluchi, M. E., & Nicolini, M., (2004). A Case Study of a Chaco Low-Level Jet Event. *Monthly Weather Review*, 132, 2669-2683.

Satyamurty, P., & Seluchi, M. E. (2007). Characteristics and structure of an upper air cold vortex in the subtropics of South America. *Meteorology and Atmospheric Physics*, 96, 203-220.

Schär, C., Sprenger, M., Lüthi, D., Jiang, Q., Smith, R. B., & Benoit, R. (2003). Structure and dynamics of an Alpine potential-vorticity banner. *Quarterly Journal of the Royal Meteorological Society*, 129, 825-855.

Seluchi, M. E., & Saulo, A. C. (2012). Baixa do Noroeste Argentino e Baixa do Chaco: Características, Diferenças e Semelhanças. *Revista Brasileira de Meteorologia*, 27, 49-60.

Seluchi, M. E., Saulo, A. C., Nicolini, M., & Satyamurty, P. (2003). The Northwestern Argentinean Low: A Study of Two Typical Events. *Monthly Weather Review*, 131, 2361-2378.

Shapiro, M. A. (1980). Turbulent mixing within tropopause folds as a mechanism for the exchange of chemical constituents between the stratosphere and the troposphere. *Journal of the Atmospheric Sciences*, 37, 994–1004.

Sinclair, M. R. (1994). An Objective Cyclone Climatology for the Southern Hemisphere. *Monthly Weather Review*, 122, 2239-2256.

Sinclair, M. R. (1995). A climatology of cyclogenesis for the Southern Hemisphere. *Monthly Weather Review*, 123, 1601–1619.

Sinclair, M. R. (1997). Objective Identification of Cyclones and Their Circulation Intensity, and Climatology. *Weather and Forecasting*, 12, 595-612.

Škerlak, B., Sprenger, M., Pfahl, S., Tyrlis, E., & Wernli, H. (2015). Tropopause folds in ERA-Interim: Global climatology and relation to extreme weather events. *Journal of Geophysical Research*, 120, 4860– 4877.

Sprenger, M., Martius, O., & Arnold, J. (2013). Cold surge episodes over southeastern Brazil – a potential vorticity perspective. *International Journal of Climatology*, 33, 2758-2767

Sprenger, M., Fragkoulidis, G., Binder, H., Croci-Maspoli, M., Graf, P., Grams, et al. (2017). Global climatologies of Eulerian and Lagrangian flow features based on ERA-Interim. *Bulletin of the American Meteorological Society*, 98, 1739–1748.

Sprenger, M., Wernli, H., & Bourqui, M. (2007). Stratosphere–Troposphere Exchange and Its Relation to Potential Vorticity Streamers and Cutoffs near the Extratropical Tropopause. *Journal of the Atmospheric Sciences*, 64, 1587-1602.

Sugahara, S. (2000). *Variação Anual da Frequência de Ciclones no Atlântico Sul*. Paper presented at 11th Congresso Brasileiro de Meteorologia, Rio de Janeiro, Brazil.

Sugahara, S., da Rocha, R. P., & Rodrigues, M. L. (1994). *Condições atmosféricas de grande escala associadas a jato de baixos níveis na América do Sul*. Paper presented at 8th Congresso Brasileiro de Meteorologia, Belo Horizonte, Brazil.

Sun, X., Cook, K. H., & Vizy, E. K. (2017). The South Atlantic Subtropical High: Climatology and Interannual Variability. *Journal of Climate*, 30, 3279-3296.

Taljaard, J. J. (1967). Development, Distribution and Movement of Cyclones and Anticyclones in the Southern Hemisphere During the IGY. *Journal of Applied Meteorology*, 6, 973-987.

Thorncroft, C. D., Hoskins, B. J., & McIntyre, M. E. (1993). Two paradigms of baroclinic-wave life-cycle behavior. *Quarterly Journal of the Royal Meteorological Society*, 119, 17-55.

Uppala, S. M., KÅllberg, P. W., Simmons, A. J., Andrae, U., Bechtold, V. D., Fiorino, M., et al. (2005). The ERA-40 re-analysis. *Quarterly Journal of the Royal Meteorological Society*, 131, 2961-3012.

Waugh, D. W., Plumb, R. A., Atkinson, R. J., Schoeberl, M. R., Lait, L. R., Newman, P. A., et al. (1994). Transport out of the lower stratospheric Arctic vortex by Rossby wave breaking. *Journal of Geophysical Research*, 99, 1071-1088.

Wernli, H., & Davies, H. C. (1997). A Lagrangian-based analysis of extratropical cyclones. I: The method and some applications. *Quarterly Journal of the Royal Meteorological Society*, 123, 467-489.

Wernli, H., & Schwierz, C. (2006). Surface Cyclones in the ERA-40 Dataset (1958-2001). Part I: Novel Identification Method and Global Climatology. *Journal of Atmospheric Sciences*, 63, 2486-2507.

Wernli, H., & Sprenger, M. (2007). Identification and ERA-15 Climatology of Potential Vorticity Streamers and Cutoffs near the Extratropical Tropopause. *Journal of the Atmospheric Sciences*, 64, 1569-1586.

Whitaker, J. S., & Davis, C. A. (1994). Cyclogenesis in a Saturated Environment. *Journal of the Atmospheric Sciences*, 51, 889-907.

WMO (1986). Atmospheric ozone 1985: Global ozone research and monitoring report. *Report 16.* World Meteorological Organization, Geneva, Switzerland, 392 pp.

Yanase, W., Niino, H., Hodges, K., & Kitabatake, N. (2014). Parameter Spaces of Environmental Fields Responsible for Cyclone Development from Tropics to Extratropics. *Journal of Climate*, 27, 652-671.

Zhou, J., & Lau, K-M. (1998). Does a Monsoon Climate Exist over South America? *Journal of Climate*, 11, 1020-1040.

A) Appendix A – Autumn and spring climatologies

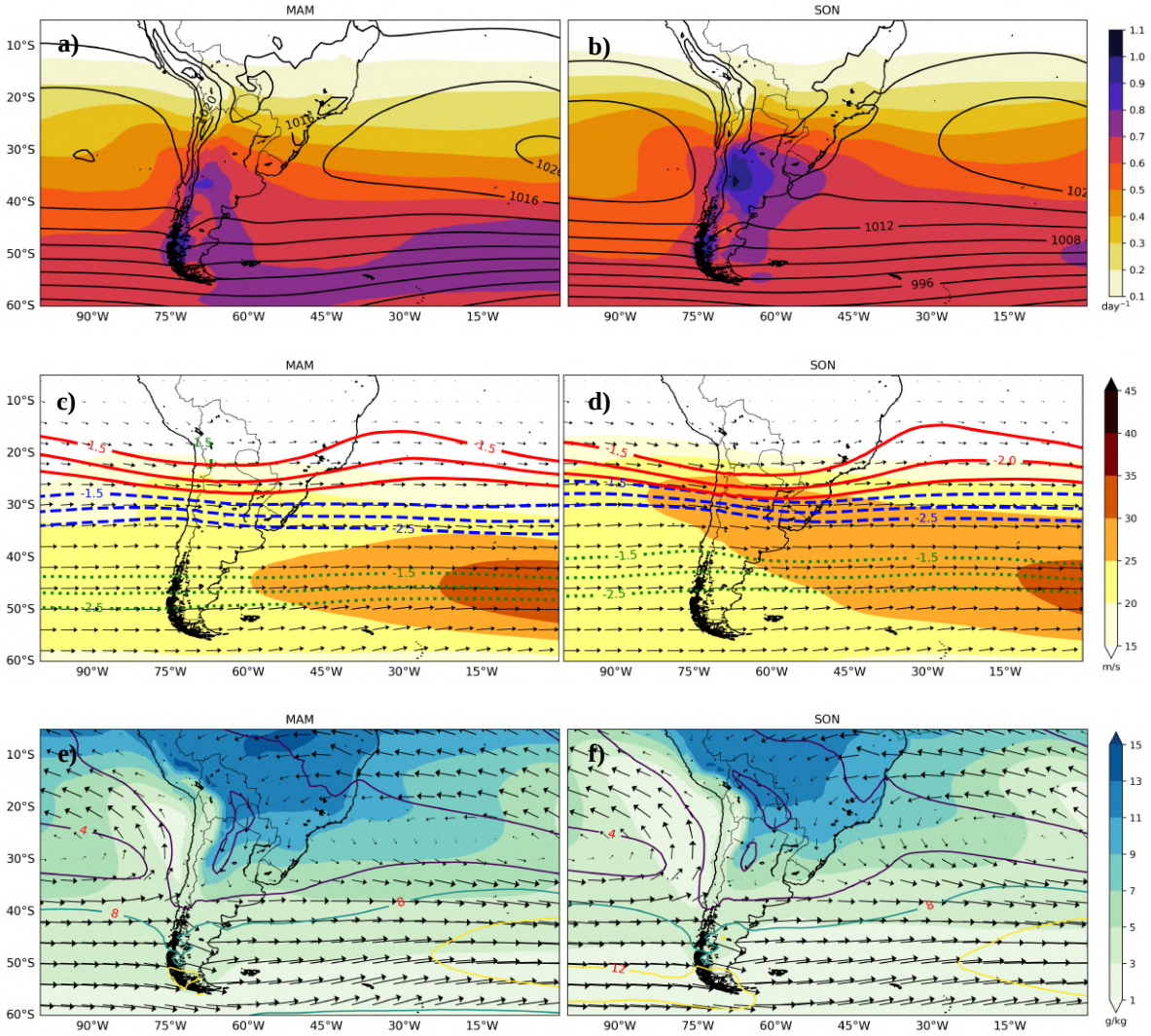

Figure A.1 Same as in Figure 5.2, but for austral autumn and spring.

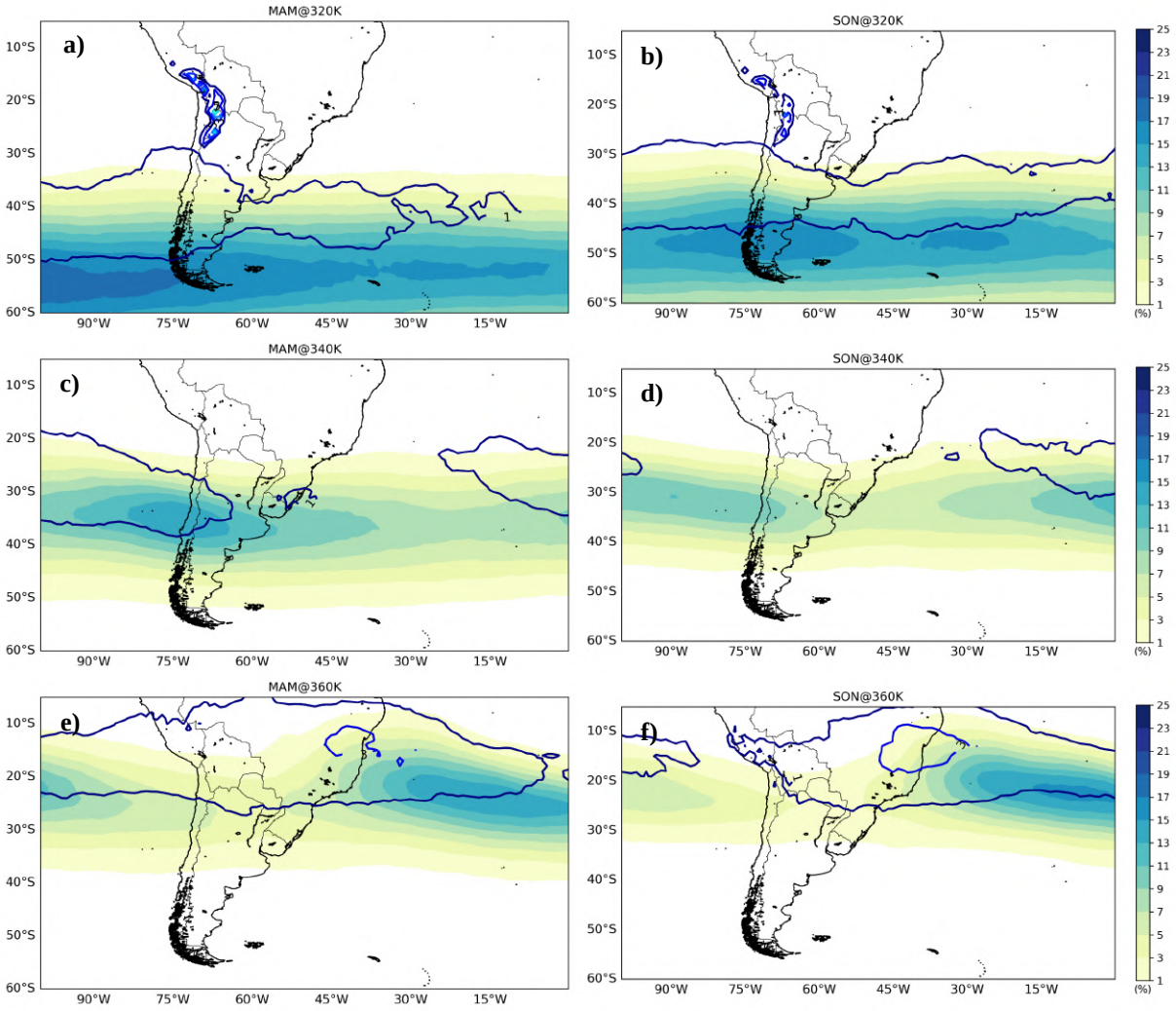

Figure A.2 Same as in Figure 5.3, but for austral autumn and spring.

B) Appendix B – Composites of PV streamers and cutoffs at 360 K

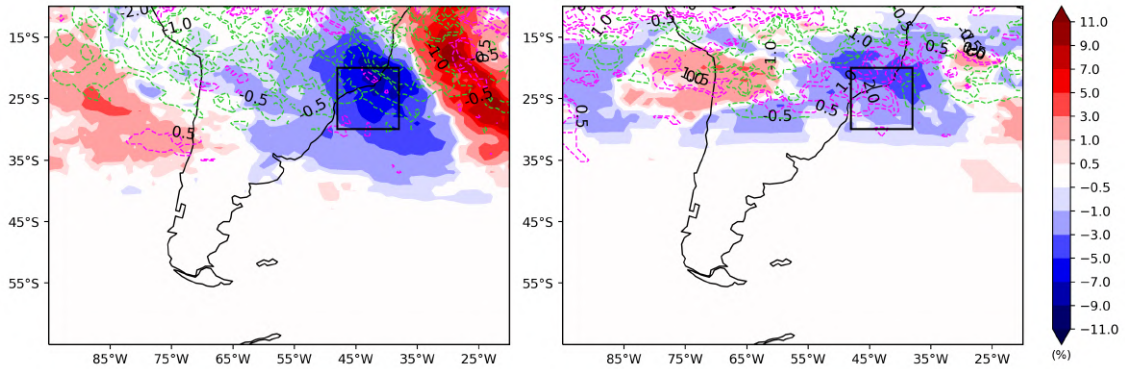

Figure B.1 Austral summer (left panels) and winter (right panels) composites (for the period 1979-2017) for *SEBrazil*: a)-b) anomaly frequencies of PV streamers (shaded) and PV cutoffs (dashed lines) frequency (%) at 360 K.

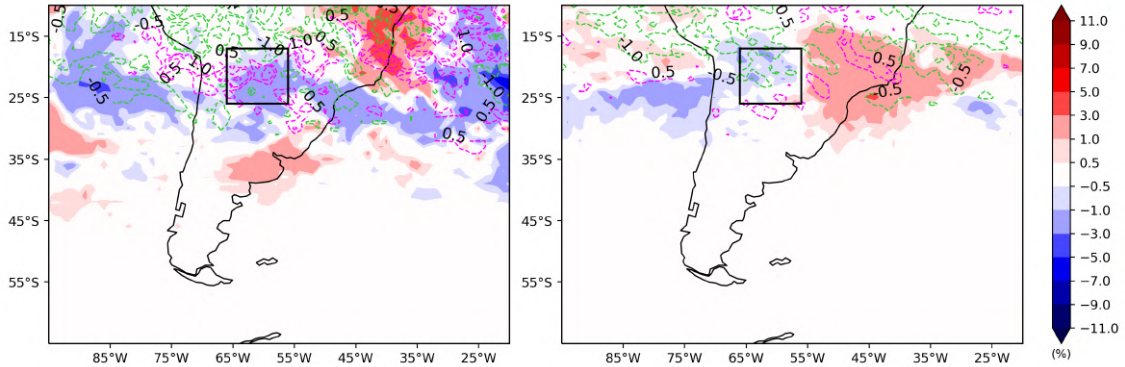

Figure B.2 Austral summer (left panels) and winter (right panels) composites (for the period 1979-2017) for *Andes*: a)-b) anomaly frequencies of PV streamers (shaded) and PV cutoffs (dashed lines) frequency (%) at 360 K.

C) Appendix C – Composites for 2 days after cyclogenesis

Argentina

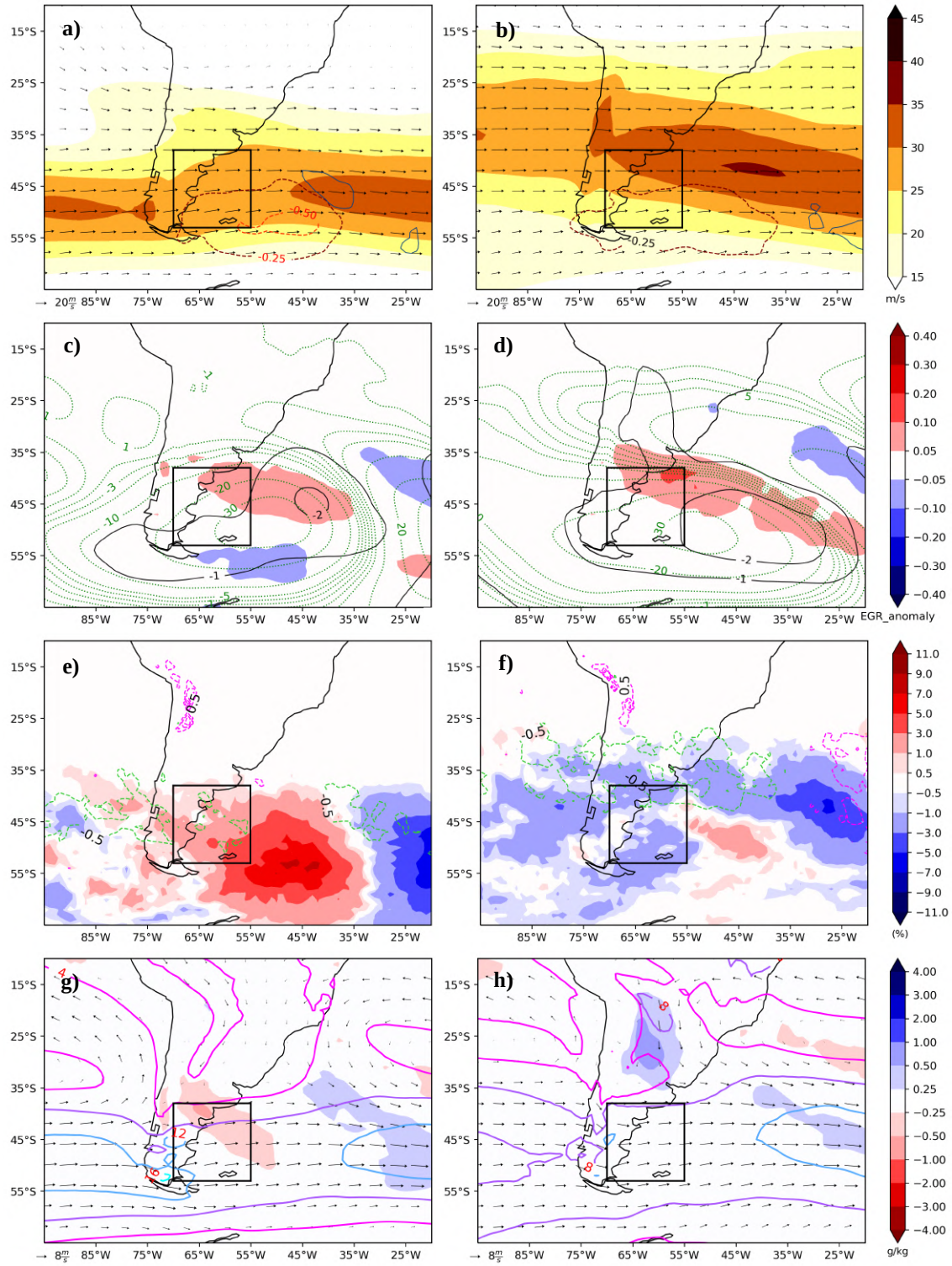

Figure C.1 As in Figures 5.6, 5.10 and 5.11 but for 48 hours after cyclogenesis.

Uruguay

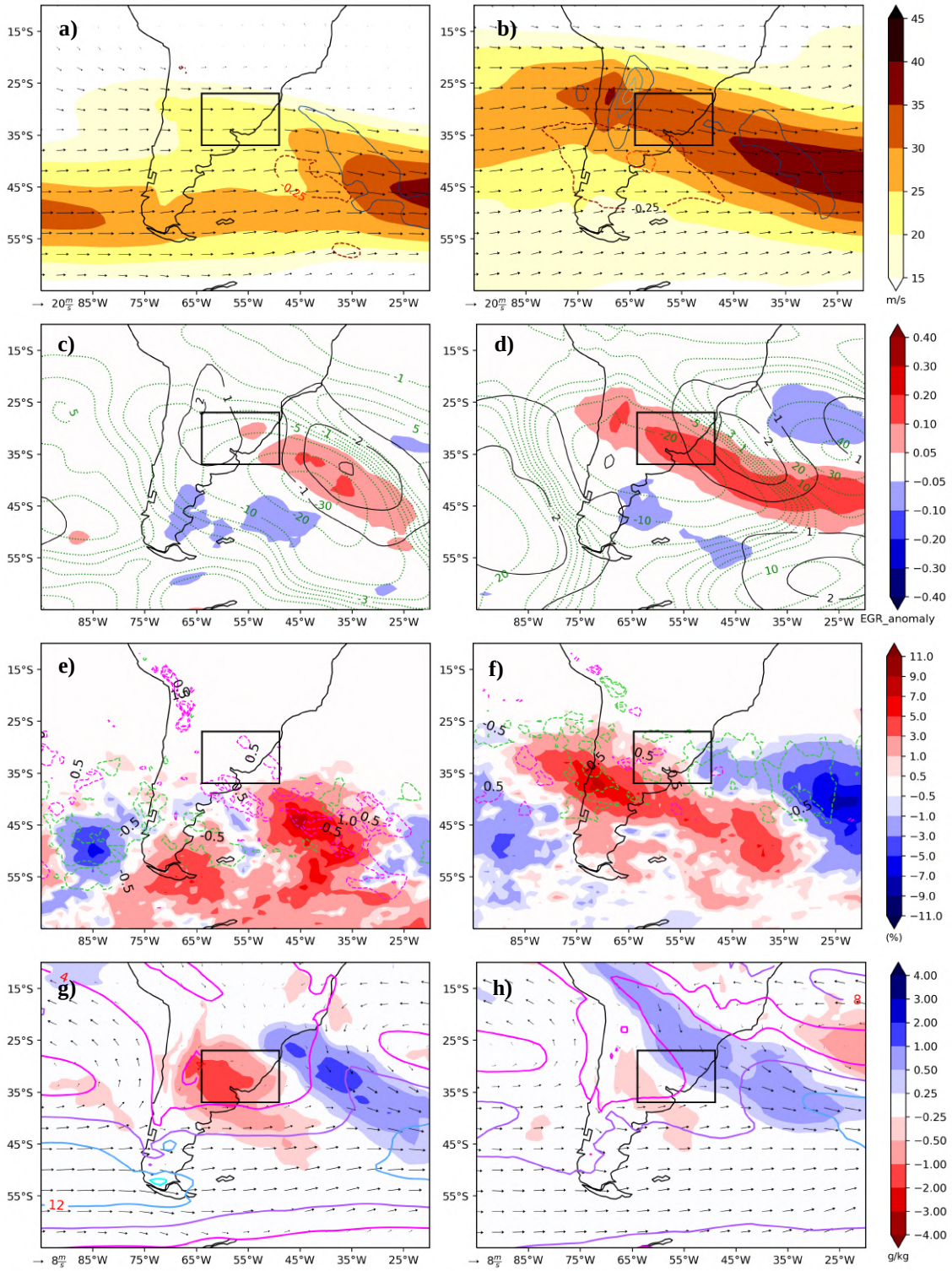

Figure C.2 As in Figures 5.7, 5.12 and 5.13, but for 48 hours after cyclogenesis.

SEBrazil

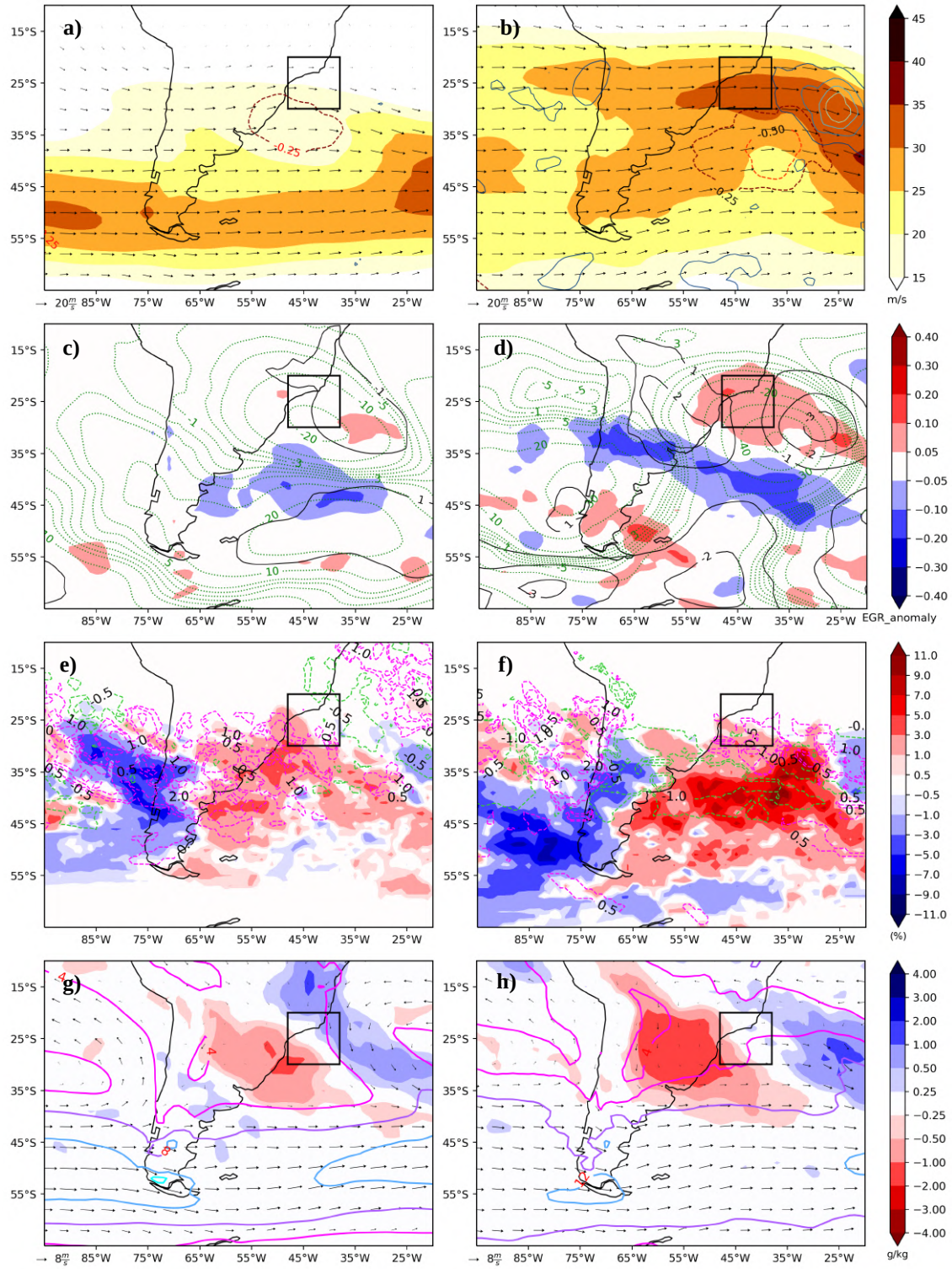

Figure C.3 As in Figures 5.8, 5.14 and 5.15, but 48 hours after cyclogenesis.

Andes

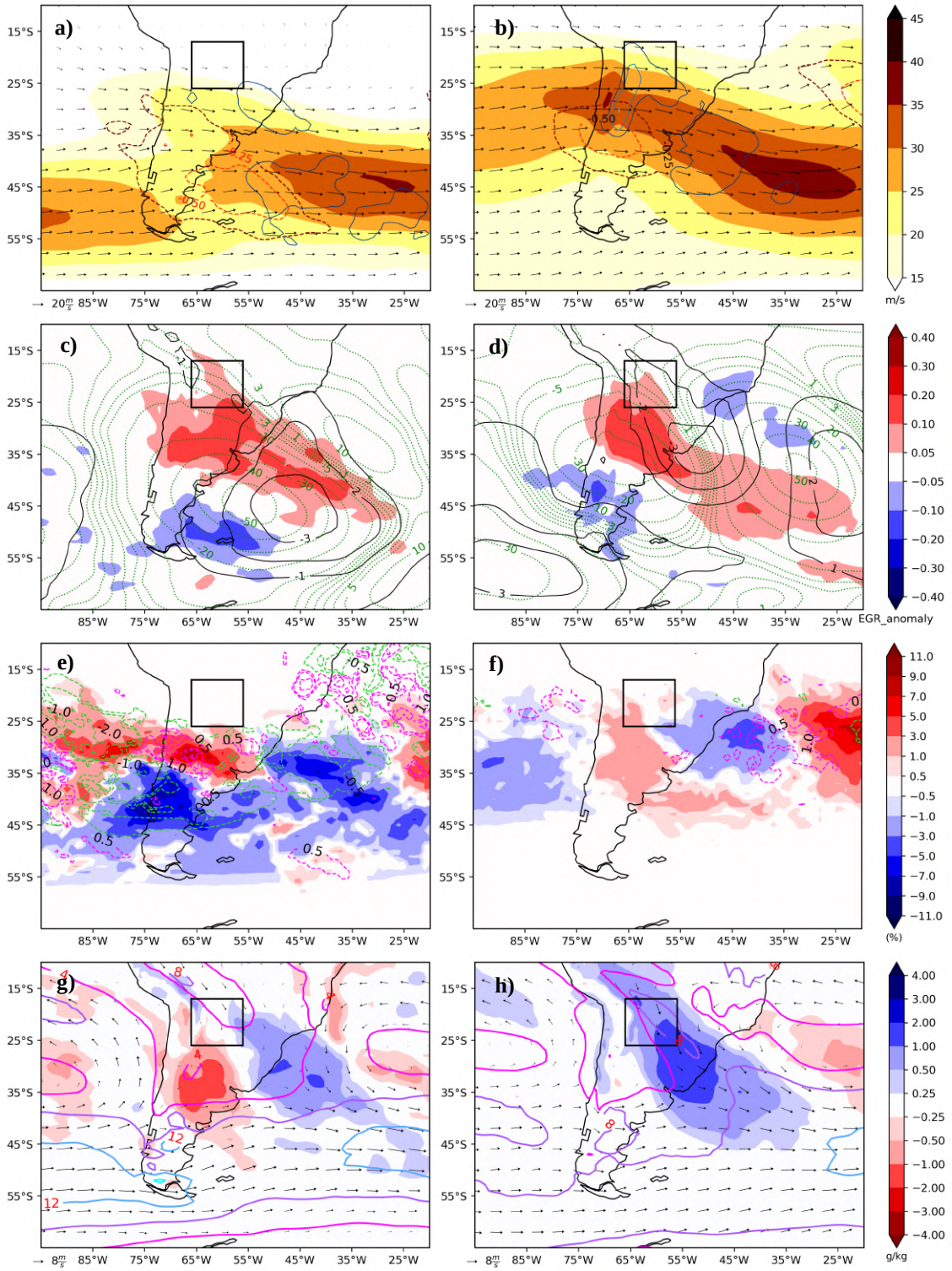

Figure C.4 As in Figure 5.9, 5.16 and 5.17, but for 48 hours after cyclogenesis.